A ROLE FOR ADAMTS5 IN REGULATING THE COMPOSITION OF THE ECM

NICHE IN MURINE PLURIPOTENT PROGENITOR CELLS

By

Daniel J Gorski

B.S. Molecular and Cellular Biology

University of Illinois at Urbana Champaign, 2009

Submitted to Rush University in partial

fulfillment of the requirements for degree of

Doctor of Philosophy

DISSERTATION APPROVAL FORM

The undersigned have examined the dissertation entitled: A ROLE FOR ADAMTS5 IN REGULATING THE COMPOSITION OF THE ECM NICHE IN MURINE PLURIPOTENT PROGENITOR CELLS

presented by: Daniel J Gorski

a candidate for the degree of

Doctor of Philosophy

and hereby certify that in their judgment it is worthy of acceptance.

_____	_____
(Chairperson)　　(date)	(Advisor)　　(date)
Hee-Jeong Im Sampen, Ph.D.	Anna Plaas, Ph.D.
Professor	Professor
Departments of Biochemistry, Orthopedic Surgery and Internal Medicine	Departments of Internal Medicine and Biochemistry
Rush University	Rush University
_____	_____
(date)	(date)
Vincent Hascall, Ph.D.	Thomas Schmid, Ph.D.
Professor	Professor
Department of Biomedical Engineering	Department of Biochemistry
Cleveland Clinic Lerner Research Institute	Rush University
_____	_____
(date)	(date)
Carol Muehleman, Ph.D.	Vincent Wang, Ph.D.
Professor Emeritus	Associate Professor
Department of Biochemistry	Department of Orthopedic Surgery
Rush University	Rush University

_____ (date)

Guozhi Xiao, Ph.D.
Professor
Department of Biochemistry
Rush University

ABSTRACT

Title of Dissertation: A ROLE FOR ADAMTS5 IN REGULATING THE COMPOSITION OF THE ECM NICHE IN MURINE PLURIPOTENT PROGENITOR CELLS

Daniel J Gorski, 2014

Dissertation directed by: Anna Plaas, Ph.D., Professor of Internal Medicine and

Biochemistry, Rush University

_____

Signature of Dissertation Advisor

ADAMTS5 (TS5), as a member of the ADAMTS-aggrecanase family of proteases is considered to be largely responsible for the turnover of aggrecan and versican in vivo. Its ablation has been shown to protect murine cartilage from a variety of joint injury models, give rise to heart valve abnormalities and cause defective wound healing, as well as affect fibroblast-myofibroblast transition due to altered versican turnover. However, a potentially broader cell biological role for this protein in signal transduction to regulate extracellular matrix turnover during tissue homeostasis and regeneration is not well understood. We have previously reported that ADAMTS5 KO mice exhibit cartilage protection after joint injury due to reduced fibrosis of the joint capsule and synovium and enhanced articular cartilage deposition. Additionally, these mice display impaired wound healing of

the skin and tendons, and this is associated with aggrecan-rich deposits at the wound sites in vivo and altered TGFb signaling in fibroblasts in vitro. We hypothesize that the multi-tissue chondrogenic wound-healing response in ADAMTS5 KO mice is due to a nodal role of TS5 in regulating the differentiation of progenitor cells into fibroblastic cell types. To address this hypothesis, we have established monolayer cultures of adipose derived stromal cells (ADSCs) from wild type and two strains of ADAMTS5 KO mice and have shown their basal capacity in vitro for versican, aggrecan, hyaluronan and collagen type I synthesis. Aggrecan synthesis was stimulated by increased (10 mM) extracellular glucose, and this was more pronounced in TS5 KO cells, which exhibited enhanced glucose uptake, under both physiological (5 mM) and hyperglycemic (10 mM) conditions.

We also investigated the catabolic turnover of aggrecan and versican in the stromal cell cultures. Both were degraded by ADAMTS-aggrecanases, and no qualitative or quantitative differences in their catabolism were detected between WT and TS5 KO cells. Notably, ADAMTS-cleavage of the core proteins occurred largely intracellularly during the secretory process, and took place both in the absence and presence of fetal bovine serum. Furthermore, a comparative analysis of aggrecan turnover in epiphyseal chondrocytes showed no differences in catabolic activity against the proteoglycan in WT and TS5 KO cells, we propose that ADAMTS5 is not essential for aggrecan cleavage in these two cells types.

In keeping with previous work on newborn skin fibroblasts we found that stromal cells from ADAMTS5 KO mice exhibited altered TGFb1 responsiveness, which in this study was shown by lack of TGFb1 stimulated hyaluronan synthase 1 and 2 gene expression and collagen type I synthesis, in TS5 KO cultures compared to WT. A non-proteolytic function for the TS5 protein was further underscored by our finding, that only fragments of TS5 were detectable in the cell associated matrix of WT stromal cells. Their absence in TS5 KO cells, their lack of proteolytic activity (size of 30kDa and 40 kDa, by reactivity on western blot analyses with 2 peptide specific antibodies), and their altered abundance in cells treated with the endocytotic/endosomal trafficking inhibitors, Dynasore or Bafilomycin, indicates a novel cell-biological role for TS5 in modulating signal transduction mechanisms by regulating growth factor receptor endocytosis and/or endosomal recycling.

ACKNOWLEDGEMENTS

TABLE OF CONTENTS

LIST OF TABLES

LIST OF FIGURES

LIST OF ABBREVIATIONS

α2M	Alpha-2-macroglobulin
ADAMTS	A disintegrin and metalloproteinase with thrombospondin motif
ADSC	Adipose Derived Stromal Cell
AMEM	Advanced Minimum Essential Medium
ALK1	Activin receptor-like kinase-1
ALK5	Activin receptor-like kinase-5
ATP	Adenosine triphosphate
Baf	Bafilomycin A1
BTM	Batimastat
bFGF	Basic Fibroblast Growth Factor
BMP	Bone Morphogenetic Protein
CD	Cluster of Differentiation
cDNA	Complementary DNA
CS	Chondroitin Sulfate
CS/DS	Chondroitin Sulfate/Dermatan Sulfate
CTGF	Connective Tissue Growth Factor
CXCR4	Chemokine (C-X-C motif) receptor 4
DE52	Diethylaminoethyl cellulose
DMEM	Dulbecco's Modified Eagle's Medium
DMSO	Dimethyl sulfoxide
DNA	Deoxyribonucleic acid
dNTPs	Deoxyribonucleotide (mixture)
Dyn	Dynasore
ECM	Extracellular matrix
EDTA	Ethylenediaminetetraacetic acid
EGF	Epidermal growth factor
FACE	Fluorophore-assisted carbohydrate electrophoresis
FAK	Focal adhesion kinase
FBS	Fetal bovine serum
FGF	Fibroblast Growth Factor
GAG	Glycosaminoglycans
GalNAc	N-Acetylgalactosamine
GLUT	Glucose transporter
HA	Hyaluronan
HABP	Hyaluronan Binding Protein
HIF-1α	Hypoxia-inducing factor-1-alpha
HRP	Horseradish Peroxidase
IFN-γ	Interferon-gamma
IGF-1	Insulin-like Growth Factor-1
IHC	Immunohistochemistry
IL	Interleukin
KO	Knockout
LRP-1	Lipoprotein receptor related protein-1
MAPK	Mitogen-activated protein kinase
MHC	Major Histocompatibility complex

MMP	Matrix metalloproteinase
mRNA	Messenger RNA
MSC	Mesenchymal stem cell
MT1-MMP	Membrane type 1-matrix metalloproteinase
OA	Osteoarthritis
PBS	Phosphate buffered saline
PCP	Procollagen C-proteinase
PCR	Polymerase chain reaction
PDGF	Platelet-derived growth factor
PG	Proteoglycan
PI3K	phosphoinositide 3-kinase
QPCR	Quantitative polymerase chain reaction
RA	Retinoic Acid
rhBMP-1	Recombinant human bone morphogenetic protein-1
rhTGFb	Recombinant human transforming growth factor beta
RNA	Ribonucleic acid
SARA	Smad anchor for receptor activation
SDS	Sodium dodecyl sulfate
SLRP	Small leucine rich proteoglycan
SMAD	Sma and Mad (Mothers against decapentaplegic) (Protein)
TBST	Tris-buffered Saline with Tween
TGFb1	Transforming growth factor beta-1
TGFbRI/II	Transforming growth factor beta receptor 1 and 2
TNF-α	Tumor necrosis factor alpha
TS4	ADAMTS4
TS5	ADAMTS5
TS9	ADAMTS9
TS15	ADAMTS15
TS5J KO	Deltagen generated ADAMTS5 knockout mouse
TS5P KO	Pfizer generated ADAMTS5 knockout mouse
TS5i	Specific ADAMTS5 inhibitor
UDP	Uridine diphosphate
WT	Wild type

I. INTRODUCTION

A. PHYSIOLOGY AND CELL BIOLOGY OF TISSUE REGENERATION

The capacity for an organism to renew itself or part of itself is a necessary biological process essential for survival after disruption or damage from its environment. The proper regeneration of tissues requires a complex orchestration of events to restore function to a damaged tissue or organ. The most sophisticated and evolutionarily refined mechanisms for regeneration in mammalian species are dermal wound-healing [1], fracture healing [2] and mucus membrane regeneration [3]. All three processes involve recruitment and activation of neutrophils and macrophages from the peripheral immune system and endogenous multi-potent progenitor cells to the injury site. In combination, these cell types achieve protection from infectious agents, removal of damaged tissue and cell debris, and generate repair tissue, which in the adult animal is also defined as "scarring". Tissue and organ regeneration involves spatially and temporally coordinated molecular responses, this sequential pathway being relatively conserved and known as the stages or 'phases' of regeneration, which include hemostasis, inflammation, proliferation and remodeling [4]. A brief summary of these stages is provided below.

1. Stages of Tissue Regeneration

A primary response at the injury site is prevention of blood loss. This is achieved by platelets aggregating to form a clot made of fibrin, fibronectin and thrombospondin [5-7]. As a temporary matrix, this allows adherence of leukocytes, which secrete growth factors such as platelet derived growth factor (PDGF), fibroblast growth factor (FGF) transforming growth factor beta 1 (TGFb1), epidermal growth factor (EGF), insulin-like growth factor-1 (IGF-1), and pro-inflammatory cytokines interleukin 1 and 6 (IL-1) and (IL-6), and further recruitment of neutrophils and macrophages [4,8], to eliminate bacteria and damaged tissue and cells. Secretion of TGFb1 by phagocytic cells induces further migration and proliferation of stromal progenitor cell populations [4,9], which embed themselves in a provisional ECM, composed of collagen types I and III, SLRP- proteoglycans [10,11], fibronectin and a hyaluronan proteoglycan network [12-15]. Prior to the production of new tissue (i.e. scar formation), remodeling of the granulation tissue is required. The residual cells are stimulated to perform ECM degradation and phagocytose fragments, and at the same time allow for activation of complex networks of autocrine stimulated signaling pathways [15-17], to induce the differentiation of stromal progenitor cells into tissue specific cell types.

2. Role of Stromal Cells in Wound Healing

Multipotent stromal cells, also known as Mesenchymal Stem Cells or (MSCs) are emerging as major regulators in nearly all parts of wound healing

from inflammation to the final repair stages [18]. They have been identified in essentially all tissues and organs, including; bone marrow, brain, kidney, liver, thymus, kidney glomeruli, muscle, lung, skin [19] and soft connective tissues [20] of the musculoskeletal system. Tissue specific activation pathways can transform those cells in vivo and in vitro to a differentiated phenotype to produce the appropriate repair tissue. This could be for example, a collagenous matrix (fibroblasts, dermal wound healing), a calcified ECM (osteoblast, fracture healing), an aggrecan/type II collagen-rich ECM (chondrocyte in fracture healing or cartilage repair), or a mucoid rich ECM (lining cells in airways and digestive system).

In addition to their capacity to differentiate into tissue-forming cells, stromal cells have been shown to have an immune-regulatory function through suppressing T-cell, natural killer cell and macrophage activation and proliferation [21,22]. They also have the ability to secrete anti-inflammatory cytokines, interleukin-10 (IL-10) and IL-4 while suppressing pro-inflammatory cytokines, tumor necrosis factor alpha (TNF-α) and interferon-γ (IFN-γ) [22,23]. This capacity clearly contributes to dampening inflammation and activation of the peripheral immune system, thus allowing the healing to proceed to completion. Stromal cells have a low immunogenic profile, with very little expression of MHC (major histocompatibility complex) class I and lack of class II [23,24]. These characteristics have been shown to be of therapeutic values; for example, one study showed the down regulation of T-helper cell driven inflammation in a murine experimental model of colitis, when stromal cells both from human and

murine sources [25] were infused. In addition to their clinical use in Crohn's disease, clinical trials are underway to test their therapeutic anti-inflammatory action in treatment of diseases such as, Graft Versus Host Disease and chronic non-healing wounds [26].

3. Stromal Cell Characteristics

'Stromal' cells were originally described as a population of adult stem cells isolated from bone marrow, which adhered to plastic and formed colonies. In more recent years, attempts have been made (such as those by the International Society for Cellular Therapy [27]) to more clearly define this cell type, and expression of cell surface markers such as CD73, CD90 and CD105 have been frequently recommended as 'marker molecules'. Furthermore, induction of osteoblastic, adipogenic, myogenic, fibrogenic and chondrogenic pathways by specialized culture media [28-30], have been used to support their 'stem-like' nature and multipotency [31,32]. In the undifferentiated form, they display a fibroblastic morphology that some describe as 'spindle like'. Indeed, several of the surface markers (CD44, CD90, and CD105) [33], multipotencies and immunomodulatory capacities are shared with fibroblasts [34,35]. A common feature for identification and localization in vivo is the so-called 'niche', which functionally could be defined as the ECM surrounding the stromal cells (**Fig. 1**). Typically, the ECM is composed of collagens I, III, IV and V, laminin, fibronectin [36], high molecular weight proteoglycans [37], HA [38-40], and SLRP-proteoglycans biglycan and decorin [41]. Communication between stromal cells

and their ECM niche is important in determining cell survival, differentiation and self-renewal. These are in turn mediated via cell surface receptors, primarily integrins, and their linkage to signal transduction pathways involving focal adhesion kinase (FAK), phosphoinositide 3-kinase (PI3K), and TGFb receptors. Growth factor delivery is also mediated by the local ECM via metalloproteinases, which serve to cleave ECM components thereby releasing soluble signals that are taken up by adjacent cells [42]. Moreover, data reported in a recent study using umbilical cord mesenchymal stem cells in a model of congenital metabolic disorder mucopolysaccharidosis VII show that once activated and present at the wound site, these cells can avoid host rejection by synthesizing a robust pericellular matrix made up of HA and versican stimulated by macrophages [43]. Furthermore, it is clear now that stromal cells are highly active in the metabolic turnover (synthesis, proteolysis and clearance) of their surrounding niches.
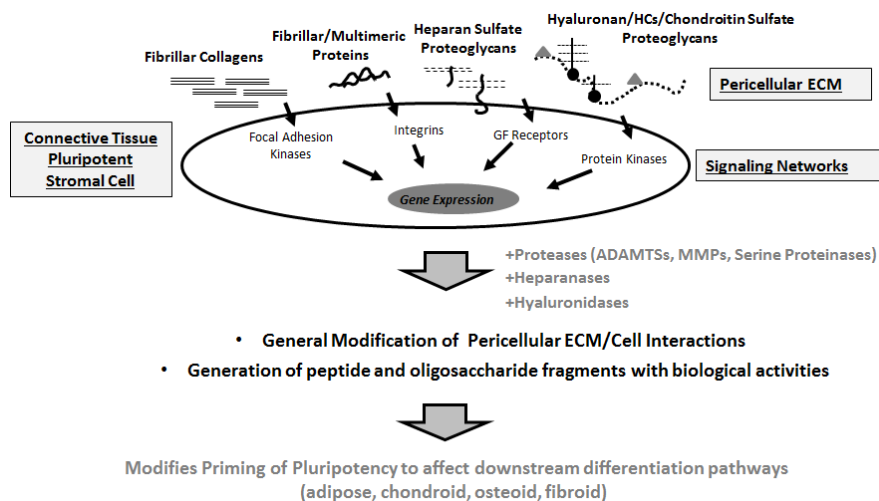
Figure 1. Schematic Diagram of Stem Cell Niche. Stems cells are surrounded by a pericellular ECM, or 'niche'; made up of collagens, proteoglycans, and growth factors. They exhibit a highly dynamic turnover of matrix proteins, generating biologically active fragments that along with growth factors signal to the cell via cell surface receptors, ultimately affecting differentiation pathways.

4. Metabolic Regulation of Stromal Cells by Extracellular O$_2$ and Glucose

Another unique feature of any stem cell 'niche' is oxygen availability. It is widely accepted that these multipotent progenitor cells reside in areas of the body with low oxygen concentrations (reviewed in [44]) and their role in wound healing requires them to function in low oxygen [45], with varying amounts of glucose and growth factors. In fact, culture conditions using hypoxic levels of oxygen (1-2%) versus room levels (~20%) have proven to be beneficial to stromal cell proliferation [46]. Studies using adipose-derived stromal cells under hypoxic conditions during cultivation [47] and expansion [46,48] report enhanced proliferation and differentiation capabilities. It has been shown that their ability to withstand hypoxic conditions may be due in part to anaerobic ATP production via glycolysis. A study using bone marrow derived stromal cells showed that as long as a sufficient glucose source is available, these cells can survive long term continuous hypoxia, without loss of proliferation or differentiation potential [49]. This idea was further solidified by a study showing that in the absence of oxygen, bone marrow derived stromal cells can survive on anaerobic ATP production, but glucose deprivation with glucose free media supplemented with 2-deoxyglucose induced rapid cell death [50]. Additionally this study suggested that glycolysis functions as a pro-survival mechanism, independent of cellular energy production, as cellular ATP levels dropped at a lower rate during glucose deprivation than they did under ischemic conditions.

5. Adipose Derived Stromal Cells express progenitor cell characteristics

Classically, the bone marrow was used as a source of pluripotent stromal cells, but as research in this area transitioned rapidly to therapeutic uses of these cells in regenerative medicine [31], the invasive procurement and relatively poor yield of cells from bone marrow aspirates has led to a search for alternative sources for these cells. To date, the most frequently used sources are umbilical cord blood and adipose tissue. Some studies even suggest that stromal cells isolated from adipose tissue display more robust multipotent differentiation capabilities than bone marrow or umbilical cord blood (reviewed in [51]). Thus, for both basic research and clinical studies, adipose-tissue provides investigators with a reliable and highly abundant source of stromal cells for in vitro use and cell based therapies in humans [52] and mice [53].

B. ROLE OF PROTEOGLYCANS AND THEIR PROTEOLYTIC TURNOVER IN THE EXTRACELLULAR MATRIX

1. Proteoglycans in ECM

The extracellular matrix produced by cells in all tissues not only provides a support structure, but plays an important role in mediating cellular communication, including proliferation, differentiation and survival. It is comprised of fibrous proteins such as collagens, fibronectins, elastins, and laminins as well as proteoglycans. Proteoglycans are a special class of macromolecules characterized by long linear chains of glycosaminoglycans (GAGs), unbranched

repeating disaccharides made up of N-acetylated or N-sulfated hexosamine and either an uronic acid (glucuronic acid or iduronic acid) or galactose; covalently attached to the protein core [54-56]. Currently, proteoglycans are divided into three main classes: small leucine-rich proteoglycans, cell surface proteoglycans and modular proteoglycans. An intensely studied subfamily of modular proteoglycans are the hyalectans, made up of aggrecan, versican, neurocan and brevican. In addition to their GAG rich central domain and C-terminal lectin interacting domain, they share the ability to bind and aggregate on hyaluronan via their N-terminal globular domain [54,57]. Neurocan and brevican are brain specific, while aggrecan and versican are more widely expressed throughout mammalian tissues.

2. Aggrecan and Versican: Large chondroitin sulfate proteoglycans with hyaluronan binding globular domains

Aggrecan is the major proteoglycan component of cartilage, where it is found as large aggregates with hyaluronan and link protein [58,59] providing cartilage with resistance to compressive forces due to its highly anionic character and space filling domain. Although it has been studied most in the setting of cartilage, aggrecan is expressed in a variety of tissues including tendons [17,60,61], skin [15], brain [62-64], and adipose [65]. It has multiple functional domains (**Fig. 2**); the amino terminal globular domain (G1) is responsible for binding hyaluronan [66]. Between G1 and G2 is a short interglobular domain, and separating G2 and G3 is a long GAG attachment domain, consisting of

chondroitin sulfate and keratan sulfate [54]. Since depletion of aggrecan from articular cartilage is an essential marker of early osteoarthritis, studies have been directed towards investigating which enzymes may play a role in aggrecan catabolism.

Versican has three major domains (**Fig. 3**); an N-terminal G1 domain for HA binding, one or both of two alternatively spliced, extended GAG attachment domains (GAGα and GAGβ) comprised of chondroitin sulfate, and a C-terminal G3 domain [67,68]. Four splice variants of versican have been characterized; V1 (formerly known as V0 in PubMed database) contains GAGα and GAGβ, V2 only GAGβ, V3 GAGα only and V4 contains neither GAG domains and lacks chondroitin sulfate [69,70]. Versican isoforms V1 and V2 are expressed by fibroblasts and vascular smooth muscle cells [71,72], whereas V3 is primarily found in the brain [73]. Functionally, versican has been implicated in many processes including neural crest cell migration [74], limb development [75-77], and cardiac formation [78]. Again, similar to aggrecan, versican was originally thought to be degraded by MMPs and certainly MMPs can degrade versican [79,80], but interest has shifted to ADAMTS proteases due to findings using transgenically altered mice [81].
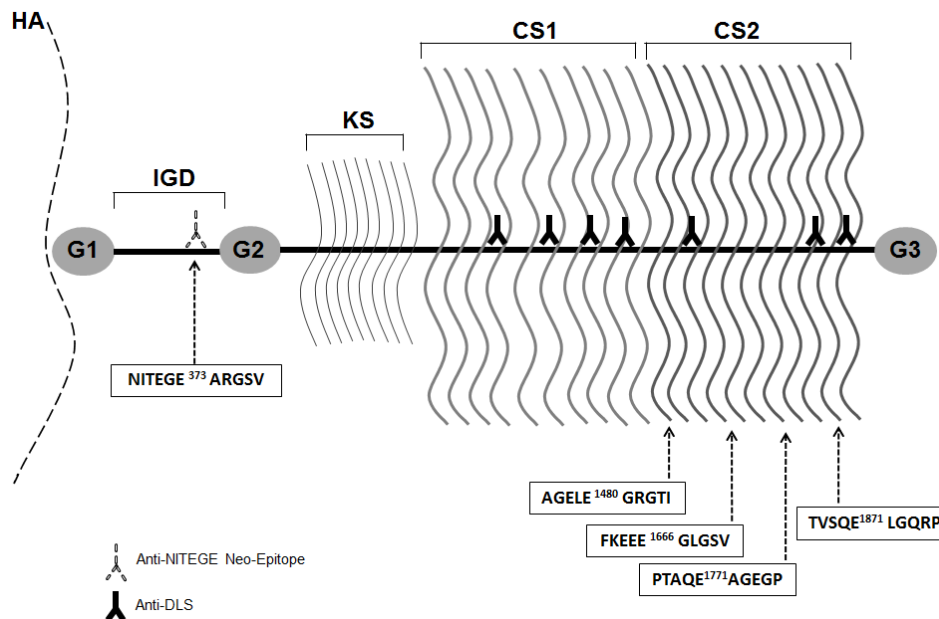
Figure 2. Schematic Diagram of Aggrecan. Aggrecan diagram, showing functional domains, ADAMTS cleavage sites (arrows) and antibody binding sites used for western analysis. Globular domains consist of G1 (HA binding), G2 and G3. IGD is inter-globular domain. KS is keratan sulfate domain, CS1, 2 are chondroitin sulfate domains 1 and 2.
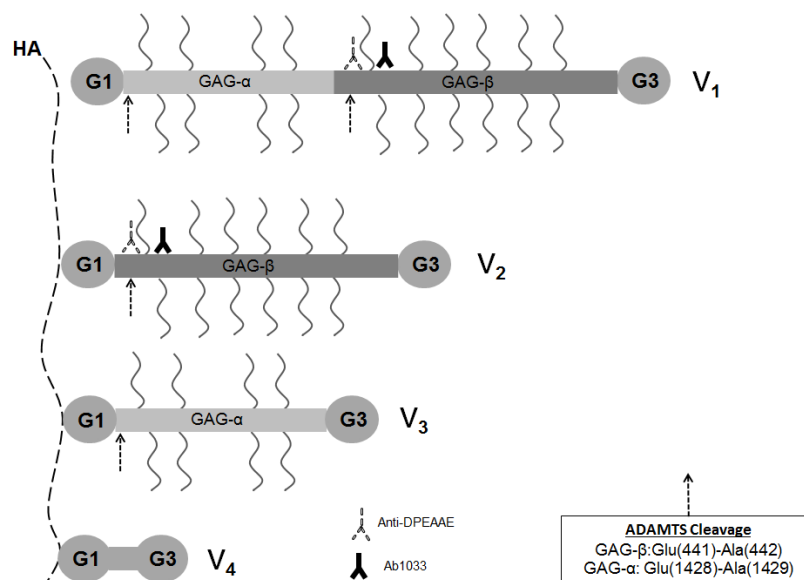
Figure 3. Schematic Diagram of Versican Isoforms. Versican diagram showing isoforms V1-4, ADAMTS cleavage sites (arrows), functional domains and antibody binding sites used for western analysis. G1 (HA binding) and G2 are globular domains, GAGα/β chains are alternatively spliced CS-bearing protein cores.

3. ADAMTS-Aggrecanases

Initially, it was thought that matrix metalloproteinases (MMPs) were responsible for the proteoglycan's destruction. But it has been shown – and is now widely accepted – that the extracellular proteolysis of aggrecan in vivo is primarily catalyzed by one or more of the ADAMTS-aggrecanase (A Disintegrin And Metalloproteinase with ThromboSpondin motifs) group of proteinases. Similarly, to function properly and maintain tissue homeostasis, aggrecan and versican have to be enzymatically degraded. As mentioned above the primary group of enzymes responsible is the ADAMTS family of proteases. ADAMTSs belong to the metzincin superfamily of metalloendopeptidases. Their discovery is relatively recent, [82] and their substrates as well as their functions are widely diverse. They share common domains, from the amino terminal; a signal peptide, a pro-domain, a catalytic domain, a disintegrin-like domain, a thrombospondin domain, a cysteine-rich and a spacer domain, and besides ADAMTS4, they contain 1 or more thrombospondin domains following the spacer domain. The prodomain is cleaved by proprotein convertases, a process that is most likely requisite for activity, and has been shown to be necessary for ADAMTS4 [83] and ADAMTS5 [84]. ADAMTS-aggrecanases include ADAMTS1, 4, 5, 8, 9 and 15. They have been shown to cleave aggrecan at five distinct sites along the core protein, one in the interglobular domain at the Glu(373)-Ala(374) bond, and four others in the CS rich domain at Glu(1480)-Gly(1481), Glu(1667)-Gly(1668), Glu(1771)-Ala(1772) and Glu(1871)-Leu(1872) bonds (bovine alignment) [85-87]. The versican V2 (formerly V1 in PubMed database) GAGβ domain has been

shown to be degraded at Glu (441)-Ala (442), and GAGα of the V1 (formerly V0

in PubMed database) isoform at Glu (1428)-Ala (1429) by ADAMTS1, 4, 5, 9 and

20 [88,89]. The GAGα of the V3 isoform can be degraded by ADAMTS4 [90].

These sites can be differentiated from ones generated by MMPs, or other

proteases by the use of neo-epitope antibodies [87,91,92]. In mice, ADAMTS5 is

thought to be the primary enzyme responsible for aggrecan degradation by

investigating its ablation [93,94]. In humans, the primary aggrecanase has yet to

be elucidated [95], it has been proposed that both ADAMTS4 and ADAMTS5 are

responsible [96]. The regulation and specificity of ADAMTS4 and ADAMTS5 on

the aggrecan substrate have been extensively investigated in vitro by using

catabolic agents such as interleukin 1 alpha and beta (IL-1α, IL-1β), retinoic acid

(RA), tumor necrosis factor-alpha (TNF-α) and oncostatin M on tissue explants

and cell cultures [91,97,98]. Treatment with these catabolic agents has shown

TS4 and TS5 to be differentially regulated. For example, some studies indicate

stimulation of TS4 with IL-1 and TNF-α, but not TS5 [97]. Others show IL-1α

together with oncostatin M (not independently) will upregulate TS4, but only IL-

1α, not oncostatin M will upregulate TS5 [98]. Conversely, studying

aggrecanolysis by inhibition of ADAMTS4 and 5 is challenging due to the high

homology of their catalytic domains, and indistinguishable cleavage fragments.

Moreover, they are both inhibited by alpha-2-macroglobulin [99], an anti-protease

readily found in serum. To differentiate these two aggrecanases and further

investigate their roles in normal physiology, research has shifted its focus to their

localization, possible secondary functions via ancillary domains, and phenotypic abnormalities caused by their genetic deletion.

4. ADAMTS5

ADAMTS5 was first cloned in 1999 [100]. Like other aggrecanases, it possesses an N-terminal prodomain, a catalytic domain, a disintegrin domain, and two thrombospondin motifs on either side of a cysteine-rich domain and a spacer domain (**Fig. 4**). The active site (HEIGHLLGLSH) binds zinc via three histidine residues, which is necessary for catalytic function, and its crystal structure, resolved in 2007, shows two calcium binding sites thought to aid structural integrity [101]. In addition to catalytic activity, ADAMTS5's ancillary domains also have key functions. In 2007, it was found that ADAMTS5 co-localizes with HA in the pericellular matrix of clonal cell clusters in articular cartilage. This interaction can be disturbed by removal of HA by streptomyces hyaluronidase, suggesting ADAMTS5 has the ability to bind HA on its own [102]. This is thought to be mediated by a double HA- binding motif seen only in ADAMTS5 within the disintegrin domain located between the catalytic site and the first thrombospondin [102,103]. Previous analyses of the fate of the aggrecan products has indicated that the N-terminal globular domain (G1-NITEGE) remains bound to HA and that the HA itself can be immobilized by interaction with CD44. In support of this was the finding that the aberrant dermal repair in the ADAMTS5 KO mouse was corrected in the ADAMTS5/CD44 double knockout, apparently due to the inability to accumulate dermal aggrecan [15]. In

addition, studies with isolated chondrocytes [104] have indicated that the HA-bound G1-NITEGE product can be endocytosed in a CD44-dependent process. Recently, ADAMTS5's activity has been shown to be regulated by lipoprotein receptor related protein-1 (LRP-1) via interaction with the first thrombospondin and spacer regions. It is thought that subsequent endocytosis removes it from the extracellular space, thereby reducing proteoglycan catabolism [105].

In the context of the current study, both ADAMTS5 protein and the G1-NITEGE fragment of aggrecan have been identified in differentiating murine adipose [65], consistent with a role for these proteins in extracellular matrix (ECM) structure of adipose stromal cells. Additionally adipose contains other ECM macromolecules such as collagen types I [65], III [106], IV [107], V [108] and VI [109], thrombospondin-1 [110] laminin and fibronectin [106], all consistent with a supportive 'niche' within adipose tissue.
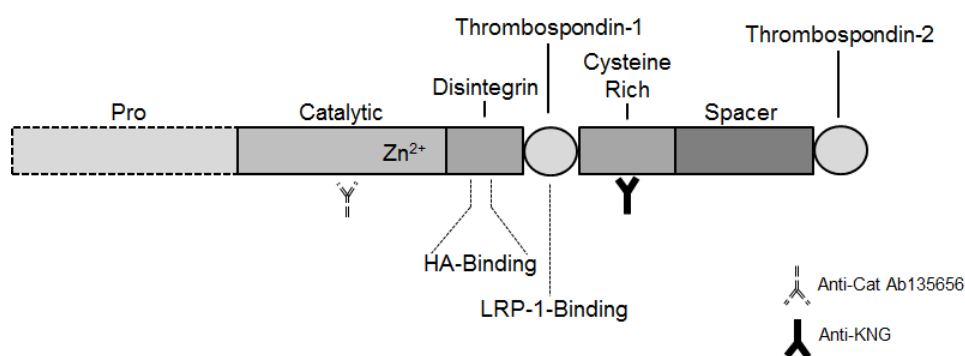
Figure 4. Schematic Diagram of ADAMTS5. ADAMS5 diagram showing functional domains and antibody binding sites used for western analysis.

5. ADAMTS5 Knock Out Mouse Strains

Four mouse strains with exon 2 or exon 3 deletions (encoding the active site) have been generated to date, and they are summarized in **Table 1**. It should be noted that the first suggested primary function of the ADAMTS5 was degradation of cartilage matrix aggrecan, and this was corroborated by reports that Adamts5 KO mice (ΔExon 3, generated by Lexicon Inc. with Wyeth Inc.) were protected against cartilage degradation in the DMM model of osteoarthritis [93], and another knockout strain (ΔExon 3, generated by Lexicon Inc. with Johnson and Johnson Inc.) was similarly protected against cartilage loss in antigen-induced inflammatory arthritis [94]. However, subsequent in vitro experiments using epiphyseal cartilage explants from these knockout strains showed that aggrecanolysis could proceed even in the absence of ADAMTS5 [94,111]. Yet another strain of Adamts5 KO mice (ΔExon 2 generated by Deltagen Inc. with Jackson Labs), referred to here as 'TS5J KO', exhibit heart valve anomalies, and this is associated with changes in local versican turnover [112], though effects on aggrecanolysis were not examined in this study. In our laboratory, we have found that when knee joints of wild type or yet another line of Adamts5 KO mice (ΔExon2, generated by Lexicon Inc. with Pfizer Inc., see [113]), referred to here as 'TS5P KO' were challenged with high doses of intra-articular TGFb1 and mechanical overuse, knockout mice showed enhanced articular cartilage deposition despite ongoing cartilage aggrecanolysis. Most notably, when compared to wild types, the knockout mice showed diminished fibrosis in the joint capsule, the synovium and the menisci [114]. This strain of

mice has shown a generalized impairment of wound healing in skin and tendons [15,61], has enhanced susceptibility and lack of resistance in dextran-sulfate induced inflammatory bowel syndrome (De la Motte, Plaas et al, unpublished) and accelerated callus formation in fracture healing (Coleman, Li, Plaas, unpublished). In general, cell groups surrounded by an HA, versican and aggrecan-rich ECM accumulate at the injury sites, which is accompanied by a deficiency in collagen-rich scar tissue deposition [17]. Further, newborn fibroblasts from this knock-out strain show a diminished capacity for SMAD2/3 phosphorylation with compensatory SMAD1/5/8 phosphorylation following TGFb1 stimulation [15]. Based on these findings our lab proposed a general hypothesis that ADAMTS5 has a nodal role in the regulation of TGFb1-mediated responses in stromal progenitor cells during tissue regeneration, and is needed for post-natal scaring.

Source (Investigators)	Deletion	Frame	Mutant mRNA	Mutant Protein Translation	Major Findings (PMID)
Lexicon/Wyeth (Glasson)	Exon 3	In	Yes	Undetermined	Protected against cartilage degradation in the DMM model of osteoarthritis (Glasson SS et al. 2005)
Lexicon/Johnson & Johnson (Fosang)	Exon 3	In	Yes	Undetermined	Protected in antigen-induced inflammatory arthritis (Stanton H et al. 2005)
Deltagen/Jackson (Apte, McCullough)	Exon 2	Out	Not detected	Undetermined	Lack of Versican cleavage causing heart valve deformation (Dupuis LE et al. 2011)
Lexicon/Pfizer (Malfait, Plaas, Wang)	Exon 2	In	Yes	Undetermined	Diminished fibrosis and enhanced articular cartilage deposition in joint injury (Li J et al. 2011) Impaired wound healing of skin and tendons (Velasco J et al. 2011, Bell R et al. 2013)

Table 1. ADAMTS5-Deficient Mouse Lines. Current list of ADAMTS5 deficient mouse lines, detailing location and type of deletion, resultant mRNA transcription and mutant protein translation along with major findings reported.

6. ADAMTS5 and TGFb1 signaling in wound healing and fibrosis

The TGFb superfamily of growth factors controls a variety of cellular responses including migration, proliferation, inflammation, matrix production and degradation. They regulate gene expression mainly through SMADs and/or mitogen-activated protein kinases (MAPKs) and are widely studied in the field of wound healing, tissue fibrosis, and extracellular matrix regulation, where they have been linked to the expression of Col1a1, Col3a1 and Col5a2. In the same framework, TGFb1 overexpression is known to cause tissue fibrosis, by an over-accumulation of fibrillar collagens [115]. Canonically, SMAD 2/3 signaling results in a fibrogenic cellular response while signaling through SMAD 1/5/8 results in a chondrogenic cellular response. The balance of these pathways is governed by the relative phosphorylation of either ALK1, directing signaling through SMAD 1/5/8 or ALK5, directing signaling down the SMAD 2/3 pathway [116]. Factors that control signaling through ALK1 or ALK5 are unclear, although certain surface receptors are known to interact with these molecules and could possibly regulate their fate.

7. Collagen synthesis and processing

Type I collagen, the most abundant protein of the body, is synthesized mainly by the osteoblast and the fibroblast in bone, skin, and tendons. The expression of type I collagen in the form of fibrosis such as lung and liver is thought to be driven by TGFb1. Type I collagen is a heterotrimeric molecule consisting of two alpha 1(I) chains and one alpha 2(I) chain. Its synthesis (**Fig. 5**)

begins inside the endoplasmic reticulum. Shortly after translation, procollagen

chains undergo proline and lysine hydroxylation by lysyl hydroxylases, a process

critical for triple helical formation. Next, procollagen triple helices are secreted

into the extracellular space, where their procollagen peptides (N and C terminal)

are removed by proteases, in a process that yields must less soluble

tropocollagen, which is then able to participate in higher order fibril assembly.

Removal of C-terminal pro-peptides of fibrillar pro-collagens are carried out by a

procollagen C-proteinase (PCP) [117] namely bone morphogenetic protein -1

(BMP-1). N-terminal propeptides are removed by ADAMTS members 2, 3 and 14

[118]. Lastly, fibrillar collagen must be cross linked by lysyl oxidase, to achieve

physiological functionality [119]. Studies using growth factors show that

regulation of collagen type I synthesis and deposition are controlled in an

extracellular manner. [120] showed that TGFb1 stimulation had minimal effect on

mRNA production, but exhibited a large increase in polypeptide synthesis and

cell layer deposition of collagen type I in osteoblast cultures. This is supported by

work done in gingival fibroblasts [121], showing that TGFb1 directly increases

lysyl oxidase levels via connective tissue growth factor. Interestingly, lysyl

oxidase activation by cleavage of its propeptide is catalyzed by BMP-1 as well.

These suggest that TGFb1 affects extracellular enzymatic events that regulate

the ultimate deposition of collagen type I rather than simply up regulating gene

transcription of the procollagens.

Transcription/Translation

Pro-collagen alpha chains

Disulfide Bond Formation
(Noiva R et al. 1992)

Intracellular

Endosomal/Lysosomal
Degradation
(Kim SI et al. 2012, Lee H et al. 2006)

N - and C-terminal Pro-peptidases

Intracellular/
Extracellular

ADAMTS 2,3,14
(Colige A et al. 2002)

BMP1
(Kessler E et al. 1978)

Extracellular

Collagen Monomer
Alignment and Fibril
Formation (Mould AP et al. 1990, Prockop DJ et al. 2005)

Figure 5. Schematic Diagram for Collagen Type I Production, Processing and Degradation via Endosomal Pathway. Collagen type I is a heterotrimer molecule consisting of two alpha 1(I) chains and one alpha 2(I) chain. After translation procollagen chains nucleate then undergo proline and lysine hydroxylation by lysyl hydroxylases, afterwards procollagen triple helices are secreted and their procollagen peptides (N and C terminal) are removed by proteases. C-terminal propeptides are cleaved by procollagen C-proteinases PCP's namely (BMP-1). N-terminal propeptides are removed by ADAMTS members 2, 3 and 14. Collagen is then cross linked by lysyl oxidase. Its degradation is achieved by an endocytotic/phagocytotic pathway, primarily by fibroblasts, where MT1-MMP functions to fragment collagen fibers before internalization and subsequent degradation via the lysosomal pathway.

8. Regulation of Collagen Turnover

Collagen degradation is a necessary step in many processes of growth and development, especially in tissue remodeling during wound healing. This is thought to be achieved by an endocytotic/phagocytotic pathway, primarily by fibroblasts [122,123], where MT1-MMP functions to fragment collagen fibers before internalization and subsequent degradation via the lysosomal pathway [124,125]. More recently, intracellular collagen degradation has been linked to

autophagy, [126], whereby investigators observed profibrotic effects (increased collagen deposition) by inhibiting autophagy with bafilomycin A1 and beclin-1 ablation. Moreover, they observed induction of both autophagy and collagen synthesis by TGFb1, further implicating this growth factor's role in multiple mechanisms relating to collagen biosynthesis, processing and degradation.

C. ENDOCYTOSIS IN REGULATION OF CELL FUNCTION

Endocyotsis is a specialized mechanism whereby cells produce membranes made up of the phospholipid bilayer to internalize cell surface ECM proteins and fluid. The reverse of the process is known as exocytosis. These processes allow specific communication between the cell and the extracellular space, for example a main focus in this area of research has been the internalization and trafficking of transmembrane receptors and the subsequent effect on their signaling cascade [127]. Of particular relevance to this study is clathrin mediated endocytosis, a process by which clathrin nucleates at the plasma membrane to induce a curved deformation near particles to be internalized. Dynamin, a GTPase, constricts the vesicle and upon hydrolysis releases it into the cell [128,129]. Afterwards, the endosome can be trafficked to the lysosome for degradation, or recycled to the cell surface [130]. Additionally, clathrin mediated endocytosis, in conjunction with lipoprotein receptor related protein-1 (LRP-1), has been well established in the turnover of ECM

macromolecules and their proteases [131], allowing cells to coordinate the availability of ECM proteases on the cell surface.

1. Endocytosis and TGFb Signaling

While early work on TGFb signaling detailed a linear mechanism of ligand binding, receptor phosphorylation and subsequent signal propagation to gene expression, it is now understood that TGFb signaling is much more complex than originally thought. TGFb receptor internalization and trafficking play important roles in deciding the cellular response to TGFb [132]. TGFb receptor endocytosis via a clathrin-dependent pathway is thought to propagate SMAD2 signaling via SARA (Smad anchor for receptor activation) in the early endosome [133-135]. These receptors can then be returned to the cell surface for another round of recycling via Rab11 [136]. Conversely, receptors internalized in a membrane raft-dependent pathway involving caveloin-1 are targeted for degradation [134,137].

2. Endocytosis and Protease Regulation

MT1-MMP is the main membrane tethered matrix metalloproteinase responsible for proteolysis of pericellular ECM proteins (mainly collagen type I) and cell surface receptors [138] such as LRP-1 [139]. It is unique when compared to MMPs in that it is not secreted extracellularly as a soluble zymogen. Instead it is directed to the cell surface via a secretory pathway and is activated by furin and/or proprotein convertases in the trans-golgi network on its route to the cell surface [140,141]. It has been discovered that its activation is not furin

dependent, but it can be autocatalytically activated [142,143]. Furthermore, it has been shown that O-glycosylation of MT1-MMP regulates autocatalytic efficiency during the secretory pathway, as well its reuptake [144]. As mentioned above, ADAMTS5 is regulated by LRP-1 in a similar manner [105] suggesting that it has a unique role on the cell surface turning over a special pericellular pool of proteoglycans and/or modulates their endocytosis.

3. Endocytotic Pathways in Stromal Cells

Multiple studies provide evidence that stromal cells have an active endosomal pathway. Human bone marrow stromal cells were shown to aggregate fluorescent-labeled particles at the cell surface, then subsequently internalize them in compartments resembling endosomes [145]. Separately, rapid recycling of homing factor CXCR4 was demonstrated in fetal bovine bone marrow stromal cells where CXCR4 was found in early endosomes, recycling endosomes, and lysosomes. Upon treatment with dynasore, an endosomal recycling inhibitor, CXCR4 was increased 5 fold on the cell surface [146]. Additionally endocytosis was shown to be inducible by stimulation with highly sulfated hyaluronan [147]. Furthermore, one study successfully delivered microRNAs to bone marrow derived stromal cells via exosomes to downregulate TGFb Receptor II expression, through clathrin mediated endocytosis and macropinocytosis [148].

4. Endocytosis and Energy Metabolism

Cellular glucose uptake from the blood stream is achieved through a family of cell membrane transporter proteins known as GLUTs. GLUT1 is the most widely expressed transporter across cell types and displays long life span at the cell membrane, whereas GLUT4 is regulated in response to glucose availability, and is expressed specifically in muscle and fat cells [149]. Both GLUT1 and GLUT4, and in turn glucose uptake are controlled by transporter availability at the cell surface, a process highly regulated by internalization and endosomal recycling [150,151] in a clathrin dependent and clathrin independent manner [152,153]. Interestingly, GLUT4 has a highly dynamic recycling process. During low blood glucose levels it is kept intracellularly in a specialized cell compartment [154,155], until insulin (released upon feeding) stimulates the recycling of GLUT4 to the cell surface to transport glucose inside [156]. Since stromal progenitor cells under hypoxia need to have an efficiently controlled glucose uptake mechanism, GLUT expression and cell surface availability are very important to survival and differentiation. In fact, a study using human umbilical cord stromal cells, showed this sensitivity. Authors demonstrated that GLUT1 expression, glucose specific consumption and lactate production were all elevated in hypoxic conditions, a response thought to be mediated via hypoxia-inducing factor-alpha (HIF-1α) [157].

D. PURPOSE STATEMENT

Based on the multi-tissue chondrogenic wound-healing response in ADAMTS5 KO mice (Pfizer), our lab proposed a general hypothesis that ADAMTS5 has a nodal role in the regulation of TGFb1-mediated responses in stromal progenitor cells during tissue regeneration, and is needed for post-natal scaring. Using adipose derived stromal cells (ADSCs) from wild type and two strains of ADAMTS5 KO mice, we aim to delineate ADAMTS5's role in aggrecanolysis and versicanolysis, as well as characterize the ECM 'niche' surrounding these stromal cells, while investigating if ADAMTS5 plays a role in its regulation. This is to better understand the broader cell biological role for this protein in signal transduction as it relates to the regulation of extracellular matrix.

II. HYPOTHESES AND SPECIFIC AIMS

Hypothesis 1: ADAMTS5 is required for the degradation of the glyco-ECM niche in stromal cells, to allow pro-fibrogenic signaling by TGFb1 and maturation of fibroblasts for robust scar formation and matrix contraction.

Specific Aim 1.1: Develop methods for preparation of monolayer cultures of murine adipose derived stromal cells and perform characterization of Adamts5 gene structure, mRNA and protein abundance in cultures from wild type and two Adamts5-deficient mouse strains.

Specific Aim 1.2: Characterize the pericellular glyco-matrix synthesized in monolayer cultures of ADSCs prepared from wild type and Adamts5 KO mice. Production of aggrecan, versican and hyaluronan were determined using a combination of QPCR, western blotting, Fluorophore assisted carbohydrate electrophoresis and immunohistochemistry.

Specific Aim 1.3: Examine the relationship between glucose utilization and glycomatrix synthesis in WT and ADAMTS5 KO ADSCs. Glucose concentrations in cell conditioned media were determined by coupled enzymatic assay using AmplexRed® reagent, and proteoglycan abundance were determined by western blotting.

Specific Aim 1.4: Examine aggrecan and versican degradation in WT and ADAMTS5 KO ADSCs following serum depletion, to induce pro-catabolic pathways. Western blot analyses of versican and aggrecan degradation products

were performed using a panel of antibodies to intact core proteins and cleavage-specific neo-epitopes generated by ADAMTS-aggrecanases.

Hypothesis 2: The "profibrogenic activity of ADAMTS5" in TGFb stimulated ADSCs is due to its effect on modulation of endocytotic pathways associated with endosomal and lysosomal trafficking. Such a function is independent of its catalytic activity and may serve to 'prime' stromal cells in a wound environment to commit to a fibrogenic, rather than a chondrogenic, adipogenic, or osteogenic response.

Specific Aim 2.1: Characterize TGFb1 responsiveness of stromal cell cultures from wild type and Adamts5 KO mice. TGFb signal transduction was monitored by QPCR assays for col1 (a1, a2), col3a and Has1 & 2 in the presence and absence of; TGFb-RI/II Kinase inhibitor, LY109761 (Selleckchem). Collagen type I synthesis, processing and secretion were assayed by western blot analyses of medium and cell extracts.

Specific Aim 2.2: Examine if the TGFb1 stimulation of WT ADSCs is altered by inhibition of ADAMTS5 catalytic activity with Batimastat, a broad spectrum MMP inhibitor and a specific ADAMTS5 inhibitor (Calbiochem).

Specific Aim 2.3: Determine the effects of endosomal and lysosomal trafficking using inhibitors, Bafilomycin A and Dynasore, on the production and half-life of the cell-associated ADAMTS5 protein species.

III. MATERIALS AND METHODS

Specialized Chemicals

These include Human recombinant bFGF (R&D Systems); Human recombinant TGFb1 (Peprotech); TGFb-RI/II Kinase inhibitor, LY109761 (Selleckchem); Bafilomycin A1 (Tocris Bioscience); BMP-7 (ProSpec); Dynasore (Sigma) ADAMTS5 specific inhibitor (CAS 929634-33-3, Calbiochem); Batimastat - MMP broad spectrum inhibitor (CAS 130370-60-4, Calbiochem); Human recombinant BMP1 (R&D Systems); Complete-Mini Protease Inhibitor Tabs (Roche)-1 tab/10mL is 1x. All other chemicals used were of the highest grade purity available.

Cell Culture Supplies

Culture Flasks (Corning); 60mm dishes (Corning); 12-well Plates (Corning); 8 well glass chamber slides (Nunc™ Lab-Tek™ II); Advanced MEM (Gibco) formulation includes ascorbic acid phosphate, transferrin, insulin, AlbuMAX® II and sodium pyruvate for enhanced ECM production and viability in low serum; DMEM no glucose (Gibco) supplemented with 1g/L D-Glucose (Sigma); CO_2-independent medium (Gibco); Fetal Bovine Serum (Atlanta Biologics); Plasmocin (Invivogen); Pen/Strep (Gibco); Glutamine (Gibco); Trypsin (Gibco).

Molecular Biology Reagents

RNeasy (Qiagen); First Strand cDNA (Invitrogen); iScript kit (Bio-Rad); Trizol (Ambion) Amplex® Red Glucose Assay (Molecular Probes via LifeTech Inc).

Mouse strains

The ADAMTS5 KO (Pfizer) 'TS5P KO', strain was obtained under an MTA with Pfizer Inc. ADAMTS5 KO (Jackson) 'TS5J KO'; strains were supplied by Di Chen, Ph.D., Rush University Medical Center. Both strains were backcrossed into wild type C57/Bl6 colony used for this study, for at least 4 generations (see also **Table 1**) All experiments were performed in accordance with the Rush University Medical Center's Institutional Animal Care and Use Committee under protocol # 11-025 and # 14-026.

Antibodies

Anti-DLS was generated with the peptide immunogen SGVEDLS and it has been shown to detect full-length aggrecan and aggrecan fragments containing one or more copies of this sequence in the CS-attachment region [158]. The ADAMTS-generated G1 product of aggrecan was detected with Anti-NITEGE [15]. ADAMTS-generated fragments from CS region truncation at Glu (1480)-Gly (1481) and Glu (1667)-Gly (1668) were detected with a mixture of Anti-TASELE/Anti-TFKEEE [159,160], calpain generated aggrecan fragments

were detected with Anti-GVA [161]. Versican was detected with Ab1033 (EMD Millipore), which reacts with intact versican V1(NP_001074718.1, formerly V0) and V2 (NP_062262.2, formerly V1) as well as truncated forms of the core protein, containing some or all of residues 1360 to 1439 of versican V1 or the same residues (400-479) of versican V2. The ADAMTS-generated G1 product of versican V2 (known as G1-DPEAAE[441]) was detected with anti-DPE [161]. This product has been found to migrate as a single ~70 kDa species when extracted from human aorta [161] , human skin [162] or cultured granulosa cells [163,164]. ADAMTS5 was detected with Ab135656 from AbCam (raised against residues 338-368 of the human catalytic domain), anti-KNG (raised against residues 636-648 of the human cysteine rich domain) [102]. Collagen type I was detected by Anti-Type I Collagen (SouthernBiotech) [165]. Lane loading was checked by probing with antibody C4 to B-Actin (SantaCruz).

Genotyping of WT, TS5P KO and TS5J KO mouse strains

All mice used were 12 week male C57Bl/6. The TS5P KO (Pfizer) and TS5J KO (Jackson) strains were back-crossed into C57Bl/6 for at least six generations before use. Genomic DNA isolated from ADSCs of the three strains was analyzed as follows. Cell layers digested with 1 mg/mL proteinase K (Invitrogen) in 50 mM TrisHCl, 50 mM EDTA, 100 mM NaCl, and 1% SDS, incubated at 55 °C overnight. DNA was isolated by phenol/chloroform extraction and ethanol precipitation (Thermo Scientific). PCR was done using the following primers 'P' for Pfizer deletion: Forward 5'–

TTTGAATTTGTCTTTGGAAGGCCTC-3', Reverse 5'-

GACAGTGTTGACTCATCCGGGGATA-3' and 'J' for Jackson/Deltagen deletion:

forward 5'-GCATACCACTCCAAACTTAGAGAGG-3', mutant neo 5'-

GGGCCAGCTCATTCCTCCCACTCAT-3' and reverse 5'-

CGCAGCTGACTGCTCTTGTGCTTG-3'.

ADAMTS5 mRNA characterization

RNA was isolated from ADSCs of the three strains, and mRNA was

purified with an RNeasy kit (Qiagen), and cDNA was prepared with an iScript kit

(Bio-Rad). PCR was done using the following primers. Primer set 'I'; 5'-

GAGCACTACGATGCAGCCAT-3', and 5'-CACAGACATCCATGCCAGGG-3'.

Primer set 'II'; 5'-TGTTCACCCGAGAGGGCATC-3' and, 5'-

TGTCAAGTTGCACTGCTGGG-3'. Primer set 'III' 5'-

AGCAAGCATCCAGCTAGACTCA-3' and 5'-

TTTGTGCATTAGAGTAAACCACAGG-3'. Amplified PCR fragments were

purified on QIAquick PCR purification columns (Qiagen) and cloned into pDrive

plasmid vector (Qiagen). Five recombinant clones from each genotype were

sequenced and compared to each other using ClustalW2 alignment (EMBL-EBI).

Isolation and culture of murine adipose derived stromal cells

ADSCs were prepared essentially as described [166]. Adipose tissue was

combined from the abdominal and groin areas of five 10-12 wk male mice and

digested with agitation in 3 mg/ml collagenase type II (Worthington) for 2 h at 37

°C in CO_2-independent medium (Gibco). The digest was centrifuged at 300g for 10 min, the adipocyte/lipid layer discarded, the pellet re-suspended in 50 mL PBS, transferred to a fresh tube and centrifuged. Red blood cells in the pellet were lysed in 1.5 mL lysis buffer (eBioscience, 00-4300-54), remaining cells washed once with 45 mL PBS and re-centrifuged at 300g. The pellet was suspended in 40 mL DMEM/ 1 g/L glucose/10% FBS containing 2 ng/mL bFGF and plated in a T175 flask. After 24 h, non-adherent cells were removed and fresh medium was added. Medium changes were performed every 48-72 h. Cells were expanded at ~90% confluency by trypsinization (1:3 split) and plated at ~ 0.7 x 10^6 cells per T25 flask, cell morphology at each passage is shown in (**Fig. 6**).
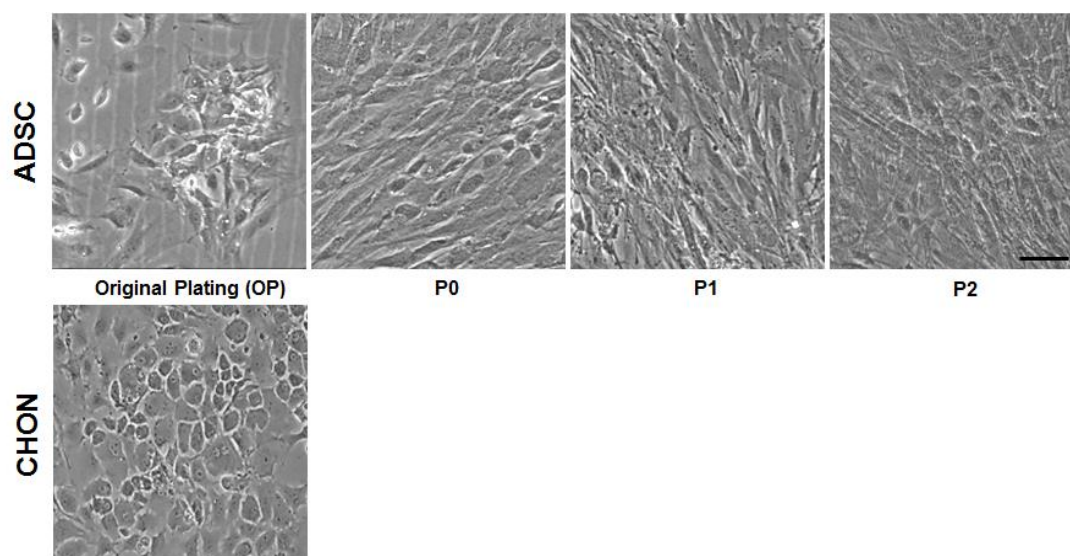
Figure 6. Phase contrast images of Adipose Derived Stromal Cell (ADSC) and Chondrocyte (CHON) cultures. Top row, phase contrast images of ADSCs in successive passages, OP to P2, cells exhibit an elongated fibroblasts-like morphology. Original plating (OP) are adherent cells directly after adipose tissue digestion. Cells were expanded at ~90% confluency by trypsinization (1:3 split), experiments were carried out on passage 2 cells (P2). Bottom left, confluent chondrocytes at original plating. 10x magnification, scale bar =30μm.

Isolation and culture of murine epiphyseal chondrocytes

Chondrocytes were from the cartilage at the epiphyseal ends of the tibia and femur of 7-10 day-old mice of mixed gender. Briefly, cartilage was washed in cold PBS, and to remove adherent soft tissue it was digested for 1 h at 37 °C in DMEM 1 g/L glucose, 3 mg/ml collagenase (Worthington, Type II). Cartilage was transferred to fresh DMEM 1 g/L glucose, 0.5 mg/ml collagenase and digested for 18 h at 37 °C. The undigested tissue was removed by filtration through a 70 µm cell strainer (BD Biosciences), cells were then pelleted at 300g, washed twice with 40 mL PBS, suspended in Advanced MEM (Gibco), 10% FBS, 2 mM glutamine (Gibco), 100 units/ml penicillin (Gibco), 100 µg streptomycin (Gibco) and plated at 71,000 cells/cm^2 in 60 mm dishes (Corning). Cells were grown to ~90% confluence (4 days) with daily medium changes. (**Fig. 6**)

QPCR analyses of stem cell surface marker gene expression

Gene expression for mesenchymal stem cell surface markers was done using Taqman probes (Life Technologies). Primer details are listed in **Table 2,** and they were targeted to exon 1-2 boundary for CD73 (5' nucleotidase), to exon 2-3 boundary for CD90 (thymus cell antigen 1), and to exon boundary 8-9 for CD105 (endoglin). QPCR reactions were performed as follows.

Gene	Life Technologies Cat. #
Acan	Mm00545794_m1
Adamts1	Mm00477355_m1
Adamts4	Mm00556068_m1
Adamts5	Mm01344180_m1
Adamts8	Mm00479220_m1
Adamts9	Mm00614433_m1
Adamts15	Mm01176187_m1
CD44	Mm01277163_m1
Col1a1	Mm00801666_g1
Col1a2	Mm00483888_m1
Col2a1	Mm01309565_m1
Col3a1	Mm00802331_m1
Eng (CD105)	Mm00468256_m1
GAPDH	Mm99999915_g1
Hapln1 (Link Protein 1)	Mm00488952_m1
Hapln3 (Link Protein 3)	Mm00724203_m1
HAS 1	Mm00468496_m1
HAS 2	Mm00515089_m1
HAS 3	Mm00515092_m1
Integrin alpha M (Mac-1)	Mm00434455_m1
Nt5e (CD73)	Mm00501910_m1
Thy1 (CD90)	Mm00493682_g1
Vcan V1	Forward 5'-CAACCTCCAAAACTCAAGAGTTGT- 3'
	Reverse 5'-CATTTATGTCAGGGTGGAACTTGGT-3'
	Reporter 5'-CTGCAGGTGTTGAAGTAG-3'
Vcan V2	Mm00490173_m1

Table 2. List of Applied Biosystems Taqman Probes used for QPCR. All primer/probe sets are inventoried in Life Technologies Inc. database. With exception to Vcan V1 (custom designed).

Experimental design for analysis of glycomatrix production

ADSCs and chondrocytes for analysis were grown to about 90% confluence in T-25 flasks and 60 mm dishes, respectively. The medium for ADSC cultures was changed into 3 ml DMEM:Advanced MEM, (3:1) containing 10% FBS and for chondrocyte cultures into 3 ml Advanced MEM/10% FBS respectively. After 24 h, cultures were terminated for T0 points for FACE, QPCR and Western blotting analyses (**Fig. 7**). To examine aggrecan and versican turnover in the two cell types, T0 cultures were changed into 3 ml DMEM/Advanced MEM (3:1) containing 1% FBS (ADSCs) or 3 ml Advanced MEM/1% FBS (Chondrocytes) and terminated at 2 and 6 hours for proteoglycan purification as described below (**Fig. 8**).
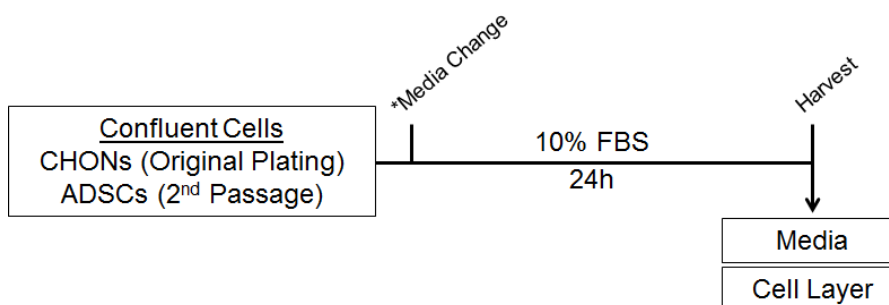
Figure 7. Experimental Scheme for Analysis of Glycomatrix Production. ADSCs and chondrocytes were grown to 90% confluence in T-25 flasks and 60 mm dishes, respectively. ADSC cultures was changed into 3 ml DMEM:Advanced MEM, (3:1) containing 10% FBS and chondrocyte cultures into 3 ml Advanced MEM/10% FBS. Incubated for 24 h then harvested for FACE, Immunohistochemistry and Western analysis.
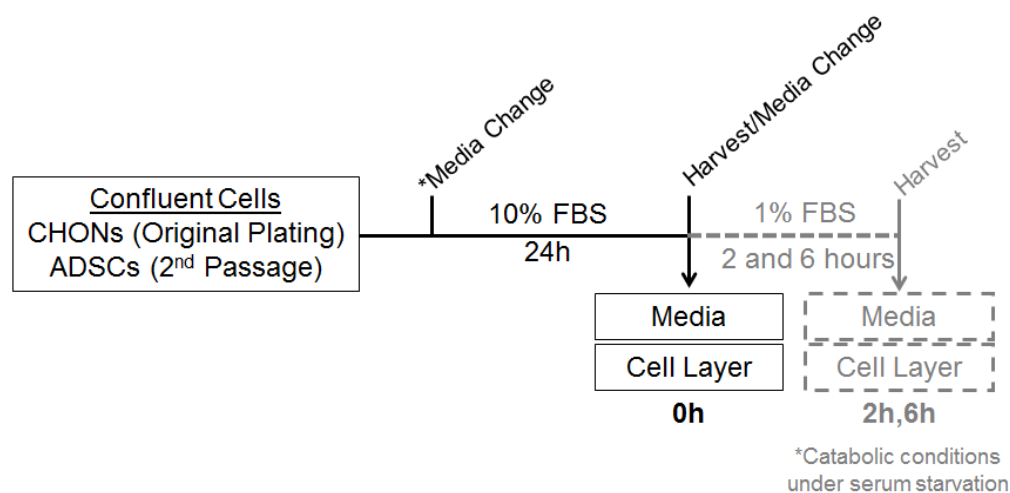
Figure 8. Experimental Scheme for Analysis of ADAMTS-mediated Aggrecan and Versican Cleavage. To examine aggrecanase mediated turnover of proteoglycans, 0 h cultures were changed into 3 ml DMEM/Advanced MEM (3:1) containing 1% FBS (ADSCs) or 3 ml Advanced MEM/1% FBS (Chondrocytes) and terminated at 2 and 6 hours for analysis.

Preparation of proteoglycans synthesized and secreted ADSCs and Chondrocytes for Western Blot Analyses

Cultures were terminated at 0, 2 and 6 h time points by placement on ice. Media were removed and adjusted to 6 M urea and 1x protease inhibitors (PIs). 10 x protease inhibitor solution is 150 mM benzamidine, 50mM ethylenediaminetetraacetic acid (EDTA), 1 mM 4- benzenesulfonyl fluoride hydrochloride, 50 mM iodoacetimide, 5 μg/mL pepstatin and 10 μg/mL leupeptin in ddH$_2$0, all supplied by Sigma. Cell layers were pretreated with 300 μL of 10x PI solution for 3 min and then dissolved in 3 mL 7 M urea, 50 mM TrisAcetate, pH 8.0. Cell extracts were transferred to 15 mL centrifuge tube and insoluble material removed by centrifugation, (14,000g for 5 min). Media and cell extracts were stored at -20 C until further analyses. To purify proteoglycan components,

media and extracts were fractionated by ion exchange chromatography. Columns consist of 1.2 mL of a 1:1 mixture of pre-swollen diethylaminoethyl cellulose (DE52 Whatman) and ddH20. Samples were poured over column, and bound fractions were washed 5x with 5 mL 7 M urea, 50 mM TrisAcetate, pH 8.0, then recovered with 2 mL of the buffer, containing 1.5 M sodium chloride. Eluates were dialyzed against multiple changes of deionized water for 8 hours, dried by Speedvac and digested with chondroitinase ABC (Seikagaku) before Western analysis [15]. In some cases they were also digested with N-glycanase (Prozyme) as described in [167]. Each lane was loaded with medium or cell extracts from one T25 flask, approximately 2.8 x 10^6 cells for ADSCs and ½ 60 mm dish approximately 1.6 x 10^6 cells for chondrocytes. In previous experiments using new born fibroblasts [15] and in a preliminary study done with chondrocytes and ADSCs, it was found that >90% of the immunoreactive proteoglycan species, including the G1-bearing catabolic products were recovered in the DE52-bound fraction.

Western Blot Analysis of Aggrecan, Versican and ADAMTS-generated digestion fragments

After chondroitinase ABC digestion, samples were Speedvac evaporated, brought up in 30 µL sample buffer and boiled at 100 °C for 5 min. Samples were electrophoresed on 4-12% Tris-Glycine gels (Novex) for 2.5 h at 100V at 4C in running buffer comprised of 50 mM Tris, 0.4M glycine, 0.2% SDS, pH 8.0. Proteins were transferred to 0.2 µM nitrocellulose (BioRad) for 2.5 h at 25V at

room temperature in transfer buffer comprised of 25 mM Tris, 192 mM glycine and 20% methanol v/v. Membranes were blocked with 10 mL 5% nonfat milk in 1x TBST, Tris Buffered Saline (BioRad)/0.1% Tween-20 (Fisher), for 1 h at room temperature with gentle rocking. Primary antibody incubation was in 5% milk TBST, overnight at 4 °C with gentle rocking. Using α-DLS for aggrecan core at 1 µg/mL, α-NITEGE for aggrecanase generated aggrecan-G1 product at 1 µg/mL, α-TASELE/TFKEEE for CS region aggrecanase cleavage at 1 µg/mL, α-GVA for calpain generated aggrecan cleavage at 1 µg/mL, Ab1033 (AbCam) for versican core at 1:1000, and α-DPEAAAE for the aggrecanase generated versican-G1 product at 1 µg/mL. Membranes were washed 3x with 15 mL TBST by gentle rocking at room temperature for 15 min/wash. Secondary antibody (goat anti-rabbit HRP) AP307P (Millipore) was incubated in 5 % milk/TBST at 1:4000, at room temperature for 1 h, then washed the 3x again. Membranes were then incubated with Immobilon Western Chemiluminescent HRP Substrate (Millipore) for 10 min at room temperature with gentle rocking, covered in polyvinyl chloride wrap and exposed to autoradiography film (Denville Scientific) for times ranging from 1 sec to 30 min.

Western Blot Analysis of ADAMTS5 Protein in Tissue Extracts, Cell Cultures and Fetal Bovine Serum

For analysis of ADAMTS5 protein gastrocnemius muscle, ~100 mg, was harvested immediately after sacrifice from 3 12 wk old male mice, into ice cold PBS containing 1X PIs, then rinsed in fresh PBS +PIs to remove blood products.

They were then frozen in liquid N2 and processed in a Bessman pulverizer. The powdered tissue was collected into 300 µL Laemmli sample buffer (BioRad) with 1X PIs, vortexed, boiled for 10 min, centrifuged at 14,000g for 15 min and 10 µl of the clear supernatant (equivalent to about 3 mg of muscle) used for Western analyses. ADSC cell layers were lysed in 100 µl of 50 mM Tris HCl pH 7.5, 150 mM sodium chloride, 5 mM EDTA, 1% NP-40, 10 mM sodium fluoride, 100 mM sodium orthovanadate with 1x Roche PIs (Roche PIs are cOmplete -Mini tablets from Roche Inc., and a 1x concentration was obtained when 1 tablet is dissolved in 10 ml of solution), scraped down and collected into a 1.5 mL microcentrifuge tube, vortexed, and kept on ice for 15 min. Lysates were cleared by centrifugation, 14,000g for 15 min, and a 5 µl aliquot (containing extracted protein from ~ 2x 10^4 cells) was loaded on a 4-12% Tris-Glycine gel and processed by Western analysis as described above. Fetal bovine serum batches used for the study were also assayed for presence of ADAMTS5 protein. For this, 0.2 µl (diluted 10x from 2 µl) of FBS batches E1101, B12027, H12120, A13005 (Atlanta Biologics) were mixed with sample buffer. Western analysis was done as described above. Using antibodies against ADAMTS5 catalytic domain, α-cat, Ab135656 (AbCam) at 0.25 µg/mL, and ADAMTS5 cysteine rich domain, α-cys, at 2 µg/mL (Anti-KNG) [102].

FACE Analyses of Chondroitin/Dermatan Sulfate and Hyaluronan

The hyaluronan and chondroitin/dermatan sulfate contents of ADSC cultures were determined by fluorophore-assisted carbohydrate electrophoresis

as described [168]. Briefly, medium was digested with 100 µg/mL of proteinase K (Invitrogen) at 37 °C, and cell layers were solubilized with 1 mL PBS containing 500 µg proteinase K, 100 mM ammonium acetate, 0.01% SDS for 1 h at 37 °C. Samples were ethanol precipitated, proteinase K was inactivated at 100 °C for 5 min and then chilled on ice, digested with chondroitinase ABC and hyaluronidase SD at 37 °C overnight, ethanol precipitated and inactivated again. Samples were then incubated with 2-aminoacridone (Molecular Probes) at 37 °C for 18 h in the dark, before being run on polyacrylamide (Glyko monosaccharide) gels. Fluorescent bands were imaged using a CCD camera and quantified by ImageJ (NIH).

Immunohistochemistry for Hyaluronan, Aggrecan and Versican

IHC was performed on cells in 8 well chamber slides (Nunc™ Lab-Tek™ II). Cells were grown to ~ 90% confluency, and maintained for 24 h in fresh basal medium. The medium was removed, and cell layers were rinsed twice with PBS before fixation in Histochoice (Amresco). Cell layers were stained for hyaluronan with biotinylated HAPB at 1 µg/mL [159,169], aggrecan with α-DLS at 1 µg/mL and versican with ab1033 (AbCam) at 1 µg/mL [15], antibody binding was visualized with the ABC kit from Vector labs, and cell nuclei were counterstained with methyl green. Streptomyces hyaluronidase treatments were done as described [15]. Non-immune controls were treated with a 1 µg/mL non-immune rabbit IgG, as the primary antibody.

Treatment of Cultures with Growth Factors

P2 ADSCs were plated into 12 well plates (Corning) and grown for 24 h-48 h in DMEM/1 g/L glucose/10% FBS/2 ng/mL bFGF, to bring the cultures to ~ 90% confluency. Media were then changed to Advanced MEM/10% FBS for 24 h. Cultures were then changed into AMEM containing 10% FBS with or without 10 ng/mL TGFb1 (Peprotech) or where indicated with 50 ng/mL BMP-7 (ProSpec). To illustrate TGFb1 dependent effects, some TGFb1 containing media were additionally supplemented with TBRI/II Kinase inhibitor, LY109761 5 µM (Selleckchem). Incubation with growth factors and RI/II inhibitor was done as described in (**Fig. 9**).
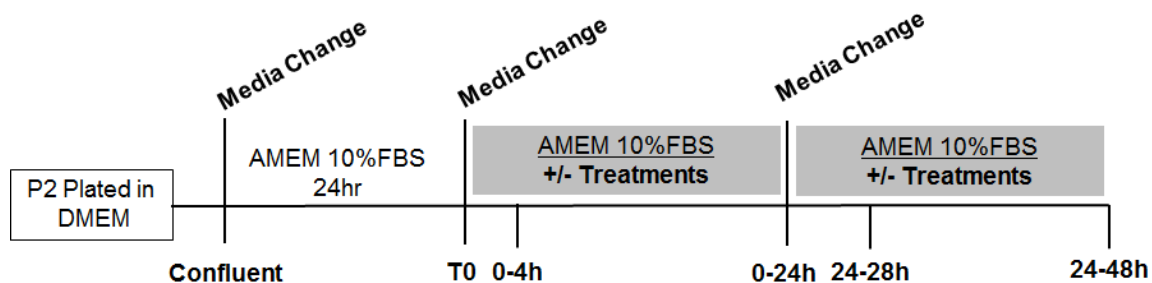
Figure 9. Experimental Scheme for Collagen Type I and ADAMTS5 Protein Analysis in ADSCs. P2 ADSCs were plated into 12 well plates and grown for 24 h-48 h in DMEM/1 g/L glucose/10% FBS/2 ng/mL bFGF, until ~ 90% confluency. Media was then changed to Advanced MEM/10% FBS for 24 h. Cultures were then changed into treatment media, as indicated in Methods, consisting of Advanced MEM/10% FBS supplemented with the one of following; 10 ng/mL TGFb1, 50 ng/mL BMP-7, 10 ng/mL TGFb1+ 5 µM TGFb RI/II Inhibitor, 80 µM Dynasore, 10 µM Bafilomycin A1, Batimastat (1, 3 or 9 µM), ADAMTS5 inhibitor (TS5i) (1, 3 or 9 µM), or Control (10% FBS only). Cultures were terminated at 4 and 24 h intervals, with fresh media changes every 24 h.

Treatment of Cultures with Protease Inhibitors

P2 ADSCs were treated with ADAMTS5 specific inhibitor (CAS 929634-33-3, Calbiochem) and MMP broad spectrum inhibitor-Batimastat (CAS 130370-60-4, Calbiochem), as illustrated in (**Fig. 9**). Concentrations used were 1, 3 and 9 µM and reflect the concentration range recommended by the supplier. The 'activity' and specificity were assessed by effects on pro-collagen processing and formation of the versican and aggrecan neoepitope. Potential cell toxicity side effects were determined by glucose uptake assay**.**

Treatment of Cultures with Bafilomycin A1 and Dynasore

P2 ADSCs were also treated with inhibitors for clathrin-mediated endocytosis, and lysosomal degradation, Dynasore 80 µM (Sigma), and Bafilomycin A1 10 µM (Tocris Bioscience) respectively, as illustrated in (**Fig. 9**). Concentrations used were according to the manufacturer's recommendations, and cell toxicity side effects were determined by glucose uptake assay.

Analyses of collagen processing and secretion in ADSC cultures

P2 ADSCs grown in 12 well plates, as described above, were terminated at the indicated time points by removing the media. The cell layers were briefly washed with 100 µL PBS, then extracted with 100 µL lysis buffer; 50 mM Tris HCl pH 7.5, 150 mM sodium chloride, 5 mM EDTA, 1% NP-40, 10 mM sodium fluoride, 100 mM sodium orthovanadate + 1 Roche PIs. Extracts were collected

on ice, vortexed and centrifuged for 15 min at 14,000g to pellet cell debris. The media were centrifuged at 14,000g for 3 min to remove floating cell debris and supernatants frozen. 40 µL aliquots were Speedvac evaporated before analysis. Portions of the cell layer extract (5 µL) and dried media (40 µL) were mixed with 30 µL of sample buffer, heated at 100 °C (for 5 min) and western blotted as described above using primary antibody Type I Collagen (SouthernBiotech) at 0.4 µg/mL and secondary anti-Goat HRP (Vector Labs PI-9500) at 1:4000. Lane loading was checked by anti-b-actin, C4 (SantaCruz) at 1:1000, with secondary goat anti-mouse (ThermoScientific # 31430) at 1:2000.

BMP-1 Treatment of Secreted Collagen

For BMP1 digestion of pro-collagen, confluent ADSCs were changed into phosphate-free DMEM (Gibco) supplemented with L-ascorbic acid 2.5 mg/L (Sigma) and sodium pyruvate 110 mg/L (Sigma*)* and cultured for 24h. Media were collected, as described above and stored at -20 °C. Samples were thawed on ice, and identical aliquots were supplemented with 5 mM $CaCl_2$ (Fisher) and digested with rhBMP-1/PCP (R&D Systems) at 37 °C for 6 h. Digests were terminated with 10 mM (EDTA) to inactivate BMP-1, controls received 10 mM EDTA only.

QPCR Assay for Gene Expression

Total RNA was isolated from cell layers with TRIzol® reagent (Ambion) 1 mL/T25 or 60 mm dish and purified to remove protein and DNA as per

manufactures guidelines. The RNA enriched pellet was suspended in 100 µl RNase/DNase free water (Gibco) and further purified using the RNeasy kit (Qiagen). RNA purity and yield were determined from the 260 nm/280 nm ratio using Synergy Mx Monochromator-Based Multi-Mode Microplate Reader (BioTek) using the Gen5™ software. cDNA was synthesized from 1 µg RNA using the First-Strand Synthesis Kit (oligo dT method). Kit contains; dNTPs, oligo dT primer, 5x reaction buffer, and superscript reverse transcriptase RTII. cDNA was diluted 10-fold and combined with Taqman Gene Expression Master Mix (Applied Biosystem, Inc). QPCR was on a 7300 System (Applied Biosystems, Inc) with the Taqman platform (Life Technologies). Details of murine primers are given in **Table 2**. Data are presented as apparent mRNA abundance relative to Gapdh, calculated as $(2^{-\Delta CT})*1000$ (arbitrary units).

DNA Assay

Cell layers were digested in 1 mg/mL proteinase K (Invitrogen), 100mM ammonium acetate, 0.01% SDS for 1 h at 37 °C, digest collected, vortexed 10-15 sec and stored at -20 °C until fluorometric analysis using Hoechst 33258 (Invitrogen) as described [170], on a LS50 B Luminescent Spectrometer (Perkin Elmer) equipped with FL WinLab Software. A standard curve, ranging from 0.375 to 7 µg was constructed, with each assay based on a calf thymus DNA (Sigma) standard.

Glucose Uptake Assay

Glucose contents of culture media before and after addition to cell cultures were determined with Amplex® Red kit A22189 from LifeTech Inc. Kit contains; glucose standard, 5x reaction buffer, horseradish peroxidase, hydrogen peroxide, DMSO, glucose oxidase and Amplex® Red reagent. Briefly, 0.1 µL media (serially diluted from 10 µL) from a total of 800 µl of medium from approximately 0.4 x 10^6 of cells was measured in a total reaction volume of 100 µL. Fluorescence was determined using a Synergy Mx Monochromator-Based Multi-Mode Microplate Reader (BioTek) using the Gen5™ software set at 530nm for excitation and 590 nm for emission. A standard curve was measured ranging from 0.25 µM to 11.5 µM glucose. Glucose was measured in fresh medium and medium collected from cells after 24 h in culture. Glucose concentrations were then calculated from the standard curve, and uptake was calculated as (glc at 0 h - glc at 24 h) and expressed as a µmoles of glucose consumed per µg DNA per 24 h.

Statistical Methods

Group differences (Mean +/- SD (n=6)) were evaluated with Students t-test and p-values are shown.

IV. RESULTS

Genotyping and mRNA analysis of wild type, TS5-deficient mice

To confirm the nature of the Adamts5 gene modification for two different knock out strains, Lexicon generated, (for Pfizer Inc) TS5P KO [113] and Deltagen generated (for Jackson Labs) TS5J KO [112], DNA was isolated from confluent cultures of ADSCs prepared as described in the Methods, from WT, TS5P KO and TS5J KO male mice.

Using the primers pairs outlined in the Method section and (**Fig. 10A**), the PCR product generated from WT DNA was 642bp, the product generated from TS5P KO DNA was 374bp and no product was detected from TS5J KO (**Fig. 10A,D**) confirming deletion of exon 2 in both KO strains. For the TS5J KO strain, deletion of exon 2 and the insertion of a LacZ+Neo cassette into the genome was confirmed using primers and conditions provided in Jackson Lab protocols (**Fig. 10A, E**).

Analysis of mRNA transcripts in ADSCs from all three genotypes were also performed using primers targeting exon 1 and 4 (**Fig. 10B**, primer set '*I')*, This PCR reaction showed the expected product in WT cells, it absence in the TS5J KO, but also showed a transcript in TS5P KO cells. Such a product would arise (**Fig. 10C,F**) if the KO resulted in an in-frame deletion of exon 2 in TS5P KO, not reported in the initial description of this KO strain [112]. This was confirmed, when we performed an additional PCR reaction using primers targeted to an overlapping sequence generated by fusion of exon 1 and 3, (**Fig.**

10C,F, primer set '*II*'). In comparison, PCR assay for transcripts in TS5J KO

cells, with primer set '*II*' gave no product, consistent with the reported out-of-

frame deletion in this KO strain (**Fig. 10C, F**). Further analysis of TS5P KO

mRNA using primers for exon 1 and 8 (**Fig. 10C, G**, primer set '*III*'), also showed

the presence of a full length transcript lacking exon 2 in ADSC cultures.

Identification of these PCR products was confirmed by sequencing (**Fig. 11**).
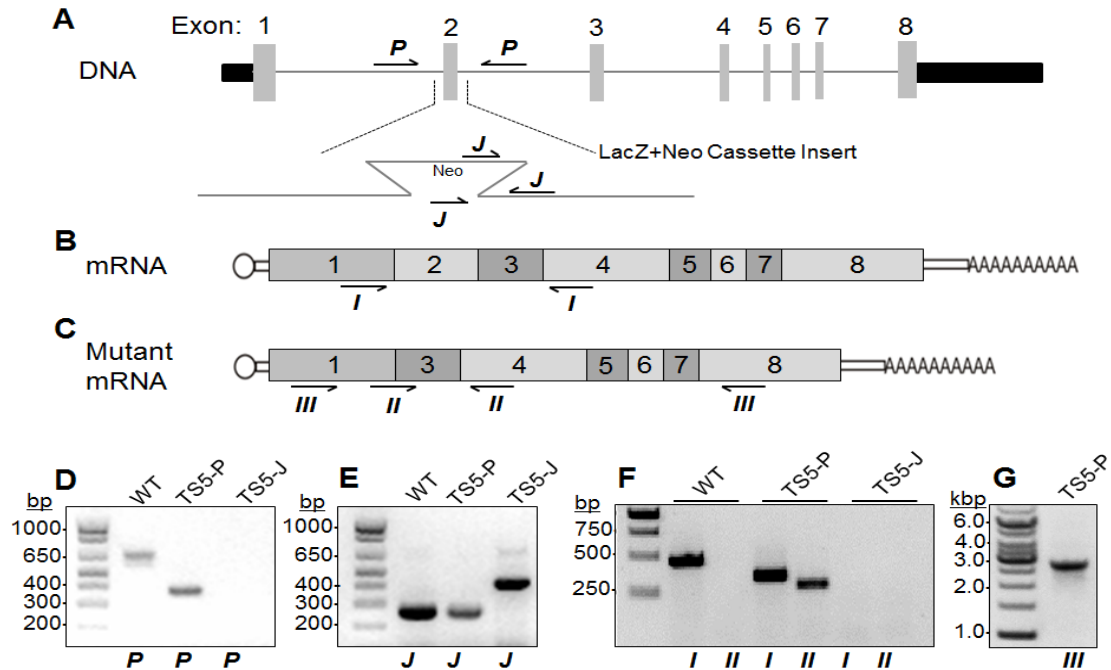
Figure 10. Genotyping and mRNA analysis of wild type and TS5-deficient ADSC cultures. (A) Diagram of ADAMTS5 gene showing genotyping primer locations for genotyping Pfizer generated '*P*' and Jackson generated '*J*' knockouts. **(B)** Diagram of full length WT Adamts5 mRNA showing locations of primer set '*I*', targeting exons 1 and 4. **(C)** Diagram of proposed mutant mRNA missing exon 2, showing locations of primer set '*II*' targeting an overlapping sequence of exons 1/3 and exon 4 and primer set '*III*' targeting exons 1 and 8. **(D)** PCR products from genotyping ADSCs with Pfizer primers '*P*', WT product 642bp, TS5P KO 374bp, confirming exon 2 deletion in TS5P KO, TS5J KO shows no amplification due to LacZ-neo insert. **(E)** PCR products from genotyping ADSCs with Jackson primers '*J*', WT and TS5P KO product is 271bp, TS5J KO product is 424bp confirming exon 2 deletion and LacZ+Neo cassette insertion in TS5J KO only. **(F)** PCR products amplified from ADSC cDNA synthesized from mRNA, using primer set '*I*' and '*II*'. Primer set '*I*' shows predicted amplification product in WT and smaller product in TS5P KO ADSCs, consistent with an 'in-frame' modification and mRNA transcription with exon 2 deleted, no product was seen in TS5J KO ADSCs, consistent with an out of frame mutation. Primer set '*II*' shows amplification of TS5P KO, not WT or TS5J KO, confirming mutant mRNA in TS5P KO ADSCs is missing exon 2 and has a fusion of exon 1 and 3 **(G)** PCR products amplified from TS5P KO ADSC cDNA using primer set '*III*', showing mutant mRNA transcript missing exon 2 is a full length transcript reaching from exon 1 to exon 8.
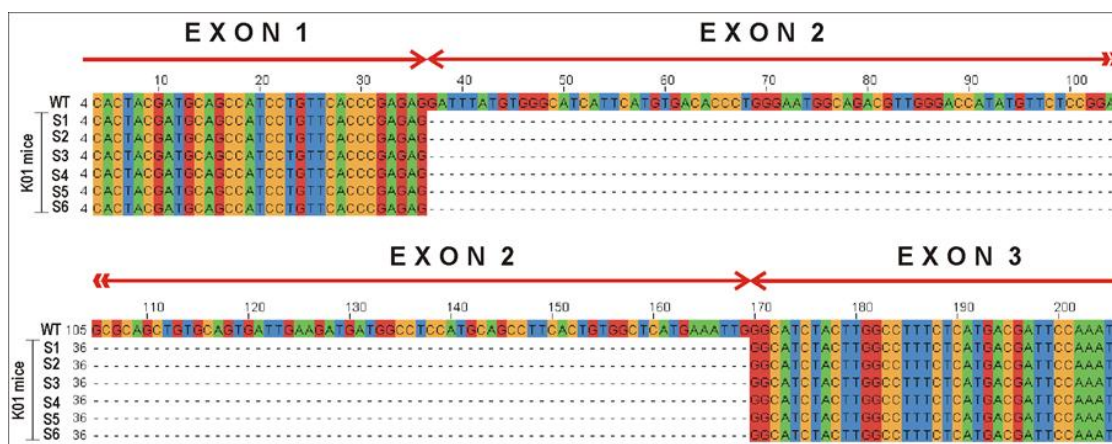
Figure 11. Sequence confirmation of mutant transcript in TS5P KO mice. Six recombinant clones 'S1-6' from TS5P KO ADSC samples were sequenced and compared to WT and each other using ClustalW2 alignment program, confirming exon 2 deletion in TS5P KO mutant mRNA.

Characterization of ADAMTS5 protein species in muscle tissue extracts, ADSC cultures and serum

Total protein extracts were prepared from skeletal muscle of WT, TS5P KO and TS5J KO male mice as described under Methods. Portions were analyzed by Western blotting using antibodies raised against residues 338-368 (Cat domain, α-Cat) and 636-648 (Cys-domain, α-Cys), (**Fig. 12A**). WT but not TS5P KO or TS5J KO samples gave a protein species migration with an apparent mwt of ~40 kDa that reacted with both antibodies consistent with its identification as a proteolytically processed form of ADAMTS5. Since the antibodies were raised against residues 338-368 (Cat domain) and 636-648 (Cys-domain), we interpret the size data to mean that WT muscle contains a species, that has an N-terminus in the catalytic domain and a C-terminus within the Cys domain. This 40 kDa species is most likely identical to that reported by

us as the major ADAMTS5 form present in fresh extracts of human OA cartilages [102] and equine tendon [171].

Analyses of extracts from ADSC cell layers showed two additional ADAMTS5 fragments that were detected only in WT samples (**Fig. 12B**). One species migrated at ~40 kDa, (fragment 'B', see **Fig. 13**) and, unlike the muscle product; it was only detected with the α-Cat antibody. The second migrated at ~30 kDa (fragment 'C', see **Fig. 13**), and it was only detected with the α-Cys antibody. Neither of those products were detected in ADSCs from TS5P KO (**Fig 12B**) or from TS5J KO (data not shown). In addition, a ~75 kDa species, (fragment 'D', see **Fig. 13**), which reacted with the α-Cys domain antibody, but not α-Cat domain antibody, was present in ADSC cultures from both wild-type and TS5P KO mice (**Fig. 12B**).

The presence ADAMTS5 fragments in both KO cell layers and also in portions of their culture media analyzed by western blotting (data not shown), raised the possibility that those were derived from fetal bovine serum, used in the culture medium. Indeed analyses of several batches of serum used in the current study showed a ~64 kDa species reactive with α-Cat (fragment 'E' see **Fig. 13**) and a ~75 kDa species, (fragment 'D' see **Fig. 13**), reactive with the α-Cys (**Fig.12C**). A schematic summary of the putative structures of the ADAMTS5 fragments identified in this study are shown in **Fig. 13**.
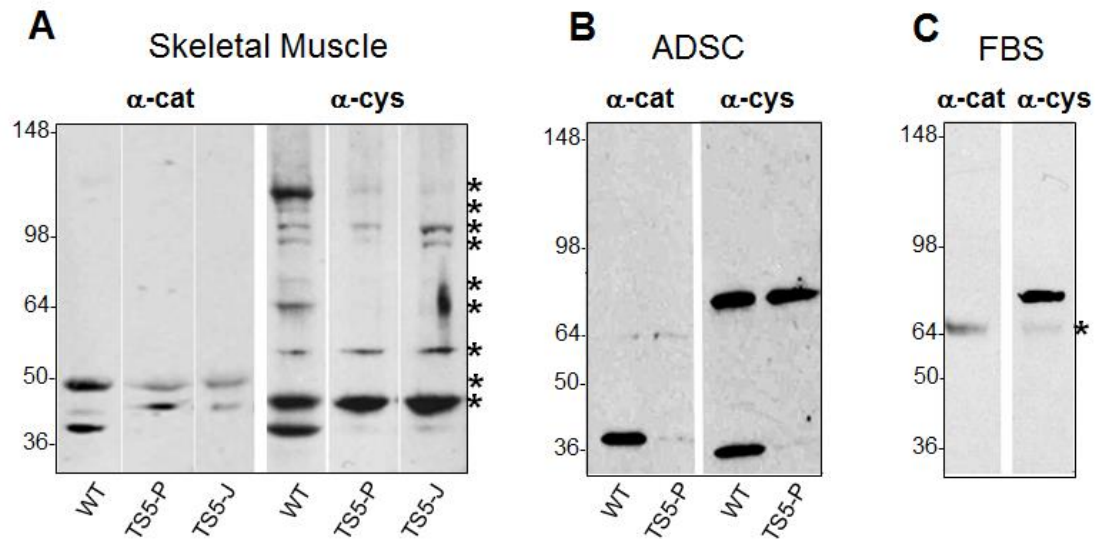
Figure 12. Western analysis of ADAMTS5 in muscle, ADSC cultures and fetal bovine serum. ADAMTS5 protein abundance was analyzed in WT and Adamts5 KO mice, in vitro and in vivo, details described in Methods. Western blots of skeletal muscle extract, ADSC cell layers and FBS used for cell culture were probed with antibodies raised against the catalytic domain (α-cat) or cysteine rich domain (α-cys) of human ADAMTS5. **(A)** Analysis of muscle extracts of WT, but not TS5P KO or TS5J KO mice detected an ADAMTS5 fragment of ~40 kDa, which reacted with both α-cat and α-cys antibodies, this presumably contains the N-terminal catalytic domain and C-terminal cysteine rich domain. **(B)** Analysis of ADSC cell layers show a ~40 kDa product reactive with α-cat, and a ~30 kDa product reactive with α-cys, in WT cultures which are not present in TS5P KO cultures. **(C)** Analysis of fetal bovine serum supplement used for cell culture shows a ~75 kDa product reactive with α-cys, and a ~64 kDa product reactive with α-cat. These products are seen in both WT and TS5P KO cultures (B), as it is serum derived. Asterisk (*) denotes non-specific bands.
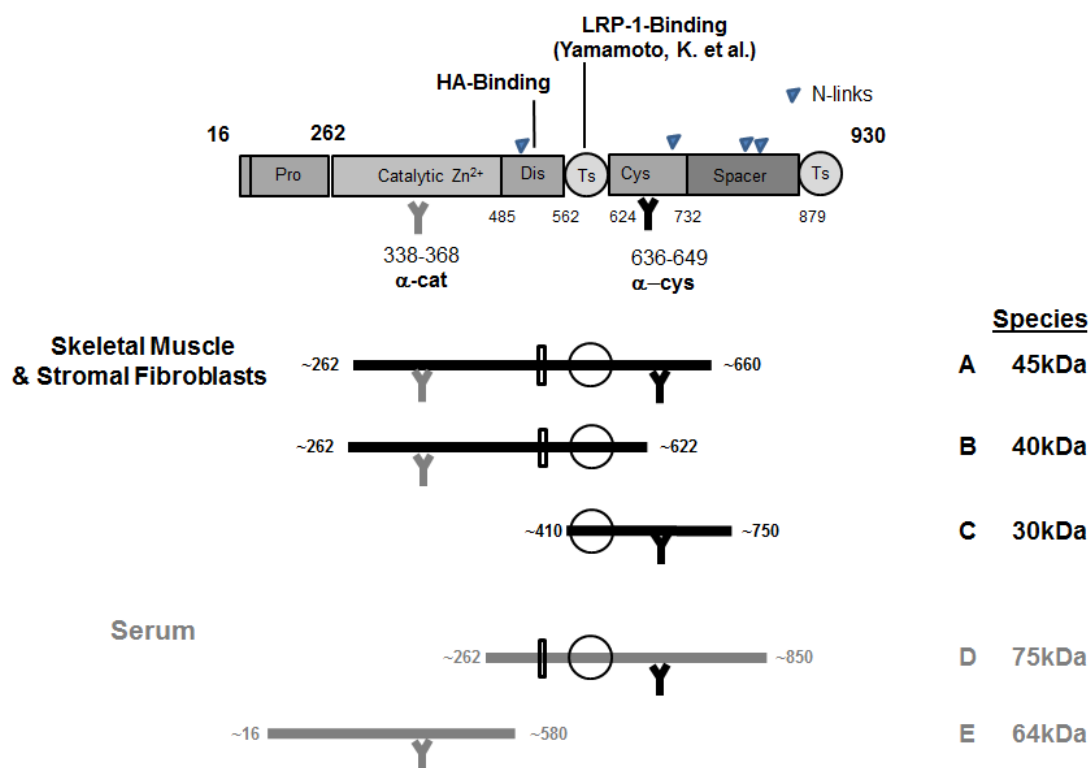
Figure 13. Proposed Structures of ADAMTS5 Fragments. Schematic diagram of proposed ADAMTS5 fragments found in ADSC cultures, with antibody reactivity and amino acid range. Fragments A (45 kDa), B (40 kDa) and C (30 kDa) are derived from ADSCs, whereas fragments D (75 kDa) and E (64 kDa) are serum derived.

Characterization of ADSC Cultures by expression of "mesenchymal stem cell" marker genes

The expressions of putative marker genes for mesenchymal stem cells (CD73, CD90, and CD105), phagocytotic cells (F4/80, Mac-1) and the HA receptor (CD44) were detected in ADSCs genotypes (**Table 3**). WT ADSCs expressed those genes in the following order of abundance; CD44>CD90>CD105>CD73>>F4/80>Mac-1.

Interestingly the same panel of genes was also assayed in epiphyseal chondrocytes, grown in high density monolayers and readily detected. In fact chondrocytes displayed a higher level of expression of CD73 and F4/80,

relatively similar expression of CD90, CD105 and CD44 compared to ADSCs.

The finding that chondrocytes express these markers may be related to our

finding that these types of cultures contained a flattened elongated cell type that

was similar in morphology to the ADSCs in monolayer (**Fig. 6**).

Some minor, yet statistically significant changes were seen when

comparing expression of the marker genes between cells from different

genotypes. For example, expression levels of CD73 and CD90 were lower

inTS5J KO than in either WT or TS5P KO cultures; CD105 and CD44 were

higher in TS5P KO than WT or TS5J KO cultures.

Genotypic differences were also seen in chondrocyte cultures, with CD90

higher in TS5J KO than WT and TS5P KO cells and F4/80 expression higher in

both TS5J KO and TS5P KO than WT cells.

Gene	WT ADSC	TS5-P ADSC	TS5-J ADSC	WT CHON	TS5-P CHON	TS5-J CHON
CD73	3.1 (0.7)	2.6 (2.3)	2.0 (0.4) **0.012	24.3 (8.45)	24.3 (1.61)	28.7 (4.70)
CD90	20.8 (2.39)	34.6 (26.39)	14.1 (1.32) ** 0.0002	12.5 (2.84)	10.8 (1.76)	21.4 (2.07) **0.002 ***0.0025
CD105	14.3 (1.4)	44.3 (23.7) *0.022 ***0.017	16.0 (2.61)	20.1 (5.00)	15.8 (1.65)	16.5 (0.90)
CD44	29.0 (6.3)	53.2 (16.6) ***0.029	20.6 (3.34)	25.7 (2.28)	Not assayed	Not assayed .
F4/80	0.12 (0.10)	0.29 (0.15)	0.20 (0.06)	1.7 (0.03)	3.7 (0.39) * 0.009	5.4 (0.93) **0.0023 ***0.042
MAC-1	0.04 (0.023)	Not detected	0.10 (0.10)	Not assayed	Not assayed	Not assayed

Table 3. mRNA transcript abundance for cell surface markers in ADSC and CHON cultures. Expression of mesenchymal marker genes; CD73, CD90 and CD105, phagocytotic marker genes; Mac-1 and F4/80 and HA binding CD44 were assayed in ADSC and Chondrocyte (CHON) cultures from WT and TS5-deficient mice using taqman based QPCR. Values are given as relative mRNA abundance (+/- SD, n=6 individual cultures), which was calculated as $(2^{\Delta Ct})*1000$ (arbitrary units), ΔCt relative to Gapdh. Not Detected = (Ct value of 35 or greater). Comparisons with statistical significance $p<0.05$ are displayed as bolded values with asterisk (*). P-values, were determined by student's t-test * WT vs TS5P KO, ** WT vs TS5J KO, *** TS5P KO vs TS5J KO.

Expression of ECM genes in ADSCs from WT and TS5-deficient mouse strains

To further describe the fibroblastic nature of undifferentiated ADSCs vs differentiated chondrocytes,   we compared the expression of a range of ECM genes (Col1a1, Col1a2, Col3a1 and Col2a1), aggrecan, versican, Has1, 2 and 3, and link proteins 1 and 3 between the two cell types (**Tables 4 and 5**). ADSCs showed a high abundance of transcripts for Col1a1 and a2, Col3a1 as well as Has1 and 2, and essentially undetectable levels of transcripts for 'chondrocyte' specific genes such as Col2a1, Acan, Hapln1, Hapln3 (link proteins 1 and 3)

Notably, for epiphyseal chondrocytes, in addition to the robust expression of Col2a1, Acan, link proteins 1 and 3, both, Col1a1 and Col3a1 were also highly expressed, with Col1a1 about 5-fold higher in the chondrocytes (5249.7+/-980.3) than in ADSCs (1749.6+/-228.3), supporting the presence of 'fibroblastic' cells in these cultures.

Genotypic differences in ECM gene expression were particularly notable for the collagen genes between genotypes. In ADSCs, Col1a1 and Col3a1 were highest in WT (1749.6+/-228.3 and 240.73+/-56.81 respectively) relative to TS5P KO (1172.7+/-484.3 and 125.90+/-59.52 respectively) and TS5J KO cells (1103.0+/-194.3 and 106.20+/-26.07 respectively). Moreover, TS5J KO cells exhibited higher expression of Col1a2 (503.4+/-32.0) than WT (142.01+/-50.0) and TS5P KO (141.0+/-37.0). As expected, transcripts for Col2a1 were present only in epiphyseal chondrocytes, and were highest in WT (49.25+/-23.67), compared to TS5P KO (21.04+/-1.36) and TS5J KO (16.01+/-3.83).

Statistically significant differences in the expression of glyco-matrix genes were seen for Hapln3, Has1 and Has2, which were elevated in TS5P KO ADSCs (0.16+/-0.03, 12.8+/-0.95 and 6.18+/-2.13 respectively) relative to WT (0.06+/-0.01, 0.46+/-0.09 and 1.80+/-0.43) and TS5J KO (0.06+/-0.01, 0.13+/-0.07 and 1.81+/-1.04) ADSCs. It should be noted that expression of the Has3 isoform was below the level of detection for ADSCs using this QPCR assay method.

Gene	WT ADSC	TS5-P ADSC	TS5-J ADSC	WT CHON	TS5-P CHON	TS5-J CHON
Col1a1	1750 (228.3)	1173 (484.3) * 0.043	1103 (194.3) **0.0006	5250 (980.3)	4427 (488.0)	988 (1153.5) ***0.0025
Col1a2	142.0 (50.0)	141.0 (37.0)	503.0 (32.0) ***0.0001	Not assayed	Not assayed	Not assayed
Col2a1	Not detected	Not detected	Not detected	49.25 (23.67)	21.04 (1.36) *0.004	16.01 (3.83) ** 0.047
Col3a1	240.7 (56.81)	125.9 (59.52) *0.014	106.2 (26.07) **0.0006	544.8 (223.4)	335.2 (84.81)	467.0 (58.59)

Table 4. mRNA transcript abundance for fibrillar collagens in ADSC and CHON cultures. Expression of collagen type I, alpha 1 and alpha 2, collagen type II alpha I and collagen type III alpha I chains were assayed in ADSC and Chondrocyte (CHON) cultures from WT and TS5-deficient mice using taqman based QPCR. Values are given as relative mRNA abundance (+/- SD, n=6 individual cultures), which was calculated as $(2^{\Delta Ct}) * 1000$ (arbitrary units), ΔCt relative to Gapdh. Not Detected = (Ct value of 35 or greater). Comparisons with statistical significance p<0.05 are displayed as bolded values with asterisk (*). P-values, were determined by student's t-test * WT vs TS5P KO, ** WT vs TS5J KO, *** TS5P KO vs TS5J KO.

Gene	WT ADSC	TS5-P ADSC	TS5-J ADSC	WT CHON	TS5-P CHON	TS5-J CHON
Acan	0.01 (0.003)	Not detected	Not detected	67.33 (16.33)	59.21 (4.87)	23.78 (8.73) **0.0027
Vcan V1	0.62 (0.21)	0.81 (0.21)	0.69 (0.20)	3.67 (0.48)	N.A.	N.A.
Vcan V2	1.40 (0.43)	1.60 (0.80)	1.70 (0.53)	5.49 (0.96)	4.35 (0.71)	2.47 (0.64) **0.0019 ***0.027
LP 1	Not detected	Not detected	Not detected	503.38 (48.18)	Not assayed	Not assayed
LP 3	0.06 (0.01)	0.16 (0.03) *0.0001 ***0.0001	0.06 (0.01)	2.96 (0.30)	Not assayed	Not assayed
Has 1	0.46 (0.09)	1.28 (0.95) *0.0001 ***0.015	0.13 (0.07)	0.16 (0.05)	0.17 (0.04)	0.21 (0.02)
Has 2	1.80 (0.43)	6.18 (2.13) *0.002 ***0.0016	1.81 (1.04)	2.96 (0.26)	3.21 (0.08)	1.57 (0.17) **0.0001 ***0.0001
Has 3	Not detected	Not detected	Not detected	0.01 (0.004)	0.005 (0.002)	0.01 (0.001)

Table 5. mRNA transcript abundance for glyco-matrix components in ADSC and CHON cultures. Expression of aggrecan (Acan), versican (Vcan) isoforms V1 and V2, link proteins 1 and 3 (LP), and hyaluronan synthases (Has) 1, 2 and 3 were assayed in ADSC and Chondrocyte (CHON) cultures from WT and TS5-deficient mice using taqman based QPCR. Values are given as relative mRNA abundance (+/- SD, n=6 individual cultures), which was calculated as $(2^{-\Delta Ct}) * 1000$ (arbitrary units), ΔCt relative to Gapdh. Not Detected = (Ct value of 35 or greater). Comparisons with statistical significance p<0.05 are displayed as bolded values with asterisk (*). P-values, were determined by student's t-test * WT vs TS5P KO, ** WT vs TS5J KO, *** TS5P KO vs TS5J KO.

CS/DS and HA production by ADSCs from WT and TS5-deficient mice

Cell layers and media from confluent WT, TS5P KO and TS5J KO ADSC cultures were processed for quantitation of CS/DS and HA content by fluorophore-assisted carbohydrate electrophoresis (FACE) as described in the methods (**Fig. 14A**). For all three genotypes, CS/DS secreted into the medium or deposited in the cell layers was predominantly (>80%) 4-sulfated with the remainder 6-sulfated. By comparison with either WT or TS5J KO, ADSCs from TS5P KO mice produced CS/DS with a higher proportion of 6-sulfated disaccharides (TS5P KO= 12.5ng/ug DNA +/-4.4 vs WT=4.4+/-1.1 and TS5J KO 4.1+/-1.3). We observed however, that TS5P KO cells accumulated more HA in cell layers (TS5P KO= 43.9ng/ug DNA +/-4.5 vs WT=29.0+/-3.0 and TS5J KO 19.3+/-8.5) and medium (TS5P KO= 44.9ng/ug DNA +/-4.7 vs WT=24.0+/-5.0 and TS5J KO 27.5+/-6.3). The increased production of in HA was accompanied by an increased [~3-fold] expression of both, Has2 and Has1 in this cell type (see **Table 5**). No statistically significant differences between genotypes were detected in the total amounts of CS/DS deposited in cell layers (~ 60 ng/μg DNA over a 3-4 day culture period) or secreted into the media (~ 25 ng/μg DNA over a 24 h period).

HA and CS-PG deposition in the ECM of ADSC cultures was confirmed by immunostaining as described in the methods (**Fig. 14B**). In cultures, from all three genotypes, HA was localized in the ECM of the fibroblastic cell layers, and was also detected as strongly stained 'capped structures' in close association with cells of an epithelioid morphology. It was also noted, that TS5P KO cultures

contained stained 'cable-like' structures extending between cell groups, and this could explain the increased HA content seen by FACE analyses in such cultures.

Versican (localized with Ab1033) showed a widespread matrix-staining, mostly organized into dense fibrillar aggregates, in a similar staining pattern that had been previously reported for fibronectin accumulation in fibroblastic cells [172-174].

On the other hand, aggrecan (localized with anti-DLS) showed a very different staining pattern. Firstly it was essentially undetectable in the predominantly fibroblastic areas of the cultures, but showed a selective strong staining in the epithelioid cell groups (which also had the distinct HA-capping staining).

Pretreatment of the cell layers with Streptomyces hyaluronidase essentially removed matrix HA and versican reactivity from the fibroblastic regions of the cultures, but did not affect the HA or aggrecan staining with the epithelioid cells suggesting that those two molecules are present intracellularly in this cell population (data not shown).
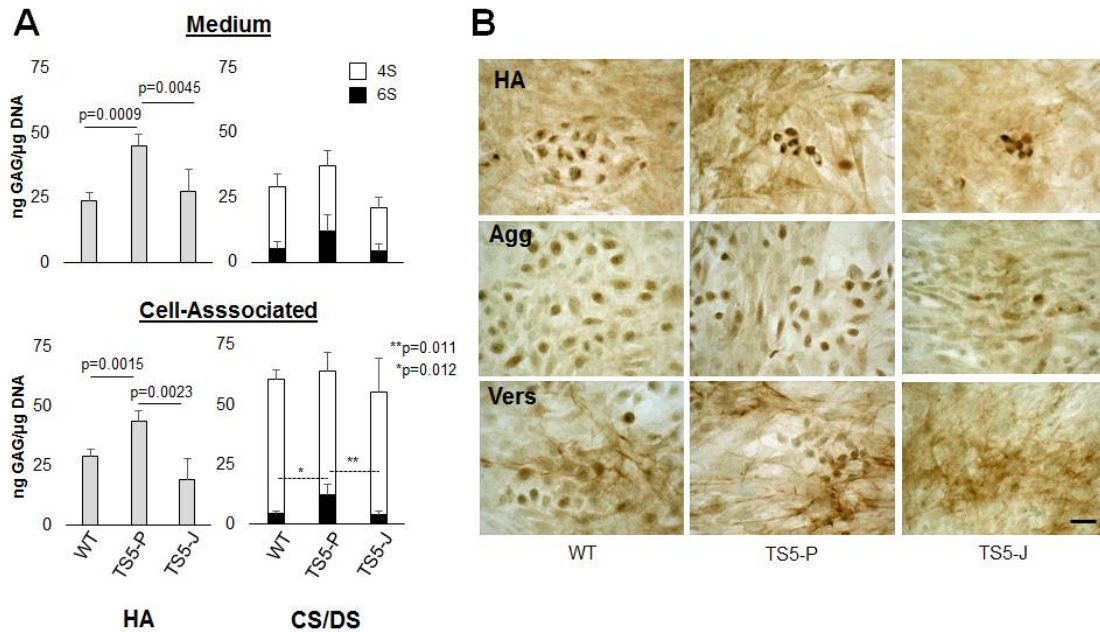
Figure 14. Identification of glyco-matrix by FACE and immunohistochemistry. (A) Media and cell layers of ADSC cultures from WT and TS5-deficient mice were analyzed for glycosaminoglycan content using FACE. Hyaluronan (HA), and chondroitin/dermatan sulfate (CS/DS) were analyzed. 4-sulfated (4S) open bars and 6-sulfated (6S) black filled bars. Data presented as the mean ng GAG/µg DNA, for n = 4 cultures. Error bars are +/- SEM, p-values are displayed. TS5P KO ADSCs show increased HA abundance in media and cell-associated compartments as well as increased 6-sulfated GalNAc in the cell-associated compartment. **(B)** Cell layers were also immunostained for hyaluronan with biotinylated HAPB, aggrecan (Agg) with anti-DLS and versican (Vers) with Ab1033. Cell nuclei were counterstained with methyl green. No large differences between genotypes are apparent. HA staining appears to be widely distributed in the ECM, as well as associated with circular 'epithelioid' cells. Versican staining distributed in the ECM, unlike aggrecan staining that only appears associated with epithelioid cells, and is virtually absent in the ECM. Scale bar= 30µm.

Versican synthesis by ADSC from WT and TS5-deficient mouse strains

Medium and cell extracts from ADSC (**Fig. 15A, B**) and chondrocytes (**Fig. 15C, D**) were also analyzed for versican V1 and V2 with Ab1033. ADSCs from all three genotypes, showed multiple products in the cell-associated and medium fractions of cells grown to confluency in 10% serum (**Fig. 15A**). Similar amounts of versican product accumulated in the cell layers and were released into the medium over 24 h. This is distinct from the distribution of aggrecan in such cultures, where after 24 h in the 10% serum, a very high proportion (~90%) of aggrecan was recovered in the medium.

Based on the electrophoretic mobility, the high molecular weight form, ~450 kDa, most likely represents full-length versican, whereas the bands migrating with apparent molecular weights of ~140 kDa, ~120 kDa, ~110 kDa and ~75 kDa would be C-terminally truncated forms and which, with the exception of the 75 kDa species, are substituted with CS/DS (**Fig. 15B**, compare +/- chondroitinase treatment). The identity of proteolytically processed species was not further investigated in the current study; however their presence in cultures with 10% serum suggests that they are generated in an environment protected from serum proteinase inhibitors, i.e. in the biosynthetic/secretory pathway, as was also the case for aggrecan (see below). Products with essentially identical electrophoretic migration at those seen in ADSC cultures were also found in the cell-associated and medium fractions from primary chondrocyte cultures from WT and TS5P KO mice (**Fig. 15C**), and chondroitin sulfate substitution, as assessed by sensitivity to chondroitinase ABC was also

similar in the two cells types and no differences seen between genotypes (**Fig. 15D**).
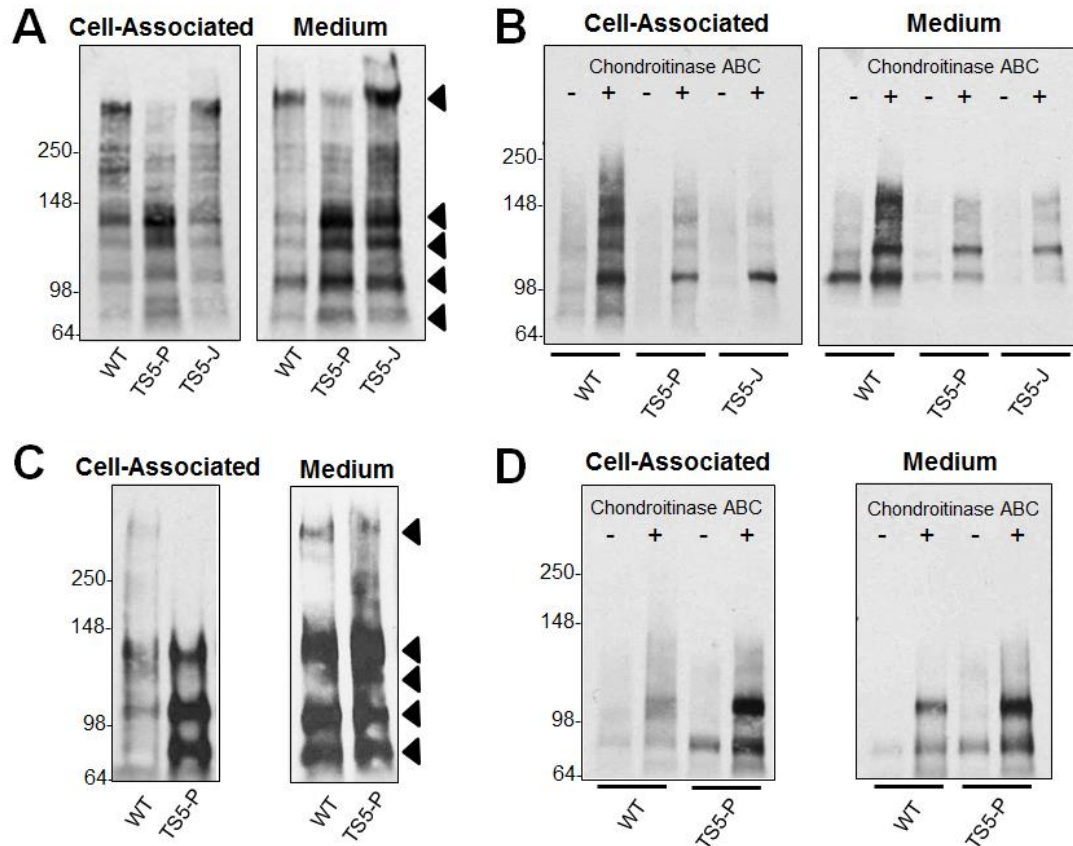
Figure 15. Western analysis of Versican core protein of ADSC and CHON cultures from WT and TS5-deficient mice. Versican isoforms V1 and V2 detected by Ab1033 **(A)** Cell-associated and media compartments from WT, TS5P KO, TS5J KO ADSCs, arrows indicate major reactive bands; full length ~450 kDa, and truncated ~140 kDa, ~120 kDa, ~110 kDa and ~75 kDa. **(B)** Portion of samples analyzed in (A) run +/- Chondroitinase ABC to determine CS-substitution, all but ~75 kDa fragment are CS-substituted. **(C)** WT and TS5P KO chondrocyte cell-associated and media compartments, showing similar banding as ADSC cultures. **(D)** Portion of samples analyzed in (C) run +/- chondroitinase ABC, showing similar CS-substitution as ADSC cultures.

Aggrecan synthesis by ADSC from WT and TS5-deficient mouse strains

Medium and cell-layers of ADSCs were processed by Western analysis for aggrecan with anti-DLS, as described in the Methods section. Portions of DE52 purified material were electrophoresed with and without chondroitinase ABC digestion, and a typical set of blots is shown in (**Fig. 16A**).The DLS-positive aggrecan core proteins species present in ADSC cultures from all three genotypes were similar, as was their distribution between medium and cell associated pool, where roughly 90% of the aggrecan core proteins were recovered in the medium (Medium membranes exposed for ~1 sec, Cell-Associated membranes exposed for ~30sec).

The blots showed three major species migrating with a molecular weight of ~ 148 kDa, ~ 110 kDa and ~ 65 kDa, all of which were substantially smaller than the 250 kDa species purified from articular cartilage as A1A1. For all three genotypes, the electrophoretic mobility of the cell layer associated aggrecan was largely unaffected by glycosidase digestion, only minor increases in the abundance of the 148 kDa species were seen. By comparison, the 148 kDa species secreted into the medium was extensively substituted with chondroitin sulfate, as its abundance on the western blot was greatly enhanced by chondroitinase ABC digestion.

To further identify the structure of the DLS-reactive aggrecan core protein species in ADSCs, western blotting of portions was also performed with antibodies to the C-terminal aggrecanase neo-epitopes TAS and KEEE (Glu(1480)-Gly(1481) and Glu(1667)-Gly(1668) respectively) and the calpain

neoepitope GVS (**Fig. 16B**). These results showed that bands, 1 (mwt ~ 250 kDa), 2 (mwt ~ 148 kDa) and 4 (mwt ~ 65 kDa) are aggrecanase generated fragments, and band 3 (mwt ~ 100 kDa) is a calpain generated fragment. Since the electrophoretic properties and the immunoreactivity of these truncated species is consistent with ADAMTS-aggrecanase-mediated cleavage of aggrecan within the CS-attachment regions, much as seen in cartilage [160] and chondrocyte cultures [86], the data strongly suggest that C-terminal truncation of aggrecan occurs in the presence of 10% serum in these cells, but that ADAMTS5 is not required for such cleavages.

To confirm the identification of aggrecan species in ADSCs, media and cell extracts were also prepared from WT and TS5P KO chondrocyte cultures and analyzed by western blotting (**Fig. 16C**). Interestingly, the four major aggrecan species identified in ADSCs were also present in these cultures, and no major differences observed between genotypes. It was noted however that on a per cell basis, chondrocytes produced ~ 3-4 times more aggrecan than ADSCs. Chondroitin sulfate substitution of aggrecan in chondrocytes was also examined by digestion with and without chondroitinase ABC (**Fig. 16C**), no major difference between ADSCs and chondrocytes were observed except that chondrocytes secreted a higher proportion of CS substituted high molecular weight core protein (arrows in +chondroitinase lanes, **Fig. 16C**).
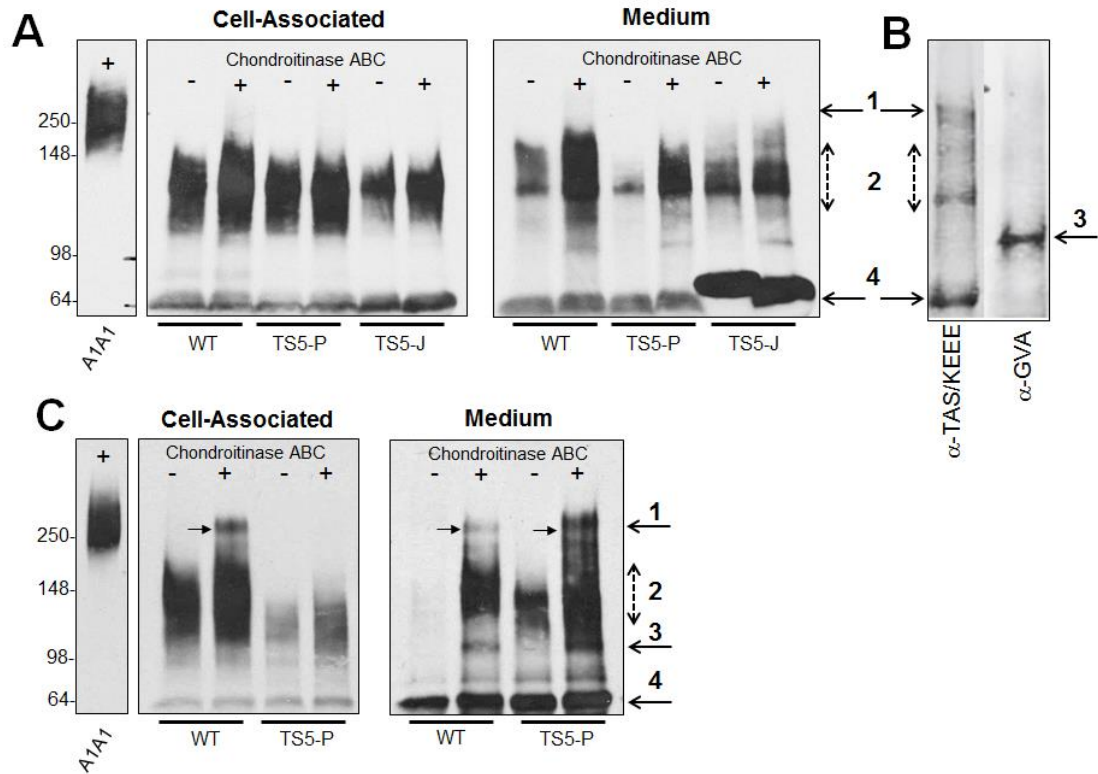
Figure 16. Identification and analysis of CS-substitution of Aggrecan core protein products by western blot. (A) Proteoglycans from cell-associated and medium compartments of ADSCs from WT and TS5-deficient mice were run +/- chondroitinase ABC to determine the degree of CS-substitution; aggrecan core protein was detected by anti-DLS. Enhanced reactivity upon chondroitinase digestion was only seen in the polydisperse band 2 of the media compartment indicating CS-substitution. **(B)** Portions of WT ADSC samples were run + chondroitinase and probed with a mixture of anti-TAS/anti-KEEE to detected CS-region aggrecanase neo-epitopes and separately with anti-GVA to detect calpain mediated aggrecan cleavage. This shows bands 1, 2 and 4 are CS-region aggrecanase neo-epitopes and band 3 is a calpain generated fragment. **(C)** Proteoglycans from cell-associated and medium compartments of chondrocyte cultures from WT and TS5P KO mice were run +/- chondroitinase ABC to determine the degree of CS-substitution; aggrecan core protein was detected by anti-DLS. All bands except band 4 were CS-substituted, the greatest of which was a high molecular weight band (small arrows). A1A1 lane is 10 µg A1A1 purified human aggrecan as positive control.

Aggrecan synthesis by ADSCs is stimulated by increased extracellular glucose, but not by TGFb1 or BMP-7

Multiple studies have shown that supplementing media with TGFb1 or BMP-7 results in increased production of a sulfated GAG rich ECM in multipotent stromal cells [175-178], and this is largely due to increased production of CS-substituted aggrecan. We therefore supplemented ADSCs from all three genotypes with the two growth factors, but did not detect any changes in the amount of aggrecan deposited in the cell layers or secreted into the medium (**Fig. 18A**), the same was seen for chondrocytes (**Fig. 18B**).

However, increasing the extracellular glucose concentration from 5 to 10 mM, (**Fig. 17A**) resulted in a notable increase in aggrecan secretion in all three genotypes. Products in both medium and cell layer pools were more highly substituted with CS and also enriched in a >250 kDa core protein species that was essentially absent in ADSCs grown in 5 mM glucose, but abundant in epiphyseal chondrocytes cultures maintained at the lower glucose concentration (see **Fig. 16C**). The enhanced aggrecan synthesis was more pronounced in TS5-deficient cells, and this may be related to their enhanced glucose uptake relative to WT cells (**Fig. 17D**). Thus, at the physiological (5 mM) concentration, TS5P KO ADSCs had a significantly increased uptake (0.53 +/-0.01 µmoles glucose /µg DNA/24h) compared to WT cultures (0.26 +/-0.03 µmoles glucose /µg DNA/24h) or TS5J KO (0.38+/-0.11) cultures. Moreover, under mildly hyperglycemic (10mM) conditions, all cultures showed a proportional increase in glucose uptake, with the TS5 deficient cells remaining more active at (1.07+/-

0.07 µmoles glucose /µg DNA/24h for TS5P KO and 1.03+/-0.02 for TS5J KO

µmoles glucose /µg DNA/24h) than WTs (0.73+/-0.05 µmoles glucose /µg

DNA/24h) cultures. Additionally, increased medium glucose caused ADSCs from

all three genotypes to deposit more 'Full Length' (~450kDa) versican into the cell

layer and medium compartments, similarly to aggrecan this was more

pronounced in TS5 KOs (**Fig. 17C**).
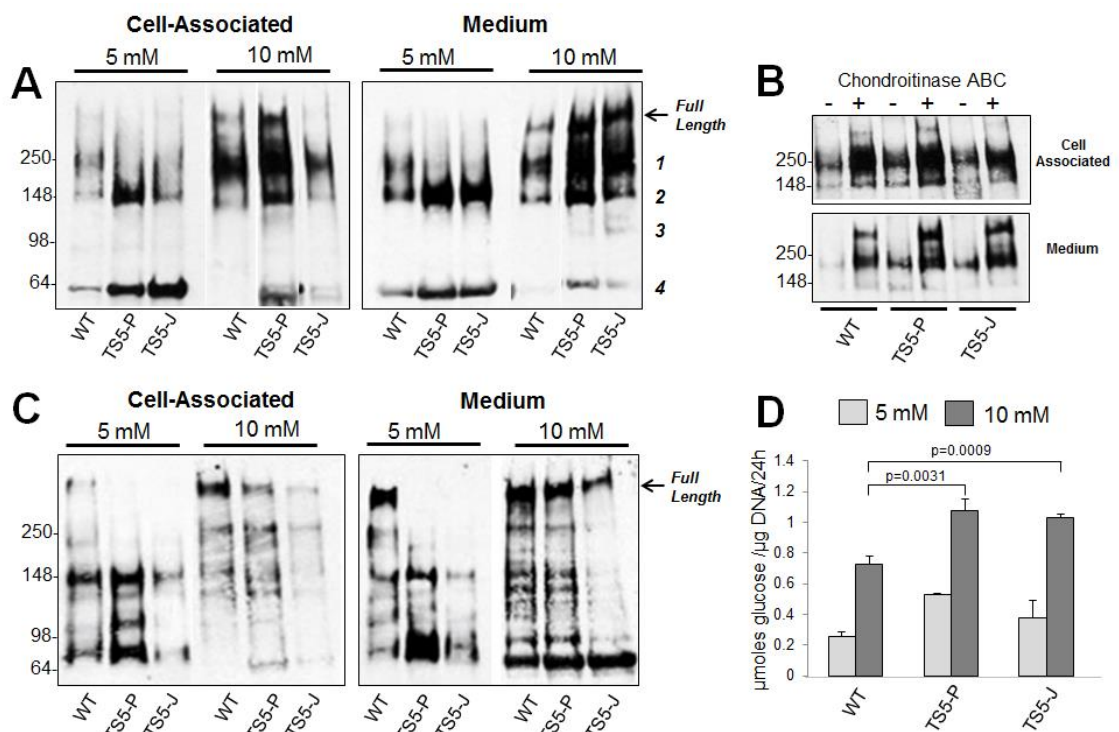
Figure 17. Aggrecan and Versican Synthesis are stimulated by extracellular glucose concentration in ADSCs from WT and TS5-deficient mice. (A) Western analysis of aggrecan core protein products generated in ADSC cultures after 24 h maintenance in medium supplemented with either 5 or 10 mM glucose, detected by anti-DLS. **(B)** Western blot assay for CS substitution of aggrecan core protein after 24 h maintenance in medium supplemented with 10 mM glucose, with and without chondroitinase ABC pretreatment of DE52 purified material (anti-DLS). **(C)** Western analysis of versican core protein products generated in ADSC cells after 24 h maintenance in medium supplemented with either 5 or 10 mM glucose (Ab1033). **(D)** Glucose uptake by ADSCs maintained in medium supplemented with 5 or 10 mM glucose. Glucose was measured in fresh medium and medium collected from cells after 24 h in culture, uptake was calculated as [glc at 0 h - glc at 24 h]. Assays were performed on n=3 individual cultures, and data are shown as µmol of glucose consumed per µg DNA per 24 h. Statistical significance (<0.05) was determined by students t-test.
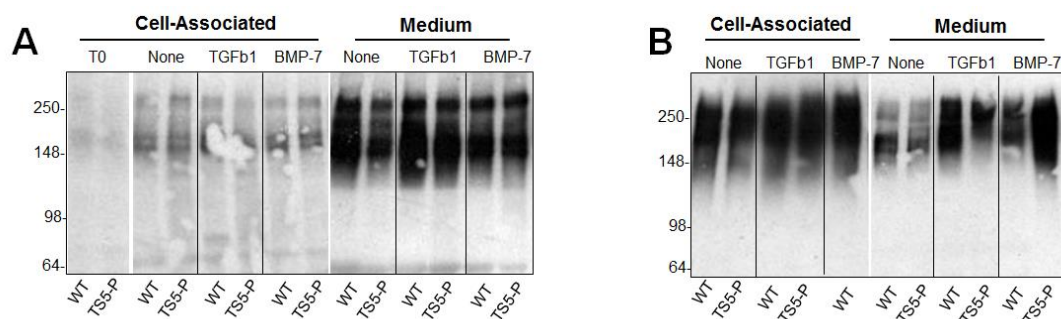
Figure 18. Aggrecan synthesis and secretion by ADSC and CHON cultures from WT and TS5P KO mice is not altered by addition of TGFb1 or BMP-7. (A) Western analysis of aggrecan core protein products generated in ADSC cultures after 24h maintenance in medium supplemented with either 10ng/mL TGFb1, 50ng/mL BMP-7 or 10% FBS only, detected by anti-DLS. T0 is Cell-Associated pretreatment. **(B)** Western analysis of aggrecan core protein products generated in chondrocyte cultures, same treatment as (A).

Aggrecan catabolism in serum deprived ADSCs from WT and TS5-deficient mouse strains

To examine if ADSCs have the capacity for ADAMTS-mediated cleavage of aggrecan, confluent cultures were washed in serum free medium and incubated in the 1% serum containing medium to promote matrix degradation (see **Fig. 8** and Methods for details). Analysis of the cell-layers prior to culture in low serum (**Fig. 19A**, 0 h) showed that all three genotypes had already accumulated the aggrecanase generated 60 kDa G1-NITEGE product, consistent with aggrecanase activity in the ADSC cultures even in the presence of 10% serum. Since serum α-2-macroglobulin is inhibitory for ADAMTS-aggrecanases [97], it is likely that the ADAMTS-mediated core protein cleavage occurs in an environment that is not accessible to the α-2-macroglobulin, which is most likely inside the cell, during the secretory process.

At 2 h and 6 h culture in low serum (**Fig. 19A**), cell layers of all three genotypes accumulated a 120 kDa NITEGE-reactive species. Furthermore, analyses of the culture medium collected during the 'catabolic' period showed that the majority of the dimeric G1-NITEGE product was retained in the cell–associated fraction in all three genotypes, and thus, as for the higher molecular weight aggrecanase fragments shown in (**Fig. 16B**), ADAMTS5 is not required for their generation in ADSCs. Validation of the identity of these species as aggrecan-derived G1 fragments was obtained from western analyses of products seen in catabolically stimulated epiphyseal chondrocyte cultures (**Fig. 19B**). Membranes in (**Fig. 19A**) were re-probed with anti-DLS (**Fig. 19C**), which confirmed the presence (at 0h only) of the 125 kDa-250 kDa forms in the cell layer of all genotypes (as in **Fig. 16A**), and these species disappeared from the cell layer and accumulated (to some extent) in the medium.

This higher molecular weight form of the aggrecanase G1 product is not due to aberrant glycosylation, since N-glycanase pre-treatment prior to western analysis did not alter the migration of the ~120 kDa NITEGE positive band (**Fig 19D**). It is highly likely that this represents the same "dimeric" form of G1-NITEGE, which had been previously reported by Yasumoto, T et al. ORS 1999, [179]) to be present in human cartilage extracts. Moreover, the formation of this dimeric form of G1-NITEGE, was not altered in cultures maintained in 10mM glucose (**Fig. 19E**), suggesting that the enhanced high molecular weight (>250 kDa) aggrecan deposition seen in 10 mM glucose cultures is not simply due to an impairment of aggrecanase-mediated catabolism.
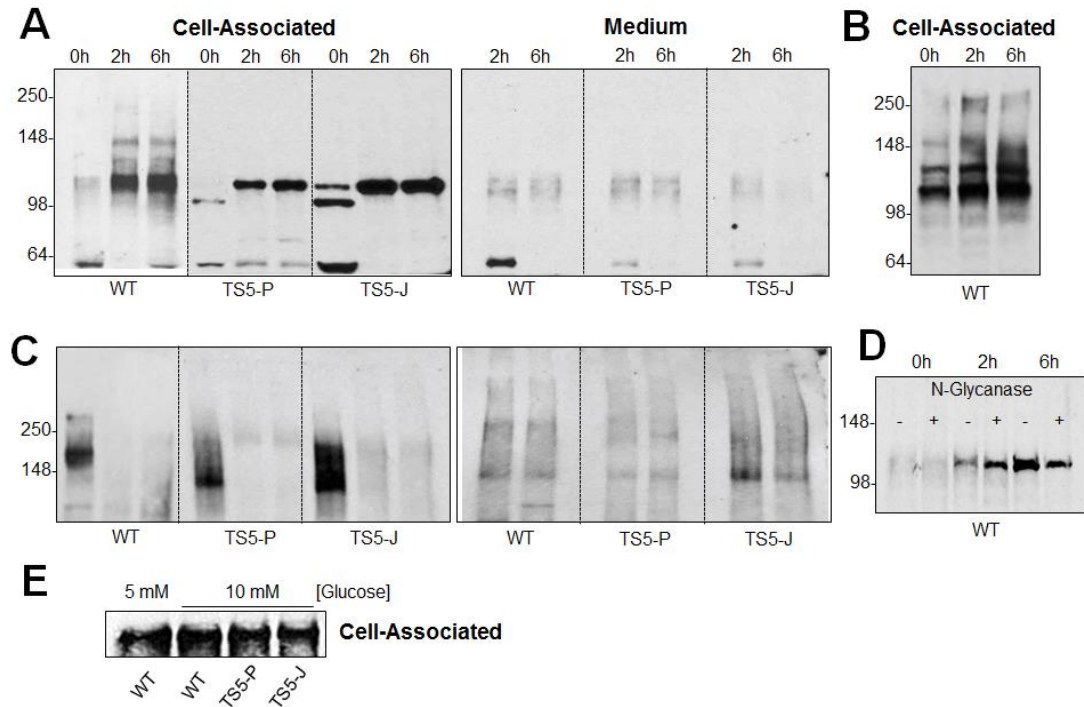
Figure 19. Western analysis of aggrecan catabolism in ADSC and CHON cultures from WT and TS5-deficient mice. Catabolic conditions were induced by changing cultures into media supplemented with only 1% serum and terminated at points indicated in Fig.8 and in the Methods. **(A)** anti-NITEGE (ADAMTS-generated G1 fragment) of cell associated products at 0, 2 and 6 h and media products at 2, 6 h from WT, TS5P KO, and TS5J KO ADSCs. **(B)** anti-NITEGE western blot of chondrocyte cell extracts, showing the presence of multimeric aggrecanase G1 products. **(C)** anti-DLS (aggrecan core protein) re-probe of panel (A) membrane showing catabolism of polydisperse aggrecan core protein upon serum starvation, with only a fraction recovered in the medium compartment at 2 and 6 h. **(D)** anti-NITEGE of separate cell-associated WT ADSC samples treated +/- N-glycanase, shows that electrophoretic mobility of aggrecanase G1 multimers is not affected by N-glycanase treatment. **(E)** anti-NITEGE of cell-associated products of WT and TS5KO ADSCs maintained in 5 mM or 10 mM glucose for 24h, shows that 10mM glucose does not affect the formation of aggrecanase G1 multimers.

Versican catabolism in serum deprived ADSCs from WT and TS5-deficient mouse strains

To examine the effect of a the low serum induced catabolic culture condition on versican degradation, media and cell extracts from ADSC cultures were examined by Western analysis with anti-DPE (**Fig. 20A**), followed by a re-probe of the membranes with Ab1033 (**Fig. 20B**). A single product of ~60 kDa (consistent with G1-DPEAAE) was detected in the cell-associated fraction at 0 h for all genotypes, showing that as for aggrecan G1-NITEGE, it was also formed in 10% FBS, and therefore perhaps generated intracellularly. The abundance of this product was not markedly altered during the 2 h or 6 h in 1% FBS, and remained distributed evenly between the cell-associated and medium compartments (unlike the G1-NITEGE which remained largely cell associated (**Fig. 19A**)). A re-probe of these membranes with Ab1033 (**Fig. 20B**) showed that in all genotypes the bulk of the ~450 kDa, ~140 kDa and ~120 kDa products were retained by the cell layer over this period, whereas the 110kDa (and ~75 kDa) products were distributed between the two compartments.
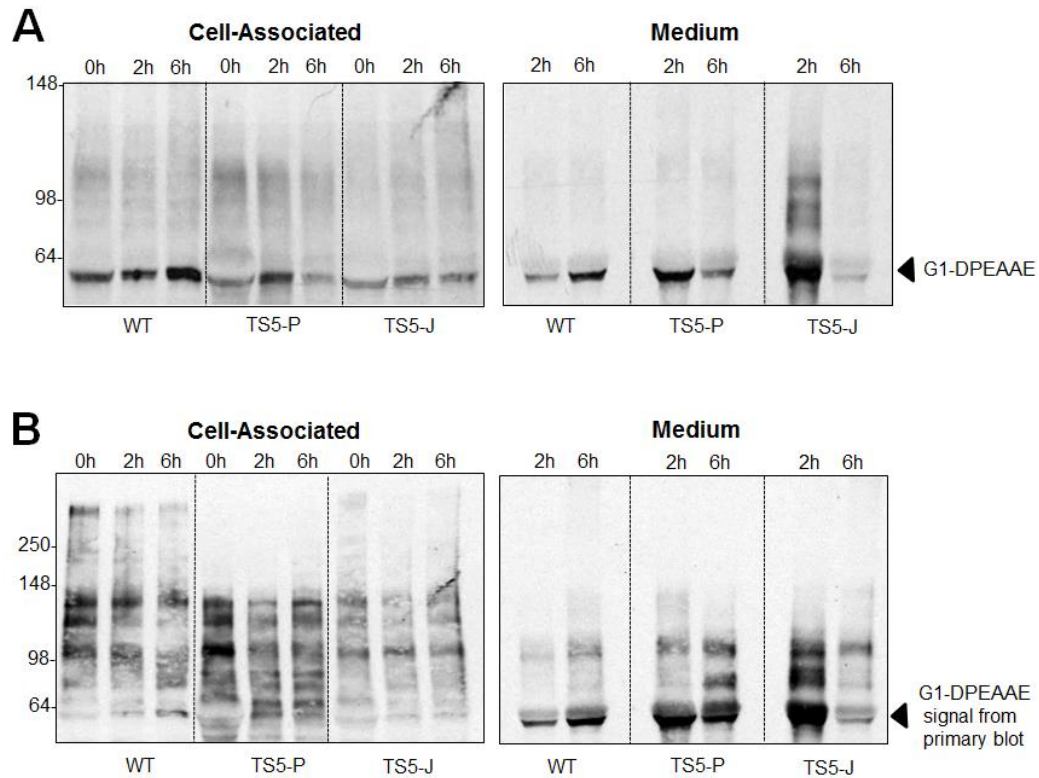
Figure 20. Western analysis of versican catabolism in ADSC cultures from WT and TS5-deficient mice. Catabolic conditions were induced by changing cultures into media supplemented with only 1% serum and terminated at points indicated in Fig. 8 and in the Methods. **(A)** anti-DPE (ADAMTS-generated G1 fragment) of cell-associated and media compartments from WT, TS5P KO, TS5J KO ADSCs. Distinct ~60 kDa G1-DPEAAE band is generated in all genotypes in 10% serum and is evenly distributed in cell layers and medium. ~60 kDa G1-DPEAAE generation does not appear to be affected by serum starvation. **(B)** Ab1033 reprobe of (A), ~450 kDa, ~140 kDa and ~120 kDa products retained in the cell layer, ~110 and ~75 kDa products are distributed in cell layer and medium, all of which are unaffected by serum starvation.
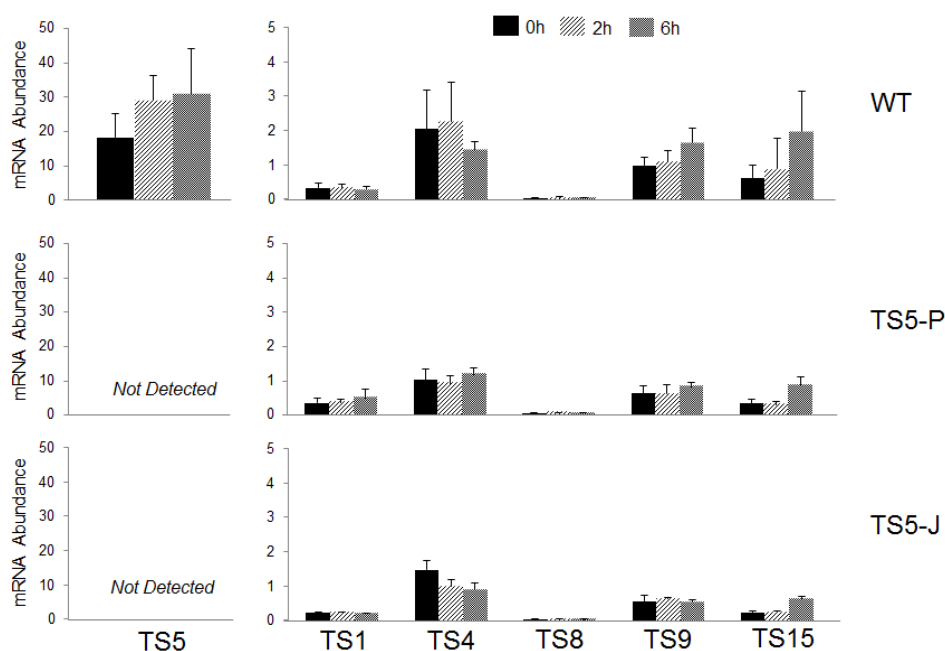
Figure 21. Gene expression of aggrecanases ADAMTS-1,-4,-5,-8,-9 and -15 in acute response to low serum in ADSCs from WT and TS5-deficient mice. Confluent cultures were changed to basal medium containing 1% serum and at 0 h, 2 h and 6 h, mRNA was isolated and QPCR done as described in 'Methods'. Data are plotted as relative mRNA abundance, error bars are standard deviation, relative abundance was calculated as $(2^{-\Delta Ct})*1000$ (arbitrary units), ΔCt relative to Gapdh. Not Detected had Ct values of 35 or greater, n = 3. Adamts5 expression is the highest out of all other aggrecanases in WT ADSCs followed by Adamts4. No compensatory up-regulation of other aggrecanases was detected in TS5-deficient ADSCs upon serum starvation.

Effect of TGFb1 stimulation on transcript abundance of Has1, Has2, Col1a1, Col1a2 and Col3a1 in ADSCs from WT and TS5P KO mice

To determine the response of ADSCs to TGFb1 stimulation, confluent monolayers were treated for 24 h in DMEM/10% FBS supplemented with TGFb1 alone or TGFb1 with TGFb RI/II Kinase inhibitor for 24 h after the 'T0' stage (see **Fig. 9** and Methods Section). TGFb1 signaling was assessed by determining changes in expression of previously reported TGFb1-sensitive genes such as Col1, [180,181], Col3 [182] and Has1 and 2 [183]. To focus the scope of this

study, the following experiments included only TS5P KO ADSCs to determine the effects of TS5 ablation.

Our results showed that transcript abundance of Has1 and Has2 was a sensitive and reproducible indicator of the TGFb1 responsiveness of the ADSC (**Table 6**). Transcripts abundance for Has1 and Has2 in unstimulated (FBS only control, 'None') WT ADSC was 0.755 +/-0.08 and 6.44 +/-1.70 respectively and following TGFb1 treatment, these levels were increased ~ 4 and 3 fold respectively. This increase was essentially completely inhibited by the inclusion of TGFb RI/II kinase inhibitor.

Surprisingly, Col1a1 transcripts were largely unaffected in WT ADSCs treated withTGFb1, and inclusion of the TGFb1+ RI/II inhibitor also had not effect. Furthermore, transcript for Col1a2 and Col3a were decreased in TGFb1 by 40 and 26 %, respectively, and RI/II inhibitor, indicating the involvement of other signaling pathways in the control of gene expression for these two collagen alpha-chains.

We next compared the response of ADSCs from TS5P KO mice to TGFb1 stimulation, and found several statistically significant changes between genotypes in the HAS1 and 2 responses. Has1 transcript abundance was increased only 1.7 fold in the KO cells and Has2 levels, which were already elevated the TS5 KO cells, were not further increased by TGFb1 stimulation. Moreover in TS5P KO cultures treated with TGFb1 and RI/II inhibitor, Has2 abundance dropped below FBS control 'None' levels (3.34+/-0.13).

Interestingly, the effect of TGFb1 on Col1 and Col3 transcript abundance was similar to that in WT cells, in that transcript levels for all three Col alpha chains assayed decreased, but this was not mediated directly by the signaling of TGFb1 through the RI/II pathways.

Gene	None		+ TGFb1		+ TGFb1 +RI/II Inhibitor	
	WT mRNA Abundance	TS5-P mRNA Abundance	WT Fold Naive	TS5-P Fold Naive	WT Fold Naive	TS5-P Fold Naive
Col1a1	1790 +/-96	2020 +/-160	1.31 +/-0.06 p=0.013	0.75 +/-0.04 p=0.0064	1.10 +/-0.05 p=0.037	0.95 +/-0.08 p=0.34
Col1a2	164 +/-11	205 +/- 17	0.40 +/-0.06 p=0.0002	0.34 +/-0.02 p=0.0001	0.28 +/-0.01 p=0.0001	0.09 +/-0.01 p=0.0001
Col3a1	141 +/-8.5	161 +/- 3.2	0.26 +/-0.03 p=0.0001	0.14 +/-0.01 p=0.0001	0.36 +/-0.02 p=0.0001	0.12 +/-0.01 p=0.0001
Has1	0.755 +/- 0.08	0.508 +/-0.041	4.12 +/-0.78 p=0.0005	1.79 +/-0.05 p=0.0015	0.24 +/-0.08 p=0.0041	0.27 +/-0.05 p=0.0012
Has2	6.44 +/-1.7	14.10 +/-1.00	3.18 0.56 p=0.0015	1.19 +/-0.14 p=0.087	0.96 +/-0.16 p=0.75	0.31 +/-0.03 p=0.0001

Table 6. Effect of TGFb1 on Fibrillar Collagen and Hyaluronan Synthase Gene Expression in WT and TS5P KO ADSC cultures. WT and TS5P KO ADSCs were treated with TGFb1, TGFb1 +RI/II Inhibitor or FBS only control (None) for 24 h and harvested for QPCR analysis as described in Methods. Values are mRNA abundance, calculated as $(2^{-\Delta Ct})*1000$ arbitrary units, +/- standard deviation, fold change was calculated by comparing treatment groups to 'None' using $2^{(-\Delta\Delta Ct)}$ method, ΔCt relative to Gapdh. n=3. p values are relative to 'None' within each genotype.

Synthesis, secretion and processing of collagen type I in ADSCs from WT mice

Collagen type I protein was assayed by Western blot using anti-Collagen type I (Southern Biotech), a rabbit polyclonal antibody raised against human collagen type I. This high affinity antibody has been used by a number of investigators in western blot analyses for collagen type I, and due to its reactivity with multiple epitopes on the collagen molecule it is a useful reagent to detect biosynthetic products in cell cultures [165]. The usefulness of this antibody for our studies is illustrated in (**Fig. 22**). A portion of 24 h conditioned medium from WT ADSCs, corresponding to the product of roughly ~ 5 x 10^3 cells was analyzed by Western blot and showed six immunoreactive species (left hand lane). These were identified based on their molecular sizes and sensitivity to BMP-1 digestion (**Fig. 22, middle and right lanes**). The ~148 kDa species represents pro-Col I a1 (containing both, proC and proN peptides); the ~125 kDa species is a mixture of proC-and proN-peptide containing Col Ia1 (pC/pN); the 115 kDa species is the fully processed Col Ia1; the 100 kDa species is the processed Col Ia2, the 35 and 25 kDa species are the Pro-C and Pro-N peptides, respectively.
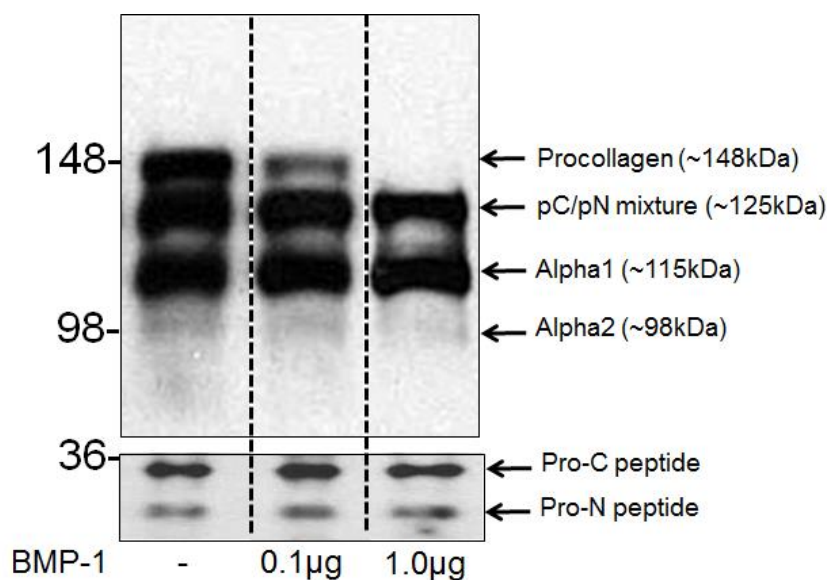
Figure 22. Western analysis of collagen type I from of ADSC cultures, digested with BMP-1. Media taken from ADSC cultures were digested with 0, 0.1 or 1.0 µg BMP-1 prior to western analysis as described in methods. Membranes were probed with anti-Collagen Type I, which reacts with 6 distinct bands (arrows); Procollagen (148 kDa), pro-C peptide containing alpha 1/pro-N containing alpha 1 mixture (125 kDa), Alpha 1 (115 kDa), Alpha 2 (98 kDa), single pro-C peptide (36 kDa) and single pro-N peptide (30 kDa). BMP-1 digest effectively cleaved the Pro-C peptide from the full collagen chains in a concentration dependent manner. Lanes are from a single gel, cut from different positions.

Effect of TGFb1 on the synthesis, secretion and processing of collagen Type I in ADSCs from WT and TS5P KO mice

Confluent ADSCs from WT and TS5P KO were maintained in DMEM medium, which does not contain ascorbate. The Western blot data of media and cell layers cultured in that medium confirmed that ascorbate is essential for collagen type I production and secretion in both, WT and TS5P KO ADSCs (**Fig. 23A, lanes 1&2**)

In the presence of ascorbate, (**Fig. 23A**) WT cells (**lane 3**) secreted significantly higher amounts Collagen I into the media and cell layers than the TS5P KO cells (**lane 6**), and this was most notable for the unprocessed pro-collagen and the fully processed alpha-1 chains. Those differences were not due to decreased cell numbers in the TS5P KO cultures, as seen by the roughly equivalent Western blot reactivity with anti-B-Actin of the cell extracts.

Addition of TGFb1 to the ADSC cultures had no major effect on the secretion of collagen I species into the culture medium. However TGFb1 markedly increased the amount of procollagen and pC/pN mixture in cell layers of WT, but not TS5P KO cultures (**Fig. 23A, lanes 4&7**). Addition of TGFbRI/II inhibitor only minimally affected the TGFb1 induced changes, suggesting that additional crosstalk between TGFb1 and other signaling networks (such as connective tissue growth factor (CTGF), and/or platelet derived growth fact (PDGF)) may be involved in the regulation of collagen type I synthesis and processing in the ADSCs.

Total collagen produced/unit cells/24 h was quantified by densitometry (using Image J (NIH) software), from band intensities of each collagen species normalized to B-Actin from the 0-24 h gels, and is shown in (**Fig. 23B**). TS5P KO cultures accumulate less collagen type I in both the media and cell-associated compartments, and TGFb1 induced increase in collagen type I production in WT ADSCs cell layers was not detected in TS5P KO ADSCs.

A

B
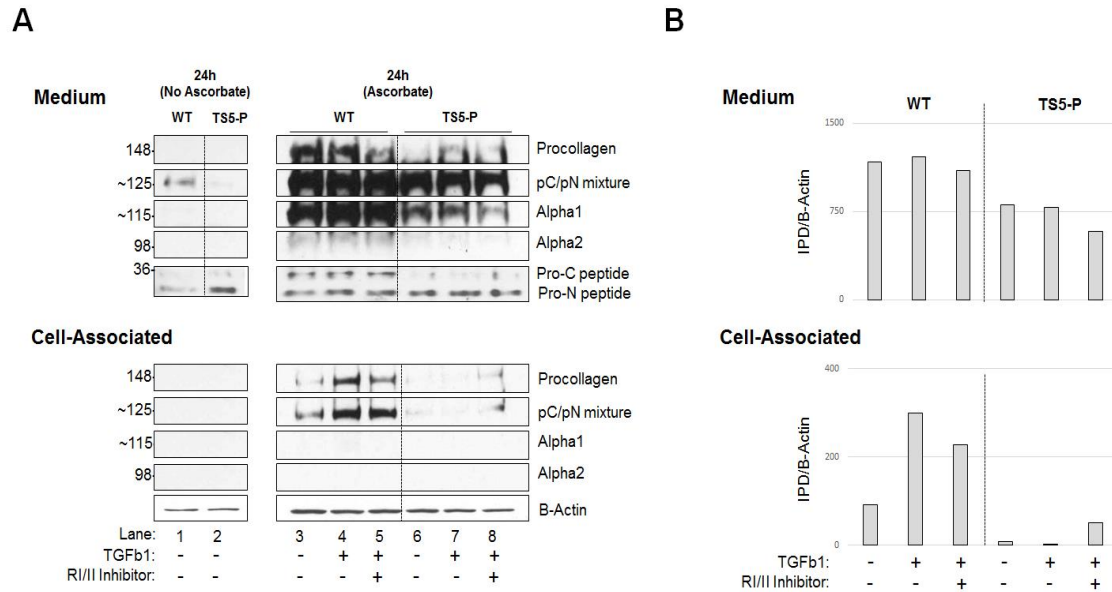
Figure 23. ADAMTS5 deletion affects TGFb1 induced collagen type I synthesis and secretion in ADSCs. **(A)** Media and cell associated compartments were harvested for western analysis with anti-Collagen Type I, from WT and TS5P KO ADSC cultures treated with FBS only control, TGFb1 and TGFb1+RI/II inhibitor as described in Methods. Cell associated membranes were reprobed with anti-B-Actin to ensure equal loading. **(B)** Densitometry of 'Total' collagen normalized to B-Actin.

Effect of MMP and ADAMTS5 protease inhibitors on collagen type I processing and secretion

To examine whether the lack of TGFb1 induced increases in cell associated collagen type I production in TS5P KO ADSCs could also be achieved in WT ADSCs through inhibition of the ADAMTS5 protease activity, WT cultures were incubated with 1, 3 and 9 µM Batimastat (BTM), a broad spectrum MMP inhibitor or with 1, 3 and 9 µM specific ADAMTS5 inhibitor (TS5i). Cells were pretreated for 60 min with the inhibitor, changed into media with ascorbate and TGFb1, and with the individual protease inhibitors for a 24 h culture period. Media and cell layers were analyzed by western blotting using anti- Collagen

type I (**Fig. 24**). BTM treatment resulted in the accumulation procollagen I in the

media and cell extracts (**compare lane 1 with lanes 2-4**), however, a parallel

decrease in Pro-C and Pro-N peptides (~35, ~25 kDa) was not observed. This

effect of BTM is most likely due to its inhibitory effect against ADAMTS 2, 3 and

14 all of which are known to cleave the collagen type I proN-peptide at a Pro-

Gln bond [43,184]**.**

The addition of TS5i to ADSC cultures did not affect the amount or type of

collagen type I species secreted into the medium (**Fig. 24 lane 1 compared to**

lanes 5-7). The presence of the inhibitor did however produce an increase in

procollagen and the pC/pN mixture in the cell associated compartment and also

resulted in appearance of lower mwt fragments (of 50 and 55 kDa, **Fig. 24 lanes**

5-7) in the cell layers in a concentration dependent manner. Although we did not

further identify these species, it is likely that they represent products of

intracellular degradation (possibly lysosomal) of newly synthesized collagens.

The interpretation of the gels was further confirmed with densitometry analysis of

single bands (**Fig. 25**) and total collagen type I (**Fig. 26**) normalized to B-Actin.

The distinct effects on collagen processing that arise from chemical

inhibition of ADAMTS5 protease activity and those seen due to ablation of the

Adamts5 gene in KO cells suggest that the catalytic site and the other domains of

the protein (see **Fig. 13**) may have separate biological functions.
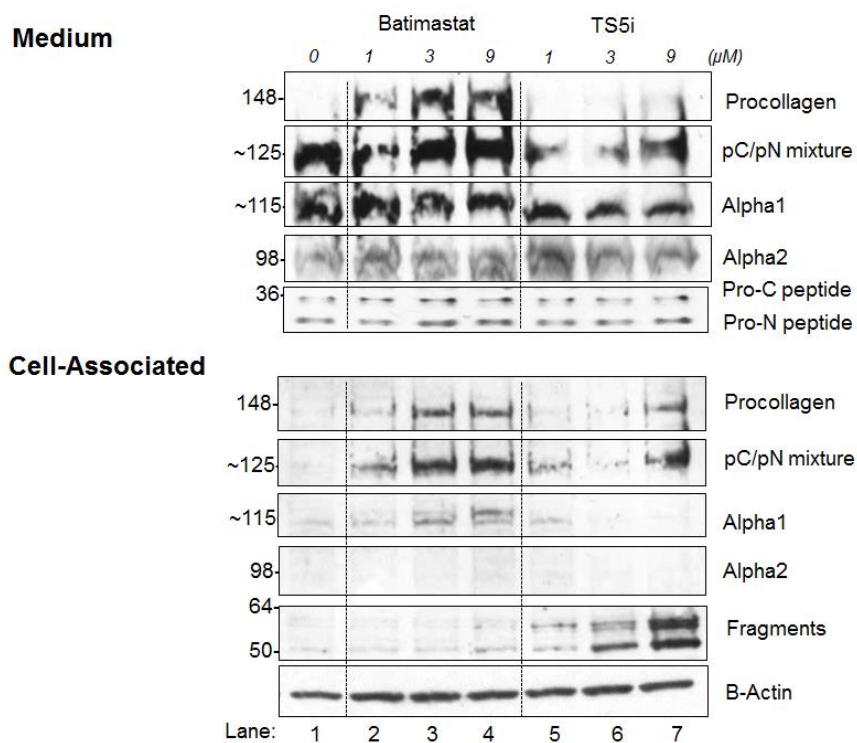
Figure 24. Effect of MMP and ADAMTS5 inhibitors on collagen type I synthesis and secretion in WT ADSCs. (A) Media and cell associated compartments were harvested for western analysis with anti-Collagen Type I, from WT ADSC cultures treated with TGFb1 and either Batimastat or TS5i at 0, 1, 3 or 9 μM as described in Methods. Cell associated membranes were reprobed with anti-B-Actin to insure equal loading.
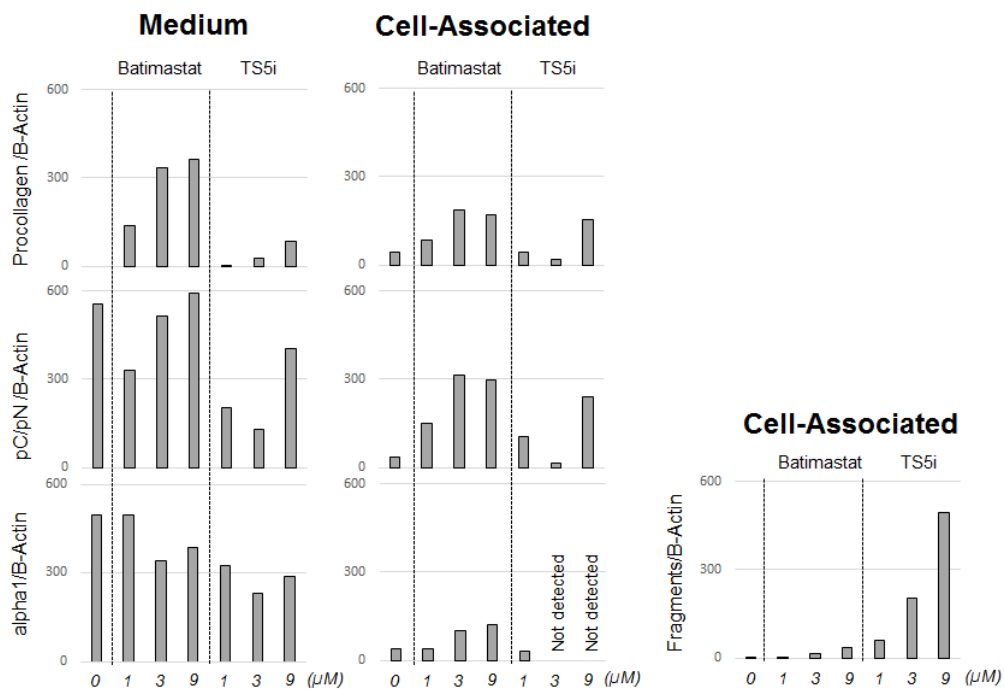
Figure 25. Quantitation of single anti-collagen type I reactive bands of MMP and ADAMTS5 inhibited WT ADSC cultures. Densitometry of single anti-collagen type I bands in Fig. 24, normalized to B-Actin.
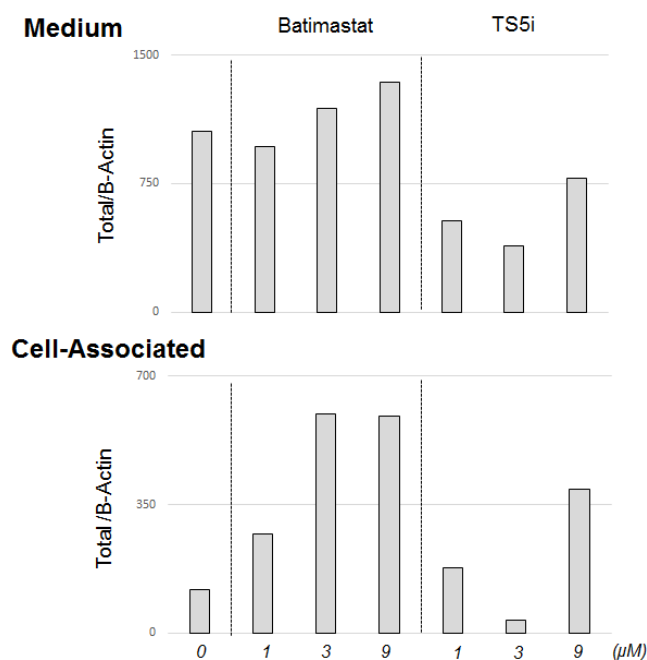
Figure 26. Quantitation of total anti-collagen type I reactive bands of MMP and ADAMTS5 inhibited WT ADSC cultures. Densitometry of 'Total' collagen (summation of all bands) in Fig. 24 normalized to B-Actin.

Detection of ADAMTS-fragments in WT ADSC cultures

Figs. 12 and 13 showed the presence of a range of proteolytically processed forms of ADAMTS5 protein in confluent monolayers of WT ADSCs. To examine the time course of formation of these fragments in both proliferating and confluent cultures, cell extracts were prepared at 24, 48, and 72 h post plating (see details in Methods). Extracts were analyzed by western blotting using the two anti-ADAMTS5 antibodies (α-Cys and α-Cat) (**Fig. 27a**), and abundance of the species relative to cell number (as B-Actin) was quantified using densitometry (**Fig. 27b**). It should be noted that ADAMTS5 protein secreted into the culture medium was not assayed due to the high content of endogenous ADAMTS5 protein and albumin in the fetal bovine serum.

All three cell-derived ADAMTS5 species (A, B, C) were generated in both, proliferating (0-24h, 24-48h) and post confluent cells (48-72 h), with fragment B being the most abundant species. All three were formed in the presence of 10 % fetal bovine serum. On a 'per cell basis", the abundance of fragment A remained fairly constant throughout the culture period, whereas fragments B and C were at the highest levels in proliferating cultures (24 and 48 h respectively) and then decreased notably in post-confluent cultures (72 h). Since we did not assay the medium compartment (see above) it is unknown whether the decreased contents of species B and C in post-confluent cultures is due to the diffusion into the medium compartment of clearance by further proteolysis and/or endocytosis.

We also examined the localization of fragments B and C to intra-cellular (trypsin-resistant) and extracellular (trypsin-sensitive) compartments (**Fig. 28a,**

b). Western blot analyses showed that at 4 h after plating, species B was only partially removed by trypsin digestion, suggesting both intra-and extracellular location of that fragment. By 24h post plating, fragment B was completely sensitive to trypsin, confirming its extracellular location. However fragment C remained only partially sensitive to trypsin even at that prolonged culture period, suggesting its association both outside the cells (cell surface or ECM) and inside the cells within the secretory [84,185,186] and/or endocytotic pathway [105].

To confirm the effectiveness of trypsin in removal of extracellular proteins in these experiments, the extracts were also assayed by western blot with anti-collagen Type I (**Fig. 28c**). The extensive removal by trypsin, of secreted procollagens from the cell layers under the conditions used, confirmed that that the conditions used here, allowed for effective enzymatic activity of the trypsin.
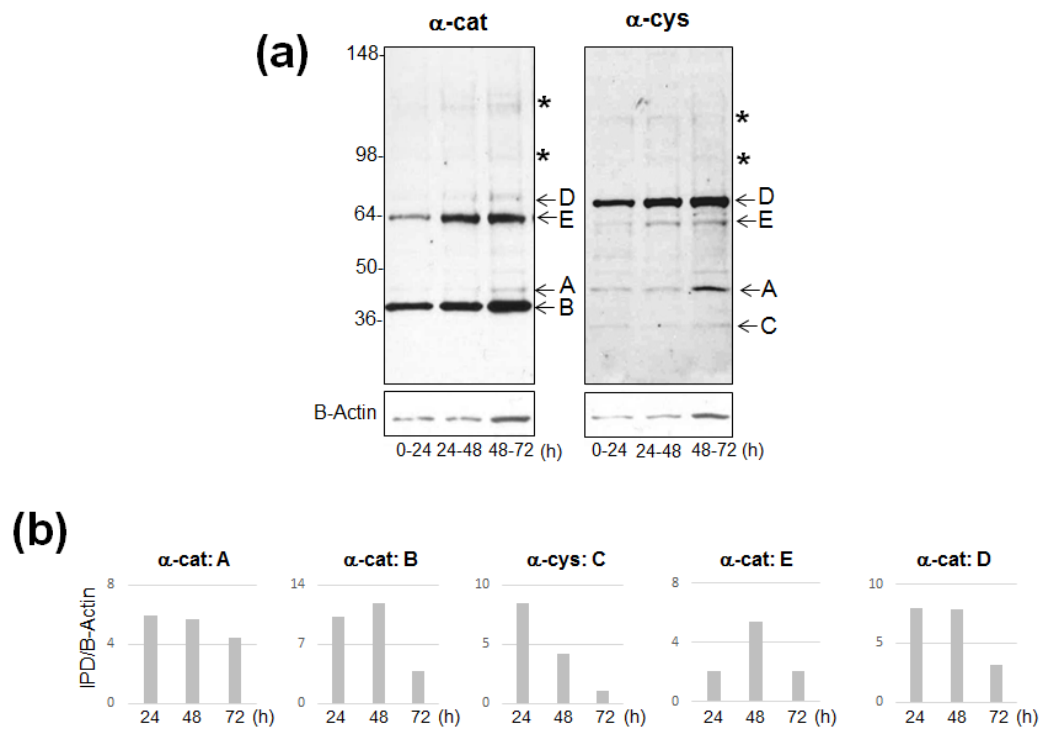
Figure 27. Western analysis of ADAMTS5 protein in proliferating and confluent ADSCs. (a) WT ADSCs were harvested throughout the culture period to determine ADAMTS5 abundance at the following time points post plating; 0-24 h (proliferating), 24-48 h (proliferating) and 48-72 h (confluent). Membranes were probed with anti-ADAMTS5 antibodies, directed towards the catalytic domain (α-cat) or the cysteine rich domain (α-cys), and then reprobed with anti-B-Actin to ensure equal loading. **(b)** Densitometry of individual fragments, normalized to B-Actin. Arrows indicate predicted fragments (A, B, C, D and E) based on Fig.13. Asterisk (*) denotes non-specific bands.
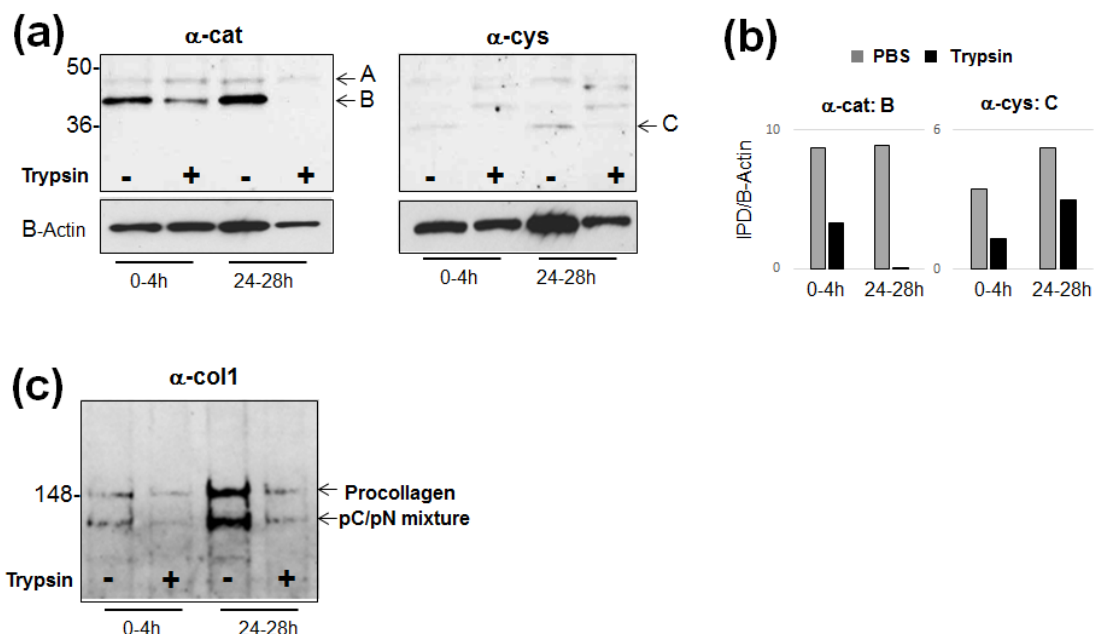
Figure 28. ADAMTS5 fragments are in an extracellular compartment. (a) ADSC cultures at 0-4 h and 24-28 h time points were digested +/- trypsin, supernatant discarded, and cell layers lysed as described in Methods prior to western analysis with anti-TS5 antibodies. Membranes were then reprobed with anti-B-Actin to ensure equal loading. Fragments A, B and C are denoted with arrows and refer to predicted species outlined in Fig. 13. **(b)** Densitometry of fragments B and C normalized to B-Actin. **(c)** α-cat membrane from (a) was reprobed with anti-collagen type I.

Effect of Protease Inhibitors on cell associated ADAMTS5

To determine if the formation of the ADAMTS5 fragments are generated by autocatalytic cleavage, as has been reported for other ADAMTS proteinases [187] or through the action of other MMPs, WT ADSCs were treated with TS5 inhibitor or the broad spectrum MMP inhibitor Batimastat as indicated in (**Fig. 29a** and in Methods). Western blot analyses of cell extracts (**Fig. 29b**) and densitometry analysis (**Fig. 29c**) showed that there was no significant decrease in the abundance of fragments A or B, when the inhibitors were added to the cultures at the 3 concentrations shown. However, the presence of either inhibitor

resulted in an apparent accumulation of the both fragments, and that was most notable for fragment A in the presence of TS5i. The mechanism for this accumulation is currently unknown but could arise from decreased clearance via proteolysis to smaller fragments (such as conversion of A to C, see **Fig. 13**), diffusion into the medium or endocytotic removal from the pericellular space. A potential role of MMP-mediated proteolysis in the generation of fragment C is shown in **Fig. 29b**, right hand panel), where both inhibitors decreased the abundance of this fragment relative to untreated cultures. Together with the accumulation of fragment A (**Fig. 29b,** left hand panel) this could indicate a precursor product relationship between those two species.
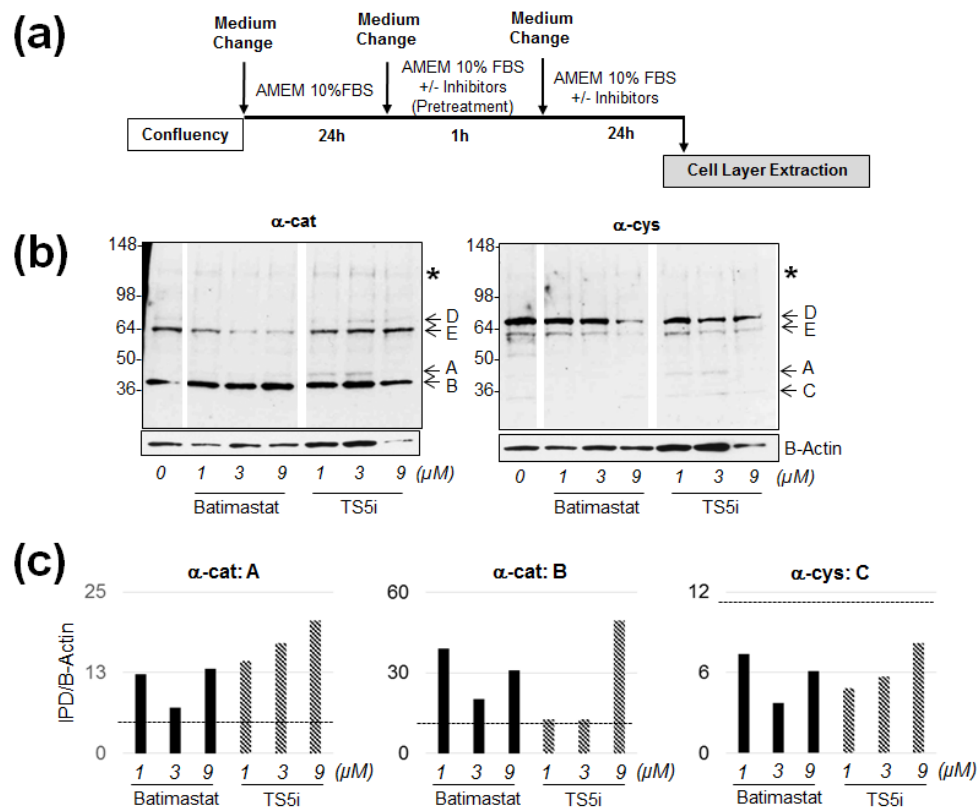
Figure 29. Effect of protease inhibitors on cell-associated ADAMT5 fragments. (a) Treatment timeline, confluent WT ADSCs were treated with Batimastat or TS5i at 0, 1, 3 or 9 μM for 24 h after a 1 h inhibitor pretreatment. **(b)** Cultures were terminated for western analysis with anti-TS5 antibodies. Membranes were then reprobed with anti-B-actin to ensure equal loading. Arrows indicate predicted fragments (A, B, C, D and E) based on Fig.13. Asterisk (*) denotes non-specific bands. **(c)** Densitometry of individual fragments normalized to B-Actin, horizontal dotted line represents control (0 μM).

TGFb1 treatment of WT ADSCs has no effect on cell associated ADAMTS-fragments

Since TS5KO fibroblasts [15] and the ADSCs used in this study displayed altered TGFb1 responsiveness, we tested the possibility that TGFb1 itself may alter the abundance of the cell associated TS5 fragments. Thus, cells were treated with growth factor using identical conditions that had resulted in the altered collagen production between WT and TS5-deficient cells (**see Figs. 23 & 24**). Western blot analyses of cell layers (**Fig. 30 a, b**) however showed no effect of TGFb1 on abundance of any of the cell generated TS5 species.
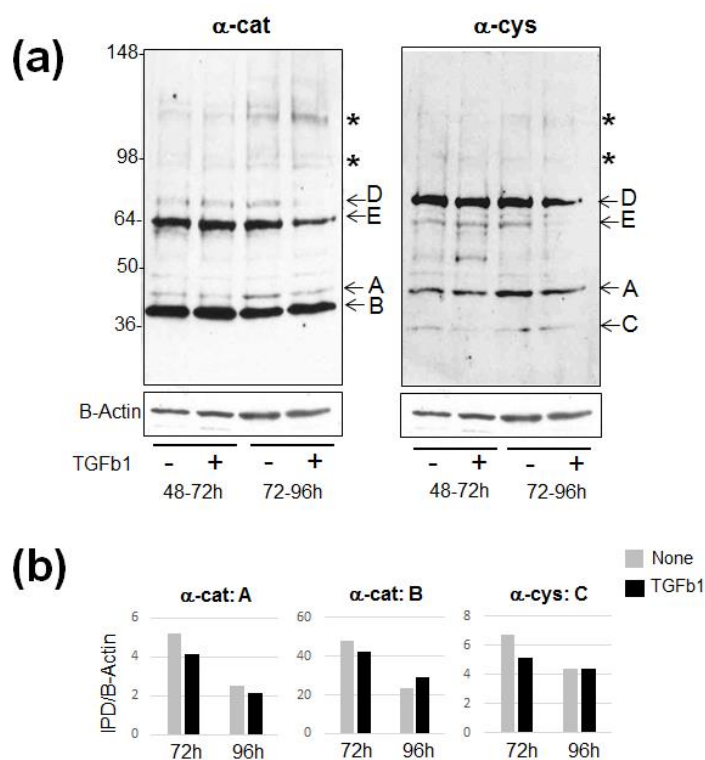
Figure 30. Western analysis of ADAMTS5 protein in confluent ADSCs stimulated with TGFb1. (a) Separate cultures were treated with or without TGFb1 at 48-72 h and 72-96 h time points, and harvested for western analysis using the same antibodies as in (Fig. 27A) **(b)** Densitometry of individual fragments, normalized to B-actin. Arrows indicate predicted fragments (A, B, C, D and E) based on Fig.13. Asterisk (*) denotes non-specific bands.

Effect of inhibitors of endosomal and lysosomal trafficking on abundance of ADAMTS5 fragments in WT ADSCs

ADAMTS5 has previously been reported to interact with LRP-1 on the cell surface [105] through the thrombospondin1 motif. Furthermore, the study also reported that Dynasore, a potent inhibitor of the clathrin-mediated endocytosis pathway in which LRP-1 participates [188], inhibited the uptake of exogenously added ADAMTS5 protein in articular cartilage. Since all three fragments detected in the ADSC cultures (A, B and C) carry the LRP-1 binding site, we have investigated whether these fragments interact with the endocytotic pathway in these cells.

In control cultures, all three fragments were detected (**Fig. 32 a, b**), and as shown above, fragment B was the most abundant and accumulated with increasing culture time (**see Fig. 27a**). When cultures were treated with Dynasore for 4 h and 24 h, and equal portions of the extracts examined by Western blotting, the accumulation of fragment B was completely inhibited, a similar effect was seen on fragment C, whereas changes were not detected for fragment A. Treatment of cultures with Bafilomycin A1, a broad spectrum inhibitor of endosomal/lysosomal acidification and trafficking, enhanced the accelerated accumulation of fragment B, relative to control conditions.

Together, these observations strongly suggest that the generation and/or accumulation of the ADAMTS5 fragments involve one or more components of the endosomal/lysosomal compartments. Whether such processes are merely required to remove the protein from the extracellular space, or whether the

specific fragments play a regulatory role in the functionality, (similar to the inactive processed form of MT1-MMP [189]) of the endosomal recycling process of cell surface receptors, including those of the TGFb-receptor family [134-136,148] remains to be determined.
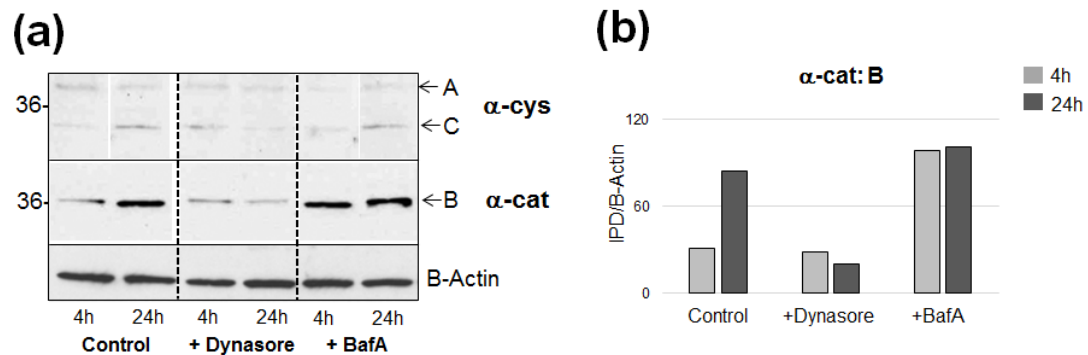
Figure 31. Abundance of ADAMTS5 fragments is altered with endocytosis and endosomal inhibitors. (a) ADSC cultures were treated with Dynasore, Bafilomycin A1 (BafA) or FBS only control, as described in Methods and harvested for western analysis using anti-TS5 antibodies at 0-4 h and 0-24 h time points. Membranes were then reprobed with anti-B-actin to ensure equal loading. Fragments A, B and C are denoted with arrows and refer to predicted species outlined in Fig. 13. **(b)** Densitometry of individual fragments normalized to B-actin.
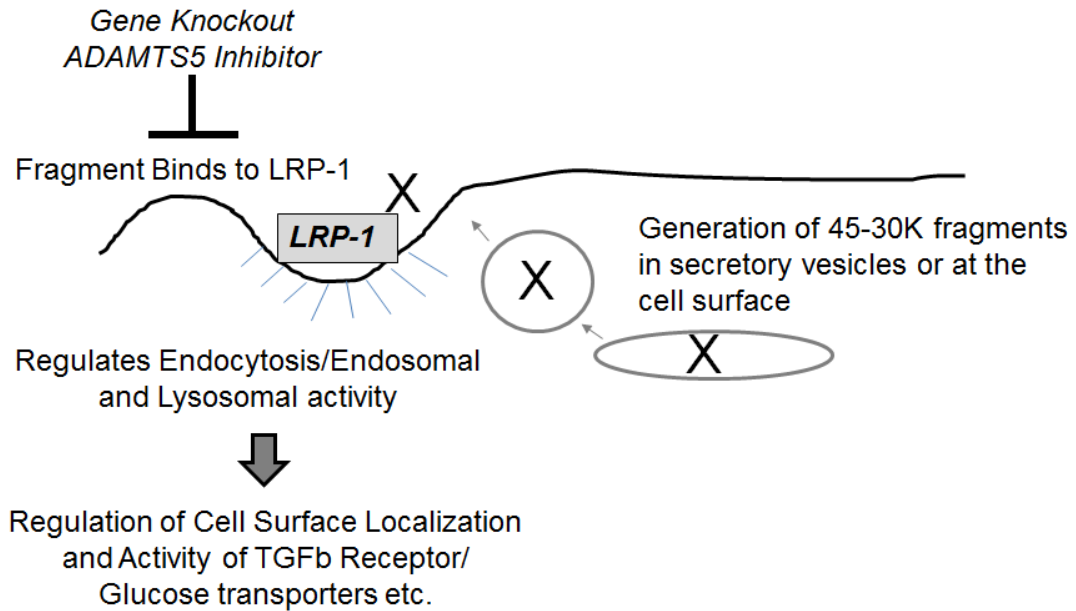
Figure 32. Proposed pathway of ADAMT5's function in progenitor cells. ADAMTS5 fragments denoted by 'X' interact with LRP-1 at the cell surface, working to regulate the endocytotic and lysosomal activity of progenitor cells, thereby affecting TGFb signaling and/or glucose transport and ultimately downstream differentiation pathways.

V. DISCUSSION

Characterization of ADSC cultures from WT and TS5 KO mice

To confirm the genetic deletions in both ADAMTS5 KO mouse strains used for this study, we genotyped ADSC cultures from WT and KO adipose tissue, using the standard genotyping primer sets for WT, TS5P KO [113] and TS5J KO (as per Jackson Labs). PCR analysis showed the expected absence of exon 2 in both KO strains and the additional LacZ+neo cassette insertion for the TS5J KO cells (**Fig. 10D, E**). Furthermore, the deletion designed for the TS5J KO had indeed resulted in an out-of-frame reading sequence in the mutated gene, as no mRNA transcripts of the mutated gene were detected [112]. However, although it was reported that the TS5P KO deletion was also designed to generate an out-of-frame mutation [113], we detected abundant mRNA transcripts for the mutated gene. These were devoid of exon 2 (**Fig. 10C, F and G**), which is indicative of an in-frame-deletion of the exon. We were however not able to detect secreted translated protein in the TS5P KO cells (**Fig. 12B**), which might result from degradation of either the mRNA or the mutated protein inside the cell. Whether this contributes to some of the differences observed between ADSCs from the two KO strains (e.g. HA production, cell surface marker expression) remains to be determined. In the same context, it is unknown as to what extent these mutations in the Adamts5 gene can affect transcriptional regulation of other genes involved in fibrogenesis, which then independently or

cumulatively give rise to the multiple connective tissue phenotypes in these mice (**Table 1**).

A common approach in studies using pluripotent cell population derived either from peripheral connective tissues (muscle, adipose tissue, synovium, bone marrow, umbilical cord, blood etc.), is the characterization of cell surface markers. In the context of this study, where we utilized progenitor cells from a 'mesenchymal' lineage and pluri-potential for differentiation into connective tissue producing cells, we have assayed for CD73, CD90, and CD105 which were described as relevant markers for such cells by the International Society for Cellular Therapy [9,27]. As has been reported previously for murine adipose derived stromal cells [20,190], ADSCs used in study also expressed these markers (**Table 3**). Although expression levels for these markers were similar between cells from all three genotypes, we observed a difference in expression of CD105. This gene was more highly expressed inTS5P KO cells than either WT or TS5J KO cells. Notably, CD105 or endoglin is a TGFb1/3 co-receptor that associates with TGFb type II receptor [191]. It has been previously reported that CD105-rich cell populations derived from human adipose derived stromal cells exhibited a more robust "chondrogenic" potential [192], whereas cells with low or deficient CD105 expression will more readily differentiate into an osteogenic phenotype [193,194]. This is in support of our previous research detailing the robust chondrogenic response in tendons [17], skin [15], and joints [114] after injury in these mice.

It is worth noting that we also detected robust expression of the three progenitor cell markers in primary cultures of epiphyseal chondrocytes. One possible explanation for these results could be the observation (**Fig. 6**) that such cultures always contain, in addition to the typically polygonally shaped chondrocytes, a population of cells with more elongated morphologies, which could represent the co-isolation of progenitor-cells from the epiphyseal growth cartilage used here [195]. Alternatively, the expression of CD73, CD90 and CD105 could be attributed to the presence of fibroblastic cells derived from adherent perichondrium, not removed in the first digestion period, as these markers have been previously reported to be abundantly expressed on 'differentiated' skin and lung fibroblasts in culture [33].

ECM gene expression and synthesis in ADSC cultures

ADSCs ECM gene expression profiling confirmed their fibroblastic characteristics [34,35], based on the high abundance of transcripts for Col1a1, Col1a2 and Col3a1, Vcan V1 (formerly V0) and V2, Has1 and Has2 as well as Halpn3 (link protein 3) (**Tables 4 and 5**). Expression for chondrogenic genes such as Acan, Col2a1 and Hapln1 (link protein 1) [28] were robustly expressed in our chondrocyte cultures (**Tables 4 and 5**) but were essentially undetectable in the ADSC cultures. In keeping with 'fibroblastic' cells in the epiphyseal chondrocyte cultures used in this study, mRNA transcripts for this cell type, namely Col1a1, Col3a1, Vcan V1, Vcan V2 and Halpn3 were readily detectable.

In all of the cultures analyzed for gene expression (n=6), we noted that both TS5KO strains had significantly lower levels of mRNA transcript abundance for Col1a1 and Col3a1, as had been observed for both skin and skin fibroblasts [15,114]. We also observed that the TS5P KO cells had increased Has1, Has2 and Hapln3 expression compared to either WT or TS5J KO cells, and that this unique effect could be related to the difference in the mutated gene between the two KO stains (**Fig. 10**).

In concurrence with the mRNA transcript abundance, versican synthesis and secretion was also readily detected in the ADSC and chondrocytes cultures, using Western blots with antibody Ab1033, which reacts with epitopes in the beta-GAG domain (**see Fig. 3**). The majority of immune-reactive versican in both, medium and cell layer compartments was in proteolytically processed fragments, with only a minor portion recovered as the intact core protein (mwt >250 kDa). All immunoreactive species were substituted with chondroitin sulfate (**Fig. 15B**) in keeping with the AB1033 epitope location in the CS-substituted region of the core protein. There were no significant qualitative or quantitative differences between the three genotypes. Moreover, equivalent analyses of versican in chondrocyte cultures showed there to be great similarity in synthesis and processing of this proteoglycan between the two cell types.

Immunostaining of ADSC cell layers with Ab1033 showed the localization of versican throughout the ECM. We believe this is in association with HA, since immunoreactivity was greatly diminished after Strep. Hyase digestion (data not shown). Although we did not assay for link protein in this manner, the lack of

mRNA transcripts for link proteins 1 and 3 in ADSC cultures might suggest that versican is not link-stabilized in association with HA, but could be associated with a cross-linked HA network [196,197] generated by heavy chain transfer from the inter-alpha-inhibitor (I-alpha-I) present in the fetal bovine serum growth supplement. Alternatively, IHC staining pattern as fibrillar structures, may indicate that versican is co-localized to the fibronectin network in the ECM of the fibroblastic cells [198,199].

Collagen type I synthesis and secretion by ADSCs from all three genotypes was assayed by Western blot and was readily detected in both media and cell associated compartments with the majority of the immunoreactive protein recovered in the media. We detected unprocessed forms (procollagen (~148 kDa), proC/proN mixture (~125 kDa)) as well as alpha I (~115 kDa) and alpha 2 (~98 kDa) chains (**Figs. 22-24**). Furthermore, western blot analyses showed that the lower mRNA transcript abundance for Col1a1 in the TS5P KO cells, relative to the WT cells, was accompanied by a decreased synthesis and secretion of the protein in these cells (**Fig. 23A**).

Previous reports from our lab [15,200] have shown that fibroblasts synthesize and secrete aggrecan, despite a very low level of transcripts for the proteoglycan core protein. It has also been widely reported that 'non-differentiated' mesenchymal progenitor cells lack transcripts for aggrecan [32], but that treatment of such cells with chondrogenic media (i.e. supplementation with dexamethasone and TGFb/BMPs) will induce gene expression and production of this proteoglycan [201,202]. The absence (or very low abundance)

of Acan transcripts was also seen in the ADSC cultures used in the present study (**Table 5**). However, western analyses of medium and cell extracts from these cultures showed the production of abundant amounts of aggrecan in an undifferentiated state, the majority of which was secreted into the media and substituted with CS [203,204]. The small amount of cell-associated aggrecan represents an intracellular pool of core protein as confirmed by IHC staining (**Fig. 14B middle row**) and the lack of CS substitution (**Fig. 16A**). As seen for versican, the majority of the aggrecan present in the ADSC cultures was in a proteolytically processed form, due to ADAMTS and calpain activities. The finding that the fragmented aggrecan and versican core proteins are generated in cultures containing fetal bovine serum, which contains potent protease inhibitors, such as α-2-macroglobulin suggests that ADSCs (as well as murine chondrocytes) display very active proteolysis of aggrecan and versican core proteins inside the cell, and that the enzymes responsible for the processing are co-localized in the secretory compartment of these proteoglycans, as has been reported for calpain [205]. Alternatively, the proteolytic step could occur at the cell surface in a compartment that might be inaccessible to the serum derived protease inhibitors [206].

The functional significance of aggrecan production by undifferentiated stromal cells and fibroblasts is unclear, since it is not required for building or maintaining an extracellular matrix, as is the case for chondrocytes. However, we considered the possibility that aggrecan core protein is an effective acceptor for the high energy (ATP) consuming synthesis of chondroitin sulfate. It is well

known that pluripotent cells at a wound site are exposed to a large number of 'stress' and 'survival' signals that may also alter metabolic pathways inside the cells that would include glycolysis and the ATP production. We considered the possibility that a pool of intracellular aggrecan core protein may serve as a regulator for elimination of excess intracellular ATP through CS substitution and secretion into the extracellular space. Therefore, we exposed ADSCs to an increased concentration of glucose and determined the relationship between glucose uptake into the cells and aggrecan production. As shown in **Fig. 17**, for WT ADSCs, a doubling of the medium glucose concentration from 5 mM to 10 mM resulted in an equivalent (~2 fold) increase of its uptake by WT ADSCs and a notable increase in secretion of CS substituted aggrecan in both cell associated and medium pools. In addition, full length unprocessed core protein was readily detected under increased glucose utilization. ADSC cultures from both TS5 KO strains also showed the proportional increase in glucose uptake and subsequent increased secretion of aggrecan. The stimulated aggrecan production was more pronounced in the KO cells, and this correlated strongly with the higher amounts of glucose taken up by the KO cells, compared to WT cells, under the same extracellular glucose concentrations. Notably, enhanced glucose uptake also modified versican accumulation, and this was seen predominantly as the high molecular weight unprocessed core protein.

Because glucose uptake is largely dependent on GLUT availability on the cell surface and since the activity of GLUT 1 and 4 are regulated by endosomal recycling pathways, including a wide range of other cell surface transporters and

receptors [150-153], ADAMTS5 may play a role in the normal turnover of glucose transporters, possibly via an endocytotic mechanism. Therefore, without ADAMTS5, GLUTs are left on the cell surface, leading to enhanced glucose uptake, resulting in increased aggrecan deposition.

Cumulatively, the data indeed support the idea that aggrecan and potentially versican core protein serve a specialized function in these cells, i.e. to stabilize the ATP levels under stimulated glucose transport into the cells. These findings need to be taken into consideration for interpreting 'chondrogenic' differentiation responses in pluripotent cells. Thus, assay of sulfated GAG accumulation as a chondrogenic differentiation indicator maybe misleading, as the cells under study may still be in a transition or even an undifferentiated state, and only display a transient response to increased glucose concentrations in the medium and/or supplementation with factors that enhance the glucose transport system.

Aggrecan and Versican Processing during ECM turnover in ADSCs

In WT ADSCs and CHONs, maintained in 10% FBS supplemented medium, ADAMTS generated fragments of both aggrecan and versican were present. For aggrecan the cleavages occurred in both the CS-domain and the interglobular domain sites, generating fragments with the C-terminal neo-epitopes KEEE/TASELE and some NITEGE respectively, that have been previously shown [159,160,167]. Proteolytic fragments of versican, including the ADAMTS-generated G1 fragment with the C-terminal neoepitope sequence DPE were also abundantly present.

Removal of serum from the culture medium resulted in an increase in the ADAMTS generated aggrecan product of ~120 kDa tentatively identified as a dimer of the established aggrecanase-G1 product, previously reported in extracts of human cartilage [179] and suggest that this type of reaction is not simply a culture artefact but actually represents a set of aggrecan processing reactions that occur in vivo.

It was also noted that the ADAMTS cleavages took place in the presence of 10% serum, in contrast to previous reports on aggrecanolysis in cultures of rat chondrosarcoma cells [86,160], where degradation could only be seen in serum free conditions, presumably due to the presence of alpha-2-macroglobulin in serum, which has been shown to be a potent inhibitor of the ADAMTS-aggrecanases [99].

The most likely explanation for this discrepancy is that under basal culture conditions, ADAMTS cleavage occurs inside the cell, possibly in the secretory pathway after ADAMTS pro-domain removal by furin [84]. In this context, intracellular processing of aggrecan core protein by the ER/Golgi associated enzyme calpain has also been described [205].

ADAMTS mediated versican processing also appeared to be intracellular in ADSCs as it readily occurred in serum supplemented cultures. Unlike for aggrecan, subsequent maintenance in low serum did not result in an increase the abundance of the versican G1 (anti-DPE ~60kDa) or other proteolytic products, suggesting that there is no broadly distributed ADAMTS-aggrecanase activity in these cultures, and that the enhanced action of ADAMTS-aggrecanases to

generate the aggrecan G1-NITEGE fragment occurs in a distinct spatial localization, potentially inside the cell or at the cell surface, as only minor amounts of the NITEGE product are recovered in the medium.

Most notable was the finding that the types of fragments and their abundances were essentially identical in chondrocyte and ADSC cultures derived from the two TS5 KO strains, confirming our previous report [114] that the proteolytic function of ADAMTS5 as an aggrecanase and versicanase is largely redundant in the murine ADSCs and chondrocytes in vitro. We examined the possibility that the lack of ADAMTS5 might induce other ADAMTS-aggrecanases, but QPCR assays of transcript abundance for those proteases did not reveal any compensatory increases in their expression in ADAMTS5-deficient ADSCs (**Fig. 21**).

A non-catalytic role for ADAMTS5 in ADSCs

A possible biological role for other domains within the ADAMTS protein, especially the thrombospondin motif with binding activity for LRP-1 [105], was supported by our observation that the predominant immunoreactive ADAMTS5 species associated with the cells were proteolytic fragments with apparent mwts of 45, 40 and 30 kDa. Based on the location of the epitopes recognized by the two anti-ADAMTS5 antibodies used here and in published studies [207], only the 45 kDa fragment contains an intact catalytic domain (**Fig. 13**). Interestingly, the 40 and 30 kDa fragments are extracellular, as established by their sensitivity to trypsin digestion, whereas the 45 kDa fragment was not.

We were unable to assay ADAMTS5 species in the medium, due to high background from the ~75 kDa and ~64 kDa serum derived species. Notably, this species also accumulated in cell layers (**Figs. 13 and 27**), indicating that there must be a receptor/binding partner in the cell layer/cell surface.

It remains to be determined which protease is responsible for the generation of ADAMTS5 fragments and which cytokine or growth factor signaling pathway that controls these steps. Thus, neither the broad spectrum MMP inhibitor Batimastat, nor the ADAMTS5 specific inhibitor blocked the formation of the fragments (**Fig. 29**). We were, however, able to demonstrate that disruption of endosomal or lysosomal trafficking and acidification by Dynasore or Bafilomycin A1, altered the abundance of the fragments (**Fig. 31**), confirming a recently published observation [105] that ADAMTS5, can bind to LRP-1 through its thrombospondin motif and thus become cargo for the clathrin mediated endocytosis pathway. It should be noted that this vesicular trafficking pathway has been implicated in regulation of abundance and thus activity of cell surface receptors and transporters. Amongst those are TGFb receptors I and II and the glucose transporters, the activities of which have been found to be altered in the TS5 KO cells [15] (**Fig. 17**). Future experiments designed to specifically alter LRP-1 expression on the cell surface in WT cells might alter the abundance and distribution of the ADAMTS5 fragments and shed light on the mechanism by which the non-catalytic domains of the ADAMTS5 protein can affect multiple cellular activities in the fibrogenic repair pathway.

We confirmed in this study the previous observation from our lab that TGFb signal transduction is impaired in the absence of ADAMTS5 protein. Using a different cell type (ADSCs, instead of fibroblasts) and downstream 'reporter' genes for TGFb1 stimulation, Has 1 and Has 2 [165,177,197-200], we found a total lack of stimulation of those two genes by TGFb1 in the TS5P KO ADSCs, and this lack of response was also seen when TGFb RI/RII inhibitor was included during TGFb1 treatment of WT ADSC cultures. Furthermore, when we examined TGFb1 stimulated collagen I secretion in ADSCs from WT and TS5P KO mice, TS5P KO cells were deficient in their response relative to WT cells. Addition of ADAMTS5 inhibitor (TS5i) during TGFb1 stimulation in WT ADSCs did not mimic the TS5P KO phenotype, which lends further support to our current hypothesis, that regulation of pro-fibrogenic TGFb1 signaling by ADAMTS5 is not primarily dependent on a functional catalytic domain of the protein. We did however, find that cell layer extracts of TS5i-treated WT cultures showed an abundance of lower mwt fragments (50-60 kDa) of collagen type I (**Fig. 24**), which are most likely of lysosomal origin [124,126] (**Fig. 5**). This observation is further support of our hypothesis for a close link between ADAMTS5 protein and endosomal/lysosomal function.

Summary and Future Directions

We are reporting two major new findings: Firstly, undifferentiated pluripotent ADSCs synthesize and secrete CS-substituted aggrecan into their medium compartment and, on a per cell basis, in amounts similar to that secreted by

chondrocytes. The correlation between the amount of glucose taken up by these cells and the synthesis of CS bearing aggrecan and versican suggests that sulfated GAG substitution on aggrecan and versican core proteins represent a convenient way to utilize excess ATP that may arise in the highly active environment of a healing wound.

The second major finding is the redundancy of ADAMTS5 as an aggrecanase and versicanase during the ECM turnover of the adipose derived stromal cells, as ADAMTS-generated fragments are quantitatively and qualitatively identical in WT and TS5-deficient cultures. Moreover, accumulation of a unique set of ADAMTS5 fragments in vivo and in vitro – which all contain the LRP-1 binding domain – favors a major functional role of the ADAMTS5 protein in regulating endosomal and lysosomal recycling and degradation of cell surface associated receptors and transport proteins (**Fig. 32**). Such a function would be entirely in keeping with range of observations linking the role of ADAMTS5 to a robust fibrogenic response required for soft tissue maintenance and regeneration (**Table 1**).

Future work will be directed towards confirming the functional association between ADAMTS5 fragments and LRP-1 mediated pathways in ADSCs. A study of such pathways in regulation of the multilineage differentiation capabilities ADSCs should shed further light on effective healing and regeneration of fibrous connective tissues such skin, tendon and ligaments.

REFERENCES

1. Singer, A. J., and Clark, R. A. (1999) Cutaneous wound healing. *The New England journal of medicine* **341**, 738-746

2. Marsh, D. R., and Li, G. (1999) The biology of fracture healing: optimising outcome. *British medical bulletin* **55**, 856-869

3. Blijlevens, N. M., Donnelly, J. P., and De Pauw, B. E. (2000) Mucosal barrier injury: biology, pathology, clinical counterparts and consequences of intensive treatment for haematological malignancy: an overview. *Bone marrow transplantation* **25**, 1269-1278

4. Velnar, T., Bailey, T., and Smrkolj, V. (2009) The wound healing process: an overview of the cellular and molecular mechanisms. *The Journal of international medical research* **37**, 1528-1542

5. Laurens, N., Koolwijk, P., and de Maat, M. P. (2006) Fibrin structure and wound healing. *Journal of thrombosis and haemostasis : JTH* **4**, 932-939

6. Pool, J. G. (1977) Normal hemostatic mechanisms: a review. *The American journal of medical technology* **43**, 776-780

7. Nurden, A. T., Nurden, P., Sanchez, M., Andia, I., and Anitua, E. (2008) Platelets and wound healing. *Frontiers in bioscience : a journal and virtual library* **13**, 3532-3548

8. Barrientos, S., Stojadinovic, O., Golinko, M. S., Brem, H., and Tomic-Canic, M. (2008) Growth factors and cytokines in wound healing. *Wound repair and regeneration : official publication of the Wound Healing Society [and] the European Tissue Repair Society* **16**, 585-601

9. Phinney, D. G., and Prockop, D. J. (2007) Concise review: mesenchymal stem/multipotent stromal cells: the state of transdifferentiation and modes of tissue repair--current views. *Stem cells (Dayton, Ohio)* **25**, 2896-2902

10. Honardoust, D., Eslami, A., Larjava, H., and Hakkinen, L. (2008) Localization of small leucine-rich proteoglycans and transforming growth factor-beta in human oral mucosal wound healing. *Wound repair and regeneration : official publication of the Wound Healing Society [and] the European Tissue Repair Society* **16**, 814-823

11. Hu, R., Xu, W., Ling, W., Wang, Q., Wu, Y., and Han, D. (2014) Characterization of extracellular matrix proteins during wound healing in the lamina propria of vocal fold in a canine model: a long-term and consecutive study. *Acta histochemica* **116**, 730-735

12. Clark, R. A. (2001) Fibrin and wound healing. *Annals of the New York Academy of Sciences* **936**, 355-367

13. Hansen, T. M., Garbarsch, C., Helin, G., Helin, P., Holund, B., Kofod, B., and Lorenzen, I. (1980) Proteoglycans, DNA, and RNA in rat granulation tissue, skin, and aorta. Biochemical and histological studies. *Acta pathologica et microbiologica Scandinavica. Section A, Pathology* **88**, 143-150

14. Tammi, R., Pasonen-Seppanen, S., Kolehmainen, E., and Tammi, M. (2005) Hyaluronan synthase induction and hyaluronan accumulation in mouse epidermis following skin injury. *The Journal of investigative dermatology* **124**, 898-905

15. Velasco, J., Li, J., DiPietro, L., Stepp, M. A., Sandy, J. D., and Plaas, A. (2011) Adamts5 deletion blocks murine dermal repair through CD44-mediated aggrecan accumulation and modulation of transforming growth factor beta1 (TGFbeta1) signaling. *The Journal of biological chemistry* **286**, 26016-26027

16. Toriseva, M., and Kahari, V. M. (2009) Proteinases in cutaneous wound healing. *Cellular and molecular life sciences : CMLS* **66**, 203-224

17. Wang, V. M., Bell, R. M., Thakore, R., Eyre, D. R., Galante, J. O., Li, J., Sandy, J. D., and Plaas, A. (2012) Murine tendon function is adversely affected by aggrecan accumulation due to the knockout of ADAMTS5. *Journal of orthopaedic research : official publication of the Orthopaedic Research Society* **30**, 620-626

18. Maxson, S., Lopez, E. A., Yoo, D., Danilkovitch-Miagkova, A., and Leroux, M. A. (2012) Concise review: role of mesenchymal stem cells in wound repair. *Stem cells translational medicine* **1**, 142-149

19. Kretzschmar, K., and Watt, F. M. (2014) Markers of Epidermal Stem Cell Subpopulations in Adult Mammalian Skin. *Cold Spring Harbor perspectives in medicine* **4**

20. da Silva Meirelles, L., Chagastelles, P. C., and Nardi, N. B. (2006) Mesenchymal stem cells reside in virtually all post-natal organs and tissues. *Journal of cell science* **119**, 2204-2213

21. Bartholomew, A., Sturgeon, C., Siatskas, M., Ferrer, K., McIntosh, K., Patil, S., Hardy, W., Devine, S., Ucker, D., Deans, R., Moseley, A., and Hoffman, R. (2002) Mesenchymal stem cells suppress lymphocyte proliferation in vitro and prolong skin graft survival in vivo. *Experimental hematology* **30**, 42-48

22. Aggarwal, S., and Pittenger, M. F. (2005) Human mesenchymal stem cells modulate allogeneic immune cell responses. *Blood* **105**, 1815-1822

23. Newman, R. E., Yoo, D., LeRoux, M. A., and Danilkovitch-Miagkova, A. (2009) Treatment of inflammatory diseases with mesenchymal stem cells. *Inflammation & allergy drug targets* **8**, 110-123

24. Tse, W. T., Pendleton, J. D., Beyer, W. M., Egalka, M. C., and Guinan, E. C. (2003) Suppression of allogeneic T-cell proliferation by human marrow stromal cells: implications in transplantation. *Transplantation* **75**, 389-397

25. Gonzalez, M. A., Gonzalez-Rey, E., Rico, L., Buscher, D., and Delgado, M. (2009) Adipose-derived mesenchymal stem cells alleviate experimental colitis by inhibiting inflammatory and autoimmune responses. *Gastroenterology* **136**, 978-989

26. Nuschke, A. (2014) Activity of mesenchymal stem cells in therapies for chronic skin wound healing. *Organogenesis* **10**, 29-37

27. Dominici, M., Le Blanc, K., Mueller, I., Slaper-Cortenbach, I., Marini, F., Krause, D., Deans, R., Keating, A., Prockop, D., and Horwitz, E. (2006) Minimal criteria for defining multipotent mesenchymal stromal cells. The International Society for Cellular Therapy position statement. *Cytotherapy* **8**, 315-317

28. Hagmann, S., Moradi, B., Frank, S., Dreher, T., Kammerer, P. W., Richter, W., and Gotterbarm, T. (2013) Different culture media affect growth characteristics, surface marker distribution and chondrogenic differentiation of human bone marrow-derived mesenchymal stromal cells. *BMC musculoskeletal disorders* **14**, 223

29. Tsukahara, S., Ikeda, R., Goto, S., Yoshida, K., Mitsumori, R., Sakamoto, Y., Tajima, A., Yokoyama, T., Toh, S., Furukawa, K., and Inoue, I. (2006) Tumour necrosis factor alpha-stimulated gene-6 inhibits osteoblastic differentiation of human mesenchymal stem cells induced by osteogenic differentiation medium and BMP-2. *The Biochemical journal* **398**, 595-603

30. Wei, X., Li, G., Yang, X., Ba, K., Fu, Y., Fu, N., Cai, X., Li, G., Chen, Q., Wang, M., and Lin, Y. (2013) Effects of bone morphogenetic protein-4 (BMP-4) on adipocyte differentiation from mouse adipose-derived stem cells. *Cell proliferation* **46**, 416-424

31. Sharma, R. R., Pollock, K., Hubel, A., and McKenna, D. (2014) Mesenchymal stem or stromal cells: a review of clinical applications and manufacturing practices. *Transfusion* **54**, 1418-1437

32. Via, A. G., Frizziero, A., and Oliva, F. (2012) Biological properties of mesenchymal Stem Cells from different sources. *Muscles, ligaments and tendons journal* **2**, 154-162

33. Halfon, S., Abramov, N., Grinblat, B., and Ginis, I. (2011) Markers distinguishing mesenchymal stem cells from fibroblasts are downregulated with passaging. *Stem cells and development* **20**, 53-66

34. Blasi, A., Martino, C., Balducci, L., Saldarelli, M., Soleti, A., Navone, S. E., Canzi, L., Cristini, S., Invernici, G., Parati, E. A., and Alessandri, G. (2011) Dermal fibroblasts display similar phenotypic and differentiation capacity to fat-derived mesenchymal stem cells, but differ in anti-inflammatory and angiogenic potential. *Vascular cell* **3**, 5

35. Haniffa, M. A., Wang, X. N., Holtick, U., Rae, M., Isaacs, J. D., Dickinson, A. M., Hilkens, C. M., and Collin, M. P. (2007) Adult human fibroblasts are potent immunoregulatory cells and functionally equivalent to mesenchymal stem cells. *Journal of immunology (Baltimore, Md. : 1950)* **179**, 1595-1604

36. Clark, B. R., and Keating, A. (1995) Biology of bone marrow stroma. *Annals of the New York Academy of Sciences* **770**, 70-78

37. Wight, T. N., Kinsella, M. G., Keating, A., and Singer, J. W. (1986) Proteoglycans in human long-term bone marrow cultures: biochemical and ultrastructural analyses. *Blood* **67**, 1333-1343

38. Chen, P. Y., Huang, L. L., and Hsieh, H. J. (2007) Hyaluronan preserves the proliferation and differentiation potentials of long-term cultured murine adipose-derived stromal cells. *Biochemical and biophysical research communications* **360**, 1-6

39. Liu, C. M., Yu, C. H., Chang, C. H., Hsu, C. C., and Huang, L. L. (2008) Hyaluronan substratum holds mesenchymal stem cells in slow-cycling mode by prolonging G1 phase. *Cell and tissue research* **334**, 435-443

40. Qu, C., Rilla, K., Tammi, R., Tammi, M., Kroger, H., and Lammi, M. J. (2014) Extensive CD44-dependent hyaluronan coats on human bone marrow-derived mesenchymal stem cells produced by hyaluronan synthases HAS1, HAS2 and HAS3. *The international journal of biochemistry & cell biology* **48**, 45-54

41. Chen, X. D. (2010) Extracellular matrix provides an optimal niche for the maintenance and propagation of mesenchymal stem cells. *Birth defects research. Part C, Embryo today : reviews* **90**, 45-54

42. Gattazzo, F., Urciuolo, A., and Bonaldo, P. (2014) Extracellular matrix: a dynamic microenvironment for stem cell niche. *Biochimica et biophysica acta* **1840**, 2506-2519

43. Coulson-Thomas, V. J., Gesteira, T. F., Hascall, V., and Kao, W. (2014) Umbilical Cord Mesenchymal Stem Cells Suppress Host Rejection: THE ROLE OF THE GLYCOCALYX. *The Journal of biological chemistry* **289**, 23465-23481

44. Haque, N., Rahman, M. T., Abu Kasim, N. H., and Alabsi, A. M. (2013) Hypoxic culture conditions as a solution for mesenchymal stem cell based regenerative therapy. *TheScientificWorldJournal* **2013**, 632972

45. Lokmic, Z., Musyoka, J., Hewitson, T. D., and Darby, I. A. (2012) Hypoxia and hypoxia signaling in tissue repair and fibrosis. *International review of cell and molecular biology* **296**, 139-185

46. Fotia, C., Massa, A., Boriani, F., Baldini, N., and Granchi, D. (2014) Hypoxia enhances proliferation and stemness of human adipose-derived mesenchymal stem cells. *Cytotechnology*

47. Kang, S., Kim, S. M., and Sung, J. H. (2014) Cellular and molecular stimulation of adipose-derived stem cells under hypoxia. *Cell biology international* **38**, 553-562

48. Choi, J. R., Pingguan-Murphy, B., Wan Abas, W. A., Noor Azmi, M. A., Omar, S. Z., Chua, K. H., and Wan Safwani, W. K. (2014) Impact of low oxygen tension on stemness, proliferation and differentiation potential of human adipose-derived stem cells. *Biochemical and biophysical research communications* **448**, 218-224

49. Deschepper, M., Oudina, K., David, B., Myrtil, V., Collet, C., Bensidhoum, M., Logeart-Avramoglou, D., and Petite, H. (2011) Survival and function of mesenchymal stem cells (MSCs) depend on glucose to overcome exposure to long-term, severe and continuous hypoxia. *Journal of cellular and molecular medicine* **15**, 1505-1514

50. Mylotte, L. A., Duffy, A. M., Murphy, M., O'Brien, T., Samali, A., Barry, F., and Szegezdi, E. (2008) Metabolic flexibility permits mesenchymal stem cell survival in an ischemic environment. *Stem cells (Dayton, Ohio)* **26**, 1325-1336

51. Kern, S., Eichler, H., Stoeve, J., Kluter, H., and Bieback, K. (2006) Comparative analysis of mesenchymal stem cells from bone marrow, umbilical cord blood, or adipose tissue. *Stem cells (Dayton, Ohio)* **24**, 1294-1301

52. Zuk, P. A., Zhu, M., Mizuno, H., Huang, J., Futrell, J. W., Katz, A. J., Benhaim, P., Lorenz, H. P., and Hedrick, M. H. (2001) Multilineage cells from human adipose tissue: implications for cell-based therapies. *Tissue engineering* **7**, 211-228

53. Zheng, B., Cao, B., Li, G., and Huard, J. (2006) Mouse adipose-derived stem cells undergo multilineage differentiation in vitro but primarily osteogenic and chondrogenic differentiation in vivo. *Tissue engineering* **12**, 1891-1901

54. (2009). in *Essentials of Glycobiology* (Varki, A., Cummings, R. D., Esko, J. D., Freeze, H. H., Stanley, P., Bertozzi, C. R., Hart, G. W., and Etzler, M. E. eds.), Cold Spring Harbor Laboratory Press, Cold Spring Harbor (NY). pp

55. Frantz, C., Stewart, K. M., and Weaver, V. M. (2010) The extracellular matrix at a glance. *Journal of cell science* **123**, 4195-4200

56. Heinegard, D. (2009) Proteoglycans and more--from molecules to biology. *International journal of experimental pathology* **90**, 575-586

57. Schaefer, L., and Schaefer, R. M. (2010) Proteoglycans: from structural compounds to signaling molecules. *Cell and tissue research* **339**, 237-246

58. Hascall, V. C., and Sajdera, S. W. (1969) Proteinpolysaccharide complex from bovine nasal cartilage. The function of glycoprotein in the formation of aggregates. *The Journal of biological chemistry* **244**, 2384-2396

59. Hardingham, T. E., and Muir, H. (1972) The specific interaction of hyaluronic acid with cartillage proteoglycans. *Biochimica et biophysica acta* **279**, 401-405

60. Berenson, M. C., Blevins, F. T., Plaas, A. H., and Vogel, K. G. (1996) Proteoglycans of human rotator cuff tendons. *Journal of orthopaedic research : official publication of the Orthopaedic Research Society* **14**, 518-525

61. Bell, R., Li, J., Shewman, E. F., Galante, J. O., Cole, B. J., Bach, B. R., Jr., Troy, K. L., Mikecz, K., Sandy, J. D., Plaas, A. H., and Wang, V. M. (2013) ADAMTS5 is required for biomechanically-stimulated healing of murine tendinopathy. *Journal of orthopaedic research : official publication of the Orthopaedic Research Society* **31**, 1540-1548

62. Bruckner, G., Brauer, K., Hartig, W., Wolff, J. R., Rickmann, M. J., Derouiche, A., Delpech, B., Girard, N., Oertel, W. H., and Reichenbach, A. (1993) Perineuronal nets provide a polyanionic, glia-associated form of microenvironment around certain neurons in many parts of the rat brain. *Glia* **8**, 183-200

63. Hockfield, S., Kalb, R. G., Zaremba, S., and Fryer, H. (1990) Expression of neural proteoglycans correlates with the acquisition of mature neuronal properties in the mammalian brain. *Cold Spring Harbor symposia on quantitative biology* **55**, 505-514

64. Matthews, R. T., Kelly, G. M., Zerillo, C. A., Gray, G., Tiemeyer, M., and Hockfield, S. (2002) Aggrecan glycoforms contribute to the molecular heterogeneity of perineuronal nets. *The Journal of neuroscience : the official journal of the Society for Neuroscience* **22**, 7536-7547

65. Voros, G., Sandy, J. D., Collen, D., and Lijnen, H. R. (2006) Expression of aggrecan(ases) during murine preadipocyte differentiation and adipose tissue development. *Biochimica et biophysica acta* **1760**, 1837-1844

66. Watanabe, H., Cheung, S. C., Itano, N., Kimata, K., and Yamada, Y. (1997) Identification of hyaluronan-binding domains of aggrecan. *The Journal of biological chemistry* **272**, 28057-28065

67. Zimmermann, D. R., and Ruoslahti, E. (1989) Multiple domains of the large fibroblast proteoglycan, versican. *The EMBO journal* **8**, 2975-2981

68. Wight, T. N. (2002) Versican: a versatile extracellular matrix proteoglycan in cell biology. *Current opinion in cell biology* **14**, 617-623

69. Dours-Zimmermann, M. T., and Zimmermann, D. R. (1994) A novel glycosaminoglycan attachment domain identified in two alternative splice variants of human versican. *The Journal of biological chemistry* **269**, 32992-32998

70. Zako, M., Shinomura, T., Ujita, M., Ito, K., and Kimata, K. (1995) Expression of PG-M(V3), an alternatively spliced form of PG-M without a chondroitin sulfate attachment in region in mouse and human tissues. *The Journal of biological chemistry* **270**, 3914-3918

71. Evanko, S. P., Angello, J. C., and Wight, T. N. (1999) Formation of hyaluronan- and versican-rich pericellular matrix is required for proliferation and migration of vascular smooth muscle cells. *Arteriosclerosis, thrombosis, and vascular biology* **19**, 1004-1013

72. Lemire, J. M., Braun, K. R., Maurel, P., Kaplan, E. D., Schwartz, S. M., and Wight, T. N. (1999) Versican/PG-M isoforms in vascular smooth muscle cells. *Arteriosclerosis, thrombosis, and vascular biology* **19**, 1630-1639

73. Schmalfeldt, M., Dours-Zimmermann, M. T., Winterhalter, K. H., and Zimmermann, D. R. (1998) Versican V2 is a major extracellular matrix component of the mature bovine brain. *The Journal of biological chemistry* **273**, 15758-15764

74. Landolt, R. M., Vaughan, L., Winterhalter, K. H., and Zimmermann, D. R. (1995) Versican is selectively expressed in embryonic tissues that act as barriers to neural crest cell migration and axon outgrowth. *Development (Cambridge, England)* **121**, 2303-2312

75. Williams, D. R., Jr., Presar, A. R., Richmond, A. T., Mjaatvedt, C. H., Hoffman, S., and Capehart, A. A. (2005) Limb chondrogenesis is compromised in the versican deficient hdf mouse. *Biochemical and biophysical research communications* **334**, 960-966

76. Shepard, J. B., Gliga, D. A., Morrow, A. P., Hoffman, S., and Capehart, A. A. (2008) Versican knock-down compromises chondrogenesis in the embryonic chick limb. *Anatomical record (Hoboken, N.J. : 2007)* **291**, 19-27

77. Capehart, A. A. (2010) Proteolytic cleavage of versican during limb joint development. *Anatomical record (Hoboken, N.J. : 2007)* **293**, 208-214

78. Cooley, M. A., Fresco, V. M., Dorlon, M. E., Twal, W. O., Lee, N. V., Barth, J. L., Kern, C. B., Iruela-Arispe, M. L., and Argraves, W. S. (2012) Fibulin-1 is required during cardiac ventricular morphogenesis for versican cleavage, suppression of ErbB2 and Erk1/2 activation, and to attenuate trabecular cardiomyocyte proliferation. *Developmental dynamics : an official publication of the American Association of Anatomists* **241**, 303-314

79. Perides, G., Asher, R. A., Lark, M. W., Lane, W. S., Robinson, R. A., and Bignami, A. (1995) Glial hyaluronate-binding protein: a product of metalloproteinase digestion of versican? *The Biochemical journal* **312 (Pt 2)**, 377-384

80. Barascuk, N., Genovese, F., Larsen, L., Byrjalsen, I., Zheng, Q., Sun, S., Hosbond, S., Poulsen, T. S., Diederichsen, A., Jensen, J. M., Mickley, H., Register, T. C., Rasmussen, L. M., Leeming, D. J., Christiansen, C., and Karsdal, M. A. (2013) A MMP derived versican neo-epitope is elevated in plasma from patients with atherosclerotic heart disease. *International journal of clinical and experimental medicine* **6**, 174-184

81. Nandadasa, S., Foulcer, S., and Apte, S. S. (2014) The multiple, complex roles of versican and its proteolytic turnover by ADAMTS proteases during embryogenesis. *Matrix biology : journal of the International Society for Matrix Biology* **35**, 34-41

82. Kuno, K., Kanada, N., Nakashima, E., Fujiki, F., Ichimura, F., and Matsushima, K. (1997) Molecular cloning of a gene encoding a new type of metalloproteinase-disintegrin family protein with thrombospondin motifs as an inflammation associated gene. *The Journal of biological chemistry* **272**, 556-562

83. Tortorella, M. D., Arner, E. C., Hills, R., Gormley, J., Fok, K., Pegg, L., Munie, G., and Malfait, A. M. (2005) ADAMTS-4 (aggrecanase-1): N-terminal activation mechanisms. *Archives of biochemistry and biophysics* **444**, 34-44

84. Longpre, J. M., McCulloch, D. R., Koo, B. H., Alexander, J. P., Apte, S. S., and Leduc, R. (2009) Characterization of proADAMTS5 processing by proprotein convertases. *The international journal of biochemistry & cell biology* **41**, 1116-1126

85. Sandy, J. D., Neame, P. J., Boynton, R. E., and Flannery, C. R. (1991) Catabolism of aggrecan in cartilage explants. Identification of a major cleavage site within the interglobular domain. *The Journal of biological chemistry* **266**, 8683-8685

86. Sandy, J. D., Thompson, V., Doege, K., and Verscharen, C. (2000) The intermediates of aggrecanase-dependent cleavage of aggrecan in rat chondrosarcoma cells treated with interleukin-1. *The Biochemical journal* **351**, 161-166

87. Sandy, J. D., and Verscharen, C. (2001) Analysis of aggrecan in human knee cartilage and synovial fluid indicates that aggrecanase (ADAMTS) activity is responsible for the catabolic turnover and loss of whole aggrecan whereas other protease activity is required for C-terminal processing in vivo. *The Biochemical journal* **358**, 615-626

88. Sandy, J. D., Westling, J., Kenagy, R. D., Iruela-Arispe, M. L., Verscharen, C., Rodriguez-Mazaneque, J. C., Zimmermann, D. R., Lemire, J. M., Fischer, J. W., Wight, T. N., and Clowes, A. W. (2001) Versican V1 proteolysis in human aorta in vivo occurs at the Glu441-Ala442 bond, a site that is cleaved by recombinant ADAMTS-1 and ADAMTS-4. *The Journal of biological chemistry* **276**, 13372-13378

89. Somerville, R. P., Longpre, J. M., Jungers, K. A., Engle, J. M., Ross, M., Evanko, S., Wight, T. N., Leduc, R., and Apte, S. S. (2003) Characterization of ADAMTS-9 and ADAMTS-20 as a distinct ADAMTS subfamily related to Caenorhabditis elegans GON-1. *The Journal of biological chemistry* **278**, 9503-9513

90. Westling, J., Gottschall, P. E., Thompson, V. P., Cockburn, A., Perides, G., Zimmermann, D. R., and Sandy, J. D. (2004) ADAMTS4 (aggrecanase-1) cleaves human brain versican V2 at Glu405-Gln406 to generate glial hyaluronate binding protein. *The Biochemical journal* **377**, 787-795

91. Hughes, C. E., Caterson, B., Fosang, A. J., Roughley, P. J., and Mort, J. S. (1995) Monoclonal antibodies that specifically recognize neoepitope sequences generated by 'aggrecanase' and matrix metalloproteinase cleavage of aggrecan: application to catabolism in situ and in vitro. *The Biochemical journal* **305 (Pt 3)**, 799-804

92. Tortorella, M. D., Pratta, M., Liu, R. Q., Austin, J., Ross, O. H., Abbaszade, I., Burn, T., and Arner, E. (2000) Sites of aggrecan cleavage

by recombinant human aggrecanase-1 (ADAMTS-4). *The Journal of biological chemistry* **275**, 18566-18573

93. Glasson, S. S., Askew, R., Sheppard, B., Carito, B., Blanchet, T., Ma, H. L., Flannery, C. R., Peluso, D., Kanki, K., Yang, Z., Majumdar, M. K., and Morris, E. A. (2005) Deletion of active ADAMTS5 prevents cartilage degradation in a murine model of osteoarthritis. *Nature* **434**, 644-648

94. Stanton, H., Rogerson, F. M., East, C. J., Golub, S. B., Lawlor, K. E., Meeker, C. T., Little, C. B., Last, K., Farmer, P. J., Campbell, I. K., Fourie, A. M., and Fosang, A. J. (2005) ADAMTS5 is the major aggrecanase in mouse cartilage in vivo and in vitro. *Nature* **434**, 648-652

95. Fosang, A. J., and Rogerson, F. M. (2010) Identifying the human aggrecanase. *Osteoarthritis and cartilage / OARS, Osteoarthritis Research Society* **18**, 1109-1116

96. Song, R. H., Tortorella, M. D., Malfait, A. M., Alston, J. T., Yang, Z., Arner, E. C., and Griggs, D. W. (2007) Aggrecan degradation in human articular cartilage explants is mediated by both ADAMTS-4 and ADAMTS-5. *Arthritis and rheumatism* **56**, 575-585

97. Tortorella, M. D., Malfait, A. M., Deccico, C., and Arner, E. (2001) The role of ADAM-TS4 (aggrecanase-1) and ADAM-TS5 (aggrecanase-2) in a model of cartilage degradation. *Osteoarthritis and cartilage / OARS, Osteoarthritis Research Society* **9**, 539-552

98. Koshy, P. J., Lundy, C. J., Rowan, A. D., Porter, S., Edwards, D. R., Hogan, A., Clark, I. M., and Cawston, T. E. (2002) The modulation of matrix metalloproteinase and ADAM gene expression in human chondrocytes by interleukin-1 and oncostatin M: a time-course study using real-time quantitative reverse transcription-polymerase chain reaction. *Arthritis and rheumatism* **46**, 961-967

99. Tortorella, M. D., Arner, E. C., Hills, R., Easton, A., Korte-Sarfaty, J., Fok, K., Wittwer, A. J., Liu, R. Q., and Malfait, A. M. (2004) Alpha2-macroglobulin is a novel substrate for ADAMTS-4 and ADAMTS-5 and represents an endogenous inhibitor of these enzymes. *The Journal of biological chemistry* **279**, 17554-17561

100. Abbaszade, I., Liu, R. Q., Yang, F., Rosenfeld, S. A., Ross, O. H., Link, J. R., Ellis, D. M., Tortorella, M. D., Pratta, M. A., Hollis, J. M., Wynn, R., Duke, J. L., George, H. J., Hillman, M. C., Jr., Murphy, K., Wiswall, B. H., Copeland, R. A., Decicco, C. P., Bruckner, R., Nagase, H., Itoh, Y., Newton, R. C., Magolda, R. L., Trzaskos, J. M., Burn, T. C., and et al. (1999) Cloning and characterization of ADAMTS11, an aggrecanase from the ADAMTS family. *The Journal of biological chemistry* **274**, 23443-23450

101. Shieh, H. S., Mathis, K. J., Williams, J. M., Hills, R. L., Wiese, J. F., Benson, T. E., Kiefer, J. R., Marino, M. H., Carroll, J. N., Leone, J. W., Malfait, A. M., Arner, E. C., Tortorella, M. D., and Tomasselli, A. (2008) High resolution crystal structure of the catalytic domain of ADAMTS-5 (aggrecanase-2). *The Journal of biological chemistry* **283**, 1501-1507

102. Plaas, A., Osborn, B., Yoshihara, Y., Bai, Y., Bloom, T., Nelson, F., Mikecz, K., and Sandy, J. D. (2007) Aggrecanolysis in human osteoarthritis: confocal localization and biochemical characterization of ADAMTS5-hyaluronan complexes in articular cartilages. *Osteoarthritis and cartilage / OARS, Osteoarthritis Research Society* **15**, 719-734

103. Yang, B., Yang, B. L., Savani, R. C., and Turley, E. A. (1994) Identification of a common hyaluronan binding motif in the hyaluronan binding proteins RHAMM, CD44 and link protein. *The EMBO journal* **13**, 286-296

104. Ariyoshi, W., Knudson, C. B., Luo, N., Fosang, A. J., and Knudson, W. (2010) Internalization of aggrecan G1 domain neoepitope ITEGE in chondrocytes requires CD44. *The Journal of biological chemistry* **285**, 36216-36224

105. Yamamoto, K., Troeberg, L., Scilabra, S. D., Pelosi, M., Murphy, C. L., Strickland, D. K., and Nagase, H. (2013) LRP-1-mediated endocytosis regulates extracellular activity of ADAMTS-5 in articular cartilage. *FASEB journal : official publication of the Federation of American Societies for Experimental Biology* **27**, 511-521

106. Nakajima, I., Yamaguchi, T., Ozutsumi, K., and Aso, H. (1998) Adipose tissue extracellular matrix: newly organized by adipocytes during differentiation. *Differentiation; research in biological diversity* **63**, 193-200

107. Chun, T. H. (2012) Peri-adipocyte ECM remodeling in obesity and adipose tissue fibrosis. *Adipocyte* **1**, 89-95

108. Huang, G., Ge, G., Wang, D., Gopalakrishnan, B., Butz, D. H., Colman, R. J., Nagy, A., and Greenspan, D. S. (2011) alpha3(V) collagen is critical for glucose homeostasis in mice due to effects in pancreatic islets and peripheral tissues. *The Journal of clinical investigation* **121**, 769-783

109. Pasarica, M., Gowronska-Kozak, B., Burk, D., Remedios, I., Hymel, D., Gimble, J., Ravussin, E., Bray, G. A., and Smith, S. R. (2009) Adipose tissue collagen VI in obesity. *The Journal of clinical endocrinology and metabolism* **94**, 5155-5162

110. Varma, V., Yao-Borengasser, A., Bodles, A. M., Rasouli, N., Phanavanh, B., Nolen, G. T., Kern, E. M., Nagarajan, R., Spencer, H. J., 3rd, Lee, M. J., Fried, S. K., McGehee, R. E., Jr., Peterson, C. A., and Kern, P. A.

(2008) Thrombospondin-1 is an adipokine associated with obesity, adipose inflammation, and insulin resistance. *Diabetes* **57**, 432-439

111. Rogerson, F. M., Stanton, H., East, C. J., Golub, S. B., Tutolo, L., Farmer, P. J., and Fosang, A. J. (2008) Evidence of a novel aggrecan-degrading activity in cartilage: Studies of mice deficient in both ADAMTS-4 and ADAMTS-5. *Arthritis and rheumatism* **58**, 1664-1673

112. Dupuis, L. E., McCulloch, D. R., McGarity, J. D., Bahan, A., Wessels, A., Weber, D., Diminich, A. M., Nelson, C. M., Apte, S. S., and Kern, C. B. (2011) Altered versican cleavage in ADAMTS5 deficient mice; a novel etiology of myxomatous valve disease. *Developmental biology* **357**, 152-164

113. Malfait, A. M., Ritchie, J., Gil, A. S., Austin, J. S., Hartke, J., Qin, W., Tortorella, M. D., and Mogil, J. S. (2010) ADAMTS-5 deficient mice do not develop mechanical allodynia associated with osteoarthritis following medial meniscal destabilization. *Osteoarthritis and cartilage / OARS, Osteoarthritis Research Society* **18**, 572-580

114. Li, J., Anemaet, W., Diaz, M. A., Buchanan, S., Tortorella, M., Malfait, A. M., Mikecz, K., Sandy, J. D., and Plaas, A. (2011) Knockout of ADAMTS5 does not eliminate cartilage aggrecanase activity but abrogates joint fibrosis and promotes cartilage aggrecan deposition in murine osteoarthritis models. *Journal of orthopaedic research : official publication of the Orthopaedic Research Society* **29**, 516-522

115. Verrecchia, F., Mauviel, A., and Farge, D. (2006) Transforming growth factor-beta signaling through the Smad proteins: role in systemic sclerosis. *Autoimmunity reviews* **5**, 563-569

116. Moustakas, A., and Heldin, C. H. (2009) The regulation of TGFbeta signal transduction. *Development (Cambridge, England)* **136**, 3699-3714

117. Kessler, E., and Goldberg, B. (1978) A method for assaying the activity of the endopeptidase which excises the nonhelical carboxyterminal extensions from type I procollagen. *Analytical biochemistry* **86**, 463-469

118. Colige, A., Vandenberghe, I., Thiry, M., Lambert, C. A., Van Beeumen, J., Li, S. W., Prockop, D. J., Lapiere, C. M., and Nusgens, B. V. (2002) Cloning and characterization of ADAMTS-14, a novel ADAMTS displaying high homology with ADAMTS-2 and ADAMTS-3. *The Journal of biological chemistry* **277**, 5756-5766

119. Pinnell, S. R., and Martin, G. R. (1968) The cross-linking of collagen and elastin: enzymatic conversion of lysine in peptide linkage to alpha-aminoadipic-delta-semialdehyde (allysine) by an extract from bone.

Proceedings of the National Academy of Sciences of the United States of America **61**, 708-716

120. Centrella, M., Casinghino, S., Ignotz, R., and McCarthy, T. L. (1992) Multiple regulatory effects by transforming growth factor-beta on type I collagen levels in osteoblast-enriched cultures from fetal rat bone. *Endocrinology* **131**, 2863-2872

121. Hong, H. H., Uzel, M. I., Duan, C., Sheff, M. C., and Trackman, P. C. (1999) Regulation of lysyl oxidase, collagen, and connective tissue growth factor by TGF-beta1 and detection in human gingiva. *Laboratory investigation; a journal of technical methods and pathology* **79**, 1655-1667

122. Ten Cate, A. R., and Deporter, D. A. (1974) The role of the fibroblast in collagen turnover in the functioning periodontal ligament of the mouse. *Archives of oral biology* **19**, 339-340

123. Melcher, A. H., and Chan, J. (1981) Phagocytosis and digestion of collagen by gingival fibroblasts in vivo: a study of serial sections. *Journal of ultrastructure research* **77**, 1-36

124. Lee, H., Overall, C. M., McCulloch, C. A., and Sodek, J. (2006) A critical role for the membrane-type 1 matrix metalloproteinase in collagen phagocytosis. *Molecular biology of the cell* **17**, 4812-4826

125. Lee, H., Sodek, K. L., Hwang, Q., Brown, T. J., Ringuette, M., and Sodek, J. (2007) Phagocytosis of collagen by fibroblasts and invasive cancer cells is mediated by MT1-MMP. *Biochemical Society transactions* **35**, 704-706

126. Kim, S. I., Na, H. J., Ding, Y., Wang, Z., Lee, S. J., and Choi, M. E. (2012) Autophagy promotes intracellular degradation of type I collagen induced by transforming growth factor (TGF)-beta1. *The Journal of biological chemistry* **287**, 11677-11688

127. Doherty, G. J., and McMahon, H. T. (2009) Mechanisms of endocytosis. *Annual review of biochemistry* **78**, 857-902

128. Schmid, E. M., Ford, M. G., Burtey, A., Praefcke, G. J., Peak-Chew, S. Y., Mills, I. G., Benmerah, A., and McMahon, H. T. (2006) Role of the AP2 beta-appendage hub in recruiting partners for clathrin-coated vesicle assembly. *PLoS biology* **4**, e262

129. Praefcke, G. J., and McMahon, H. T. (2004) The dynamin superfamily: universal membrane tubulation and fission molecules? *Nature reviews. Molecular cell biology* **5**, 133-147

130. Lamb, C. A., Dooley, H. C., and Tooze, S. A. (2013) Endocytosis and autophagy: Shared machinery for degradation. *BioEssays : news and reviews in molecular, cellular and developmental biology* **35**, 34-45

131. Etique, N., Verzeaux, L., Dedieu, S., and Emonard, H. (2013) LRP-1: a checkpoint for the extracellular matrix proteolysis. *BioMed research international* **2013**, 152163

132. Le Roy, C., and Wrana, J. L. (2005) Clathrin- and non-clathrin-mediated endocytic regulation of cell signalling. *Nature reviews. Molecular cell biology* **6**, 112-126

133. Hayes, S., Chawla, A., and Corvera, S. (2002) TGF beta receptor internalization into EEA1-enriched early endosomes: role in signaling to Smad2. *The Journal of cell biology* **158**, 1239-1249

134. Di Guglielmo, G. M., Le Roy, C., Goodfellow, A. F., and Wrana, J. L. (2003) Distinct endocytic pathways regulate TGF-beta receptor signalling and turnover. *Nature cell biology* **5**, 410-421

135. Runyan, C. E., Schnaper, H. W., and Poncelet, A. C. (2005) The role of internalization in transforming growth factor beta1-induced Smad2 association with Smad anchor for receptor activation (SARA) and Smad2-dependent signaling in human mesangial cells. *The Journal of biological chemistry* **280**, 8300-8308

136. Mitchell, H., Choudhury, A., Pagano, R. E., and Leof, E. B. (2004) Ligand-dependent and -independent transforming growth factor-beta receptor recycling regulated by clathrin-mediated endocytosis and Rab11. *Molecular biology of the cell* **15**, 4166-4178

137. Kavsak, P., Rasmussen, R. K., Causing, C. G., Bonni, S., Zhu, H., Thomsen, G. H., and Wrana, J. L. (2000) Smad7 binds to Smurf2 to form an E3 ubiquitin ligase that targets the TGF beta receptor for degradation. *Molecular cell* **6**, 1365-1375

138. Hernandez-Barrantes, S., Bernardo, M., Toth, M., and Fridman, R. (2002) Regulation of membrane type-matrix metalloproteinases. *Seminars in cancer biology* **12**, 131-138

139. Selvais, C., D'Auria, L., Tyteca, D., Perrot, G., Lemoine, P., Troeberg, L., Dedieu, S., Noel, A., Nagase, H., Henriet, P., Courtoy, P. J., Marbaix, E., and Emonard, H. (2011) Cell cholesterol modulates metalloproteinase-dependent shedding of low-density lipoprotein receptor-related protein-1 (LRP-1) and clearance function. *FASEB journal : official publication of the Federation of American Societies for Experimental Biology* **25**, 2770-2781

140. Kang, T., Nagase, H., and Pei, D. (2002) Activation of membrane-type matrix metalloproteinase 3 zymogen by the proprotein convertase furin in the trans-Golgi network. *Cancer research* **62**, 675-681

141. Yana, I., and Weiss, S. J. (2000) Regulation of membrane type-1 matrix metalloproteinase activation by proprotein convertases. *Molecular biology of the cell* **11**, 2387-2401

142. Deryugina, E. I., Ratnikov, B. I., Yu, Q., Baciu, P. C., Rozanov, D. V., and Strongin, A. Y. (2004) Prointegrin maturation follows rapid trafficking and processing of MT1-MMP in Furin-Negative Colon Carcinoma LoVo Cells. *Traffic (Copenhagen, Denmark)* **5**, 627-641

143. Rozanov, D. V., and Strongin, A. Y. (2003) Membrane type-1 matrix metalloproteinase functions as a proprotein self-convertase. Expression of the latent zymogen in Pichia pastoris, autolytic activation, and the peptide sequence of the cleavage forms. *The Journal of biological chemistry* **278**, 8257-8260

144. Remacle, A. G., Chekanov, A. V., Golubkov, V. S., Savinov, A. Y., Rozanov, D. V., and Strongin, A. Y. (2006) O-glycosylation regulates autolysis of cellular membrane type-1 matrix metalloproteinase (MT1-MMP). *The Journal of biological chemistry* **281**, 16897-16905

145. Lorenz, M. R., Holzapfel, V., Musyanovych, A., Nothelfer, K., Walther, P., Frank, H., Landfester, K., Schrezenmeier, H., and Mailander, V. (2006) Uptake of functionalized, fluorescent-labeled polymeric particles in different cell lines and stem cells. *Biomaterials* **27**, 2820-2828

146. Pelekanos, R. A., Ting, M. J., Sardesai, V. S., Ryan, J. M., Lim, Y. C., Chan, J. K., and Fisk, N. M. (2014) Intracellular trafficking and endocytosis of CXCR4 in fetal mesenchymal stem/stromal cells. *BMC cell biology* **15**, 15

147. Kliemt, S., Lange, C., Otto, W., Hintze, V., Moller, S., von Bergen, M., Hempel, U., and Kalkhof, S. (2013) Sulfated hyaluronan containing collagen matrices enhance cell-matrix-interaction, endocytosis, and osteogenic differentiation of human mesenchymal stromal cells. *Journal of proteome research* **12**, 378-389

148. Tian, T., Zhu, Y. L., Zhou, Y. Y., Liang, G. F., Wang, Y. Y., Hu, F. H., and Xiao, Z. D. (2014) Exosome uptake through clathrin-mediated endocytosis and macropinocytosis and mediating miR-21 delivery. *The Journal of biological chemistry* **289**, 22258-22267

149. Mueckler, M., and Thorens, B. (2013) The SLC2 (GLUT) family of membrane transporters. *Molecular aspects of medicine* **34**, 121-138

150. Wieman, H. L., Wofford, J. A., and Rathmell, J. C. (2007) Cytokine stimulation promotes glucose uptake via phosphatidylinositol-3 kinase/Akt regulation of Glut1 activity and trafficking. *Molecular biology of the cell* **18**, 1437-1446

151. Corvera, S., Chawla, A., Chakrabarti, R., Joly, M., Buxton, J., and Czech, M. P. (1994) A double leucine within the GLUT4 glucose transporter COOH-terminal domain functions as an endocytosis signal. *The Journal of cell biology* **126**, 979-989

152. Antonescu, C. N., Foti, M., Sauvonnet, N., and Klip, A. (2009) Ready, set, internalize: mechanisms and regulation of GLUT4 endocytosis. *Bioscience reports* **29**, 1-11

153. Wu, N., Zheng, B., Shaywitz, A., Dagon, Y., Tower, C., Bellinger, G., Shen, C. H., Wen, J., Asara, J., McGraw, T. E., Kahn, B. B., and Cantley, L. C. (2013) AMPK-dependent degradation of TXNIP upon energy stress leads to enhanced glucose uptake via GLUT1. *Molecular cell* **49**, 1167-1175

154. Li, D., Randhawa, V. K., Patel, N., Hayashi, M., and Klip, A. (2001) Hyperosmolarity reduces GLUT4 endocytosis and increases its exocytosis from a VAMP2-independent pool in l6 muscle cells. *The Journal of biological chemistry* **276**, 22883-22891

155. Huang, S., and Czech, M. P. (2007) The GLUT4 glucose transporter. *Cell metabolism* **5**, 237-252

156. Foley, K., Boguslavsky, S., and Klip, A. (2011) Endocytosis, recycling, and regulated exocytosis of glucose transporter 4. *Biochemistry* **50**, 3048-3061

157. Lavrentieva, A., Majore, I., Kasper, C., and Hass, R. (2010) Effects of hypoxic culture conditions on umbilical cord-derived human mesenchymal stem cells. *Cell communication and signaling : CCS* **8**, 18

158. Struglics, A., and Hansson, M. (2010) Calpain is involved in C-terminal truncation of human aggrecan. *The Biochemical journal* **430**, 531-538

159. Stewart, M. C., Fosang, A. J., Bai, Y., Osborn, B., Plaas, A., and Sandy, J. D. (2006) ADAMTS5-mediated aggrecanolysis in murine epiphyseal chondrocyte cultures. *Osteoarthritis and cartilage / OARS, Osteoarthritis Research Society* **14**, 392-402

160. Sandy, J. D., Gamett, D., Thompson, V., and Verscharen, C. (1998) Chondrocyte-mediated catabolism of aggrecan: aggrecanase-dependent cleavage induced by interleukin-1 or retinoic acid can be inhibited by glucosamine. *The Biochemical journal* **335 (Pt 1)**, 59-66

161. Oshita, H., Sandy, J. D., Suzuki, K., Akaike, A., Bai, Y., Sasaki, T., and Shimizu, K. (2004) Mature bovine articular cartilage contains abundant aggrecan that is C-terminally truncated at Ala719-Ala720, a site which is readily cleaved by m-calpain. *The Biochemical journal* **382**, 253-259

162. Carrino, D. A., Calabro, A., Darr, A. B., Dours-Zimmermann, M. T., Sandy, J. D., Zimmermann, D. R., Sorrell, J. M., Hascall, V. C., and Caplan, A. I. (2011) Age-related differences in human skin proteoglycans. *Glycobiology* **21**, 257-268

163. Russell, D. L., Doyle, K. M., Ochsner, S. A., Sandy, J. D., and Richards, J. S. (2003) Processing and localization of ADAMTS-1 and proteolytic cleavage of versican during cumulus matrix expansion and ovulation. *The Journal of biological chemistry* **278**, 42330-42339

164. Brown, H. M., Dunning, K. R., Robker, R. L., Boerboom, D., Pritchard, M., Lane, M., and Russell, D. L. (2010) ADAMTS1 cleavage of versican mediates essential structural remodeling of the ovarian follicle and cumulus-oocyte matrix during ovulation in mice. *Biology of reproduction* **83**, 549-557

165. Ghosh, A. K., Bhattacharyya, S., Lakos, G., Chen, S. J., Mori, Y., and Varga, J. (2004) Disruption of transforming growth factor beta signaling and profibrotic responses in normal skin fibroblasts by peroxisome proliferator-activated receptor gamma. *Arthritis and rheumatism* **50**, 1305-1318

166. Pazdro, R., and Harrison, D. E. (2013) Murine adipose tissue-derived stromal cell apoptosis and susceptibility to oxidative stress in vitro are regulated by genetic background. *PloS one* **8**, e61235

167. Frank, J. E., Thompson, V. P., Brown, M. P., and Sandy, J. D. (2009) Removal of O-linked and N-linked oligosaccharides is required for optimum detection of NITEGE neoepitope on ADAMTS4-digested fetal aggrecans: implications for specific N-linked glycan-dependent aggrecanolysis at Glu373-Ala374. *Osteoarthritis and cartilage / OARS, Osteoarthritis Research Society* **17**, 777-781

168. Calabro, A., Midura, R., Wang, A., West, L., Plaas, A., and Hascall, V. C. (2001) Fluorophore-assisted carbohydrate electrophoresis (FACE) of glycosaminoglycans. *Osteoarthritis and cartilage / OARS, Osteoarthritis Research Society* **9 Suppl A**, S16-22

169. Ripellino, J. A., Bailo, M., Margolis, R. U., and Margolis, R. K. (1988) Light and electron microscopic studies on the localization of hyaluronic acid in developing rat cerebellum. *The Journal of cell biology* **106**, 845-855

170. Kim, Y. J., Sah, R. L., Doong, J. Y., and Grodzinsky, A. J. (1988) Fluorometric assay of DNA in cartilage explants using Hoechst 33258. *Analytical biochemistry* **174**, 168-176

171. Plaas, A., Sandy, J. D., Liu, H., Diaz, M. A., Schenkman, D., Magnus, R. P., Bolam-Bretl, C., Kopesky, P. W., Wang, V. M., and Galante, J. O. (2011) Biochemical identification and immunolocalizaton of aggrecan, ADAMTS5 and inter-alpha-trypsin-inhibitor in equine degenerative suspensory ligament desmitis. *Journal of orthopaedic research : official publication of the Orthopaedic Research Society* **29**, 900-906

172. Zuckerman, K. S., and Wicha, M. S. (1983) Extracellular matrix production by the adherent cells of long-term murine bone marrow cultures. *Blood* **61**, 540-547

173. Somanath, P. R., Kandel, E. S., Hay, N., and Byzova, T. V. (2007) Akt1 signaling regulates integrin activation, matrix recognition, and fibronectin assembly. *The Journal of biological chemistry* **282**, 22964-22976

174. Monaghan, E., Gueorguiev, V., Wilkins-Port, C., and McKeown-Longo, P. J. (2004) The receptor for urokinase-type plasminogen activator regulates fibronectin matrix assembly in human skin fibroblasts. *The Journal of biological chemistry* **279**, 1400-1407

175. Shen, B., Wei, A., Whittaker, S., Williams, L. A., Tao, H., Ma, D. D., and Diwan, A. D. (2010) The role of BMP-7 in chondrogenic and osteogenic differentiation of human bone marrow multipotent mesenchymal stromal cells in vitro. *Journal of cellular biochemistry* **109**, 406-416

176. Iwakura, T., Sakata, R., and Reddi, A. H. (2013) Induction of chondrogenesis and expression of superficial zone protein in synovial explants with TGF-beta1 and BMP-7. *Tissue engineering. Part A* **19**, 2638-2644

177. Cals, F. L., Hellingman, C. A., Koevoet, W., Baatenburg de Jong, R. J., and van Osch, G. J. (2012) Effects of transforming growth factor-beta subtypes on in vitro cartilage production and mineralization of human bone marrow stromal-derived mesenchymal stem cells. *Journal of tissue engineering and regenerative medicine* **6**, 68-76

178. Solorio, L. D., Dhami, C. D., Dang, P. N., Vieregge, E. L., and Alsberg, E. (2012) Spatiotemporal regulation of chondrogenic differentiation with controlled delivery of transforming growth factor-beta1 from gelatin microspheres in mesenchymal stem cell aggregates. *Stem cells translational medicine* **1**, 632-639

179. Yasumoto, T. B., M. Bird, J. Mason, R. (1999) Species And Age-Related Differences In The Turnover Of Aggrecan And Link Protein (ABSTRACT).

45th Annual Meeting, Orthopaedic Research Society, February 1-4, 1999, Anaheim, California **24**, 82

180. Bhattacharyya, S., Ghosh, A. K., Pannu, J., Mori, Y., Takagawa, S., Chen, G., Trojanowska, M., Gilliam, A. C., and Varga, J. (2005) Fibroblast expression of the coactivator p300 governs the intensity of profibrotic response to transforming growth factor beta. *Arthritis and rheumatism* **52**, 1248-1258

181. Pan, X., Chen, Z., Huang, R., Yao, Y., and Ma, G. (2013) Transforming growth factor beta1 induces the expression of collagen type I by DNA methylation in cardiac fibroblasts. *PloS one* **8**, e60335

182. van Nieuwenhoven, F. A., Hemmings, K. E., Porter, K. E., and Turner, N. A. (2013) Combined effects of interleukin-1alpha and transforming growth factor-beta1 on modulation of human cardiac fibroblast function. *Matrix biology : journal of the International Society for Matrix Biology* **32**, 399-406

183. Sugiyama, Y., Shimada, A., Sayo, T., Sakai, S., and Inoue, S. (1998) Putative hyaluronan synthase mRNA are expressed in mouse skin and TGF-beta upregulates their expression in cultured human skin cells. *The Journal of investigative dermatology* **110**, 116-121

184. Colige, A., Beschin, A., Samyn, B., Goebels, Y., Van Beeumen, J., Nusgens, B. V., and Lapiere, C. M. (1995) Characterization and partial amino acid sequencing of a 107-kDa procollagen I N-proteinase purified by affinity chromatography on immobilized type XIV collagen. *The Journal of biological chemistry* **270**, 16724-16730

185. Mayer, G., Hamelin, J., Asselin, M. C., Pasquato, A., Marcinkiewicz, E., Tang, M., Tabibzadeh, S., and Seidah, N. G. (2008) The regulated cell surface zymogen activation of the proprotein convertase PC5A directs the processing of its secretory substrates. *The Journal of biological chemistry* **283**, 2373-2384

186. Longpre, J. M., and Leduc, R. (2004) Identification of prodomain determinants involved in ADAMTS-1 biosynthesis. *The Journal of biological chemistry* **279**, 33237-33245

187. Flannery, C. R., Zeng, W., Corcoran, C., Collins-Racie, L. A., Chockalingam, P. S., Hebert, T., Mackie, S. A., McDonagh, T., Crawford, T. K., Tomkinson, K. N., LaVallie, E. R., and Morris, E. A. (2002) Autocatalytic cleavage of ADAMTS-4 (Aggrecanase-1) reveals multiple glycosaminoglycan-binding sites. *The Journal of biological chemistry* **277**, 42775-42780

188. Kirchhausen, T., Macia, E., and Pelish, H. E. (2008) Use of dynasore, the small molecule inhibitor of dynamin, in the regulation of endocytosis. *Methods in enzymology* **438**, 77-93

189. Cho, J. A., Osenkowski, P., Zhao, H., Kim, S., Toth, M., Cole, K., Aboukameel, A., Saliganan, A., Schuger, L., Bonfil, R. D., and Fridman, R. (2008) The inactive 44-kDa processed form of membrane type 1 matrix metalloproteinase (MT1-MMP) enhances proteolytic activity via regulation of endocytosis of active MT1-MMP. *The Journal of biological chemistry* **283**, 17391-17405

190. Danoviz, M. E., Bassaneze, V., Nakamuta, J. S., dos Santos-Junior, G. R., Saint-Clair, D., Bajgelman, M. C., Fae, K. C., Kalil, J., Miyakawa, A. A., and Krieger, J. E. (2011) Adipose tissue-derived stem cells from humans and mice differ in proliferative capacity and genome stability in long-term cultures. *Stem cells and development* **20**, 661-670

191. Barbara, N. P., Wrana, J. L., and Letarte, M. (1999) Endoglin is an accessory protein that interacts with the signaling receptor complex of multiple members of the transforming growth factor-beta superfamily. *The Journal of biological chemistry* **274**, 584-594

192. Jiang, T., Liu, W., Lv, X., Sun, H., Zhang, L., Liu, Y., Zhang, W. J., Cao, Y., and Zhou, G. (2010) Potent in vitro chondrogenesis of CD105 enriched human adipose-derived stem cells. *Biomaterials* **31**, 3564-3571

193. Levi, B., Wan, D. C., Glotzbach, J. P., Hyun, J., Januszyk, M., Montoro, D., Sorkin, M., James, A. W., Nelson, E. R., Li, S., Quarto, N., Lee, M., Gurtner, G. C., and Longaker, M. T. (2011) CD105 protein depletion enhances human adipose-derived stromal cell osteogenesis through reduction of transforming growth factor beta1 (TGF-beta1) signaling. *The Journal of biological chemistry* **286**, 39497-39509

194. Yamamoto, M., and Nakata, H. (2014) Osteogenic Potential of Mouse Adipose-Derived Stem Cells Sorted for CD90 and CD105 In Vitro. **2014**, 576358

195. Grogan, S. P., Miyaki, S., Asahara, H., D'Lima, D. D., and Lotz, M. K. (2009) Mesenchymal progenitor cell markers in human articular cartilage: normal distribution and changes in osteoarthritis. *Arthritis research & therapy* **11**, R85

196. Milner, C. M., Tongsoongnoen, W., Rugg, M. S., and Day, A. J. (2007) The molecular basis of inter-alpha-inhibitor heavy chain transfer on to hyaluronan. *Biochemical Society transactions* **35**, 672-676

197. Rugg, M. S., Willis, A. C., Mukhopadhyay, D., Hascall, V. C., Fries, E., Fulop, C., Milner, C. M., and Day, A. J. (2005) Characterization of

complexes formed between TSG-6 and inter-alpha-inhibitor that act as intermediates in the covalent transfer of heavy chains onto hyaluronan. *The Journal of biological chemistry* **280**, 25674-25686

198. LeBaron, R. G., Zimmermann, D. R., and Ruoslahti, E. (1992) Hyaluronate binding properties of versican. *The Journal of biological chemistry* **267**, 10003-10010

199. Hattori, N., Carrino, D. A., Lauer, M. E., Vasanji, A., Wylie, J. D., Nelson, C. M., and Apte, S. S. (2011) Pericellular versican regulates the fibroblast-myofibroblast transition: a role for ADAMTS5 protease-mediated proteolysis. *The Journal of biological chemistry* **286**, 34298-34310

200. Karamanos, N. K. (2012) *Extracellular matrix : pathobiology and signaling*, Walter de Gruyter, Berlin, Germany

201. Bae, S. E., Choi, D. H., Han, D. K., and Park, K. (2010) Effect of temporally controlled release of dexamethasone on in vivo chondrogenic differentiation of mesenchymal stromal cells. *Journal of controlled release : official journal of the Controlled Release Society* **143**, 23-30

202. Mackay, A. M., Beck, S. C., Murphy, J. M., Barry, F. P., Chichester, C. O., and Pittenger, M. F. (1998) Chondrogenic differentiation of cultured human mesenchymal stem cells from marrow. *Tissue engineering* **4**, 415-428

203. Sugahara, K., and Kitagawa, H. (2000) Recent advances in the study of the biosynthesis and functions of sulfated glycosaminoglycans. *Current opinion in structural biology* **10**, 518-527

204. Silbert, J. E., and Sugumaran, G. (2002) Biosynthesis of chondroitin/dermatan sulfate. *IUBMB life* **54**, 177-186

205. Alonso, M., Hidalgo, J., Hendricks, L., and Velasco, A. (1996) Degradation of aggrecan precursors within a specialized subcompartment of the chicken chondrocyte endoplasmic reticulum. *The Biochemical journal* **316 (Pt 2)**, 487-495

206. Loike, J. D., Silverstein, R., Wright, S. D., Weitz, J. I., Huang, A. J., and Silverstein, S. C. (1992) The role of protected extracellular compartments in interactions between leukocytes, and platelets, and fibrin/fibrinogen matrices. *Annals of the New York Academy of Sciences* **667**, 163-172

207. Gendron, C., Kashiwagi, M., Lim, N. H., Enghild, J. J., Thogersen, I. B., Hughes, C., Caterson, B., and Nagase, H. (2007) Proteolytic activities of human ADAMTS-5: comparative studies with ADAMTS-4. *The Journal of biological chemistry* **282**, 18294-18306

COPYRIGHT STATEMENT

I hereby guarantee that no part of the dissertation entitled, <u>A ROLE FOR ADAMTS5 IN REGULATING THE COMPOSITION OF THE ECM NICHE IN MURINE PLURIPOTENT PROGENITOR CELLS</u>, which I have submitted for publication, has been copied from a copyrighted work, except in cases of passages properly quoted from a copyrighted work, copied with permission of the author, or copied from a work in which I own the copyright; that I am the sole author and proprietor of the dissertation; that the dissertation in all respects complies with the Copyright Revision Act of 1976; that the dissertation) contains no matter which, if published, will be libelous or otherwise injurious to, or infringe in any way the copyright of any other party; and that I will defend, indemnify and hold harmless Rush University Medical Center against all suits and proceedings which may be brought and against all claims which may be made against Rush University Medical Center by reason of the publication of the dissertation.

_____

      Date   Author's Signature